STUDIES OF SURFACE ACOUSTIC WAVE INTERDIGITATED TRANSDUCERS

by

© PETER MORLEY SMITH, B.Eng.Mgt., M.Eng.

A Thesis

Submitted to the School of Graduate Studies

in Partial Fulfilment of the Requirements

for the Degree

Doctor of Philosophy

McMaster University

August 1987

INTERDIGITATED SAW TRANSDUCERS

DOCTOR OF PHILOSOPHY (1987)
(Electrical Engineering)

McMaster University
Hamilton, Ontario

TITLE: Studies of Surface Acoustic Wave Interdigitated Transducers.

AUTHOR: Peter M. Smith, B.Eng.Mgt. (McMaster University)
M.Eng. (McMaster University)

SUPERVISOR: Professor C. K. Campbell

NUMBER OF PAGES: xi, 177

ABSTRACT.

The subject of this Thesis is the theoretical and experimental investigation of the capabilities and the limitations of Surface Acoustic Wave (SAW) Interdigitated Interdigital Transducer (IIDT) filters. These devices provide the means of achieving low-loss SAW filters with percentage bandwidths exceeding 10%. During the course of developing an analytical tool for IIDTs, a menu driven computer program based on a modified version of the Coupling of Modes (COM) theory was written to allow the frequency response of arbitrary SAW device structures, composed of transducers, reflector arrays and spaces, to be evaluated without further programming. Several IIDT filters were fabricated and tested with the aim of reducing the inherent ripple in the frequency response of the structures. Techniques are proposed for achieving losses of less than 6 dB with acceptable ripple suppression. In addition, some studies are performed on IIDT comb filters and their application to multimode oscillators.

ACKNOWLEDGEMENTS

The author would like to express his appreciation for the consideration and supervision received from the supervisor, Dr. C. K. Campbell. Without his help and constructive criticism this Thesis would not have been possible.

I would also like to thank my colleagues, specially Mr. C. B. Saw and Miss S. F. Yuen, for their good humour and the stimulating work environment that they helped create.

Finally, I thank my wife, Ute, for her patience and continued support during the last four years.

TABLE OF CONTENTS

TABLE OF FIGURES

CHAPTER 1

INTRODUCTION

1.0 Introduction.

Surface waves were first studied by John William Strutt, Lord Rayleigh, in 1885 [4]. He investigated, among many other topics, the behaviour of surface waves on a homogeneous isotropic elastic surface. The most important direct application of his work was in the study of earthquakes.

In 1965 the first paper describing a working Surface Acoustic Wave (SAW) device was published [9]. It consisted of two aluminium Interdigital Transducers (IDT) on the surface of quartz. One IDT generated a Rayleigh wave which propagated along the surface of the crystal and was detected by the other IDT. It was observed that, by means of this device, a delay and a filtering action could be obtained in a very compact package. The potential of this invention was soon understood, and this quickly lead to the multi-million

dollar SAW industry of today.

This chapter will present a very brief overview of SAW devices with only those SAW devices that are relevant to the rest of the Thesis being described in any detail. For more information on SAW devices in general, the reader is referred to one of the many excellent SAW text books [1, 2, 3, 4, 5, 6, 7, 8].

1.1 Basic SAW Device Principles.

The most simple SAW device is illustrated in Figure 1.1. It consists of a polished piezoelectric crystal, usually quartz or lithium niobate ($LiNbO_3$), with two Interdigital Transducers. The latter are made of a thin metal layer ($\simeq$ 1000 Å), usually of Aluminium, deposited by means of evaporation.

When an a.c. signal is applied to the bus bars of the input IDT, the resulting electric fields between adjacent fingers produce mechanical deformation in the piezoelectric crystal. At a resonant frequency, the effect of each of the IDT fingers adds constructively, and a wave is produced which propagates away from the transducer in both directions. Half the input energy will therefore propagate across the distance between the two transducers,

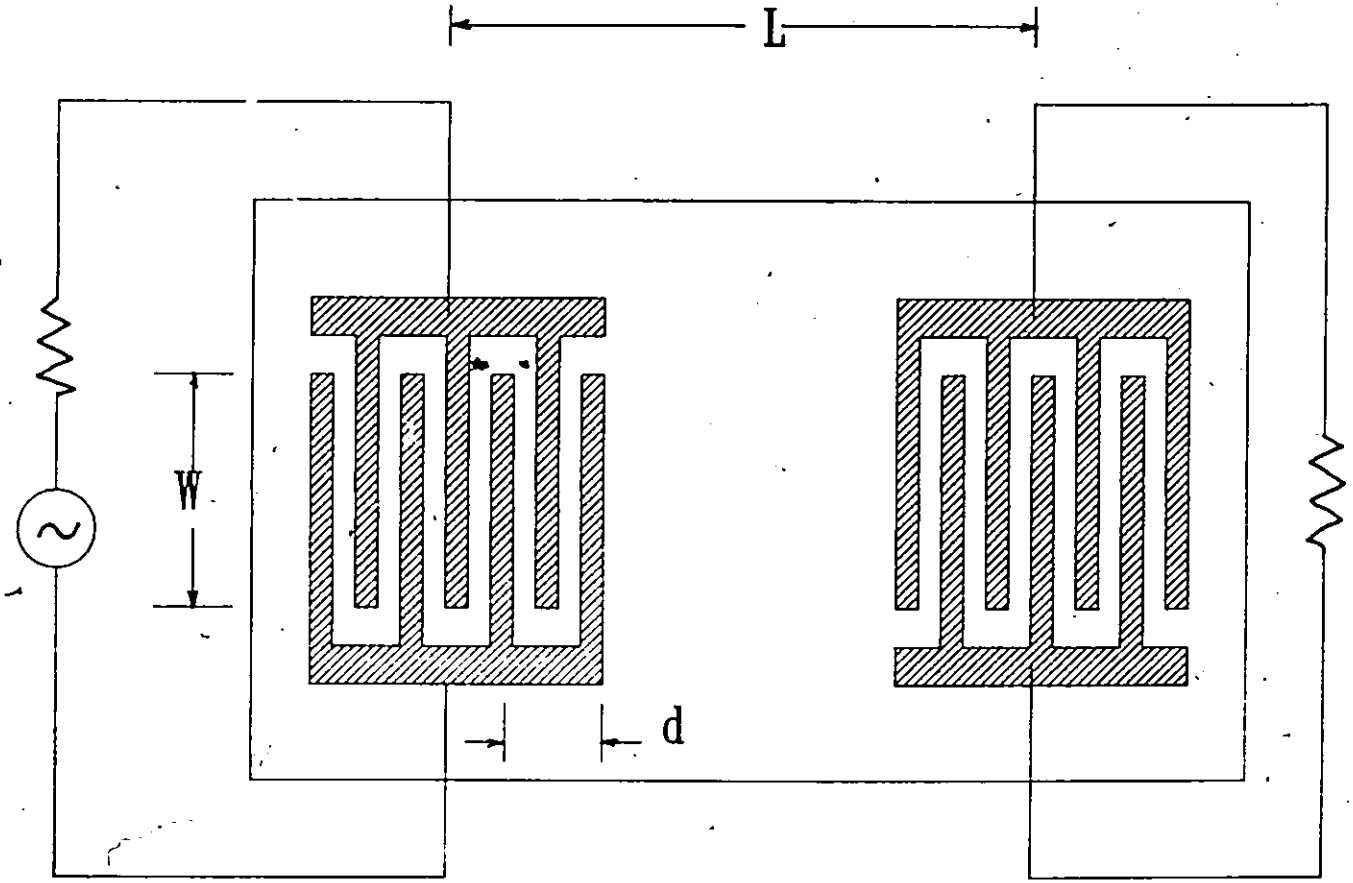

Figure 1.1: The basic SAW device

and reach the output IDT. Here the reverse effect is observed, and the crystal deformations generate electric fields between adjacent fingers, which then add to generate the output signal. The main design parameters in this case are the number of fingers **N** in each transducer, the aperture **W**, the adjacent finger spacing **d**, the finger width **a** and the IDT separation **L**.

1.1.1 Band Shaping.

The frequency response of a delay line with identical input and output transducers approximates that of a $(\sin x/x)^2$ function, where the bandwidth is inversely proportional to the number of fingers in each transducer, and the first sidelobes are 26 dB below the main lobe. This is because, to the first order, the impulse response of each transducer is a square wave with an RF carrier and, from Fourier theory, the frequency response is the Fourier Transform of the impulse response.

In order to improve upon the suppression, the impulse response must be modified to correspond to the inverse Fourier Transform of the desired frequency response. This requires a spatial variation in the coupling efficiency within each transducer. Two common techniques are used to

achieve this: the first, called withdrawal weighting, involves removing fingers where a decrease in coupling is desired (see Figure 1.2a). This technique is only effective in very long transducers, where the quantization of the weighting has little effect on the response. The second method involves controlling the length of individual fingers (see Figure 1.2b). Here it is assumed that the coupling due to one finger is constant over the aperture of the transducer. The efficiency of each finger will then be proportional to the effective length of that finger. Note, however, that in this case the average power in the outgoing wavefront is not constant over the aperture of the transducer.

Since the wavefront generated by an apodized input IDT is no longer constant, the weighting associated with each finger in the output IDT will not be a simple function of its length, but will depend as well on the input transducer. The net result is that the frequency response of the SAW filter will not in general be the product of the frequency responses of each IDT, unless at least one of them is not apodized.

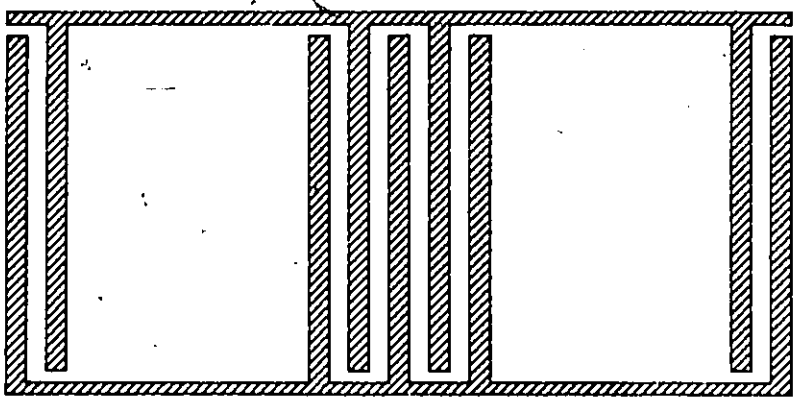

(a)

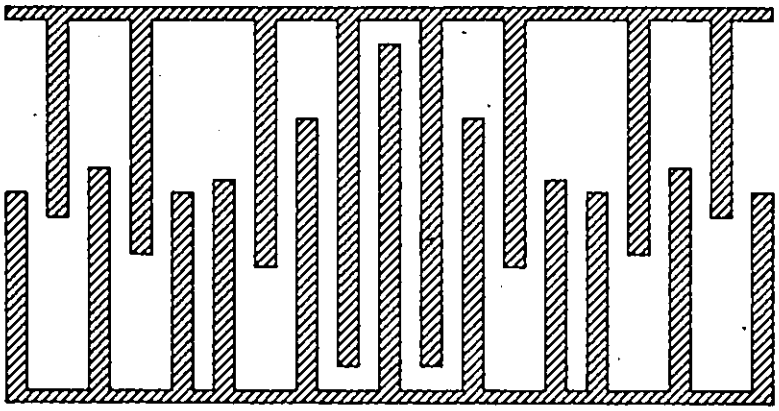

(b)

Figure 1.2: Transducer weighting
(a) Withdrawal weighting
(b) Apodization

1.1.2 Second order effects.

The simplified analysis given above ignores many effects which will degrade the performance, often significantly.

To begin with, the output IDT will not operate as an ideal energy absorber. It can be shown [10] that a lossless three port reciprocal device cannot be matched at all ports simultaneously. As a consequence, if an attempt is made to present a match at the electrical output of the SAW device, the acoustic ports in the output IDT will not be matched, and some of the incident wave will be regenerated. The wave will in turn be partly regenerated by the input IDT, and will reach the output again after further delays of 2τ, 4τ, ..., where τ is the one-path delay. This multipath effect causes ripple with periodicity 2τ in the frequency response of the device [11].

To reduce this effect, known as Triple-Transit-Interference (TTI), the electrical ports must be purposely mismatched at the expense of some additional insertion loss. Since, because of the bidirectionality of the standard IDT, the minimum loss of a SAW device is 6 dB, the mismatching often leads to losses in the order of 20 to 30 dB.

Another effect that degrades performance in a manner very similar to TTI is finger reflection. In this case, a

wave traveling from metalized to non-metalized regions encounters different characteristic impedances and is partially reflected. Unlike TTI, finger reflections are not sensitive to the external load, but depend instead on metal thickness. Because of the finger periodicity of $\lambda_o/2$ at center frequency, reflections add constructively. To combat these reflections, fingers can be split, as illustrated in Figure 1.3. As shown in the figure, the reflections now add destructively [12].

While these second order effects can be predicted quite accurately using one-dimensional models, others require considerably more complicated models, and are usually compensated for through trial and error. These include diffraction [13], bulk wave generation and detection [1], spurious reflections, and electromagnetic feedthrough. This last effect is caused by direct and instantaneous radiation between the input and output ports of the device.

1.2 SAW Device Models.

Most SAW device models in use today are one-dimensional because these require a limited amount of computer time and provide quite usable results. Three of these are in wide use, and are known as the Impulse Response

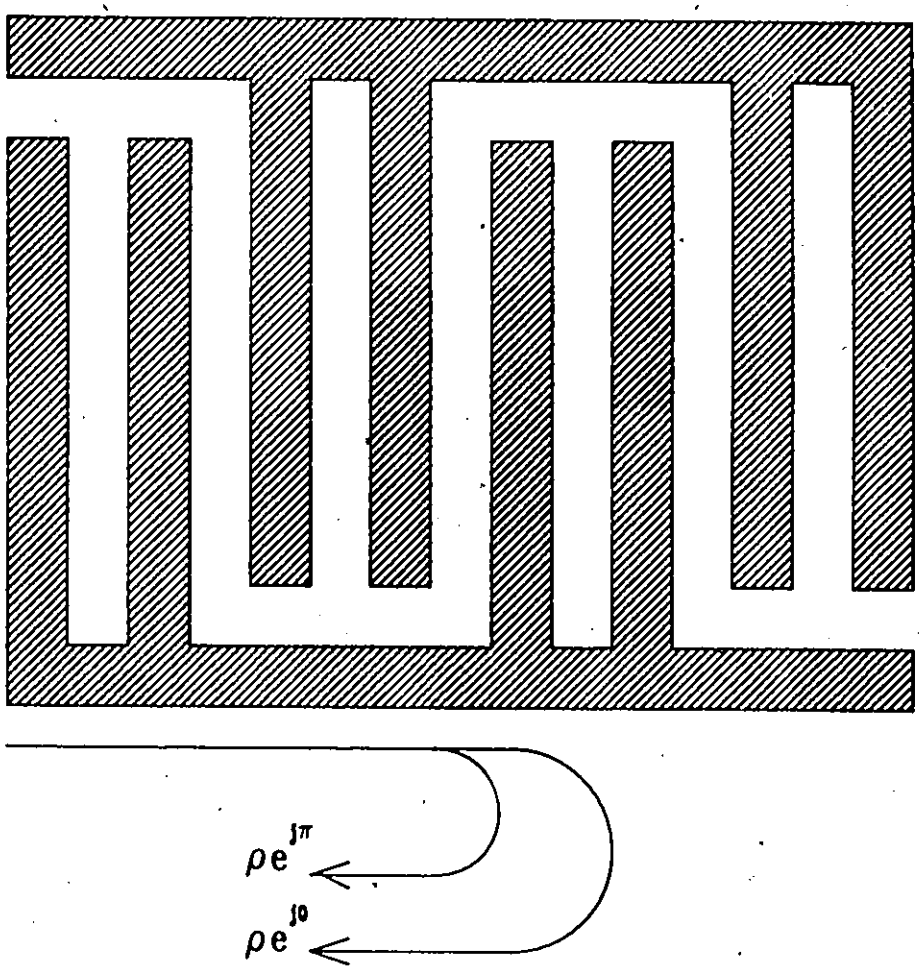

Figure 1.3: Split fingers to combat finger reflections

Model [14], the Generalized Circuit Model [15], and the Coupling-of-Modes (COM) Model [16].

The Impulse Response Model is by far the simplest of the three. It allows the synthesis of the required apodization function for a desired frequency response, but gives no information on second-order effects or insertion loss. Each finger in modeled as a point source, and is related to the desired frequency response by means of the Discrete Fourier Transform. Finite transducer lengths are taken into account either by means of window functions [17], or by using optimization programs such as the Remez Exchange Algorithm [18].

Extensions to the model are necessary for more accurate designs. The distributed nature of the IDT fingers can be incorporated into the design by first pre-distorting the desired frequency response with an element factor [18]. Information on impedances and insertion loss can be included by using Smith's equivalent circuit [19]. With these extensions, the Impulse Response Model has become the most commonly used synthesis tool. For a detailed analysis though, other models provide more information.

The Crossed Field model [15] is based on the equivalent circuit for bulk wave piezoelectric devices, which is shown in Figure 1.4 for one finger. It involves a transmission line representation for the acoustic wave,

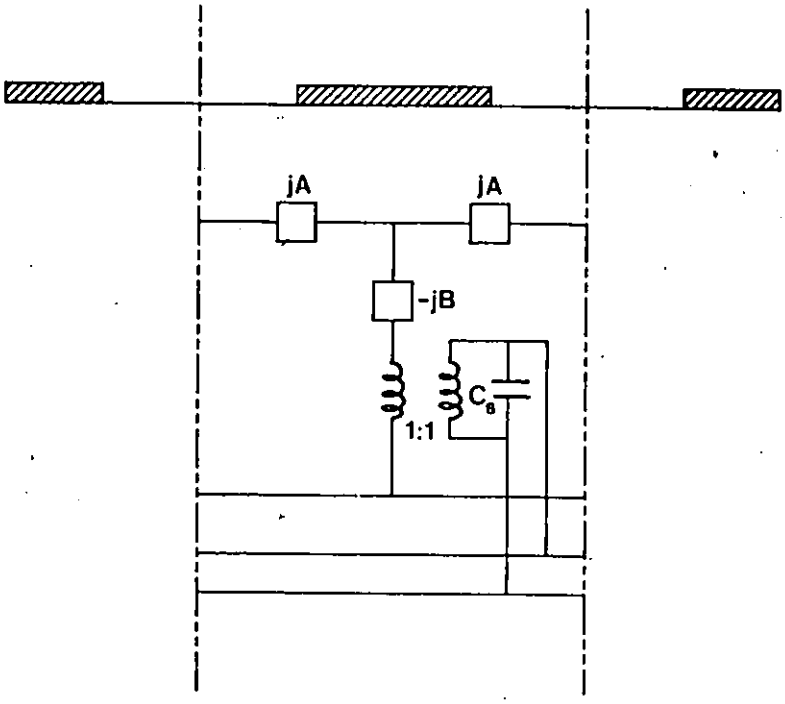

Figure 1.4: Crossed field model circuit

with appropriate electrical coupling circuitry. It can describe finger reflections, regeneration and energy storage with appropriate modifications.

More recently, Coupling-of-Modes theory has gained favour in analyzing structures, particularly resonators and narrow-band low-loss filters. Details will be left to Chapter 2 of this Thesis, but the theory describes the coupling of two waves propagating in opposite directions. It allows the derivation of closed-form expressions for many structures.

1.3 Low Loss SAW Filters.

Conventional (non-resonant) SAW filters have a minimum insertion loss of 6 dB since the bidirectionality of each IDT results in 3 dB loss under matched conditions. To reduce TTI, the filters are usually purposely mismatched, and this results in further losses, often in the order of 20 to 30 dB. While this may be of little consequence in intermediate frequency (IF) stages with signal levels usually in the millivolt range, it precludes the use of SAW filters in processing microvolt level signals found in the front-end of receivers. In these applications, losses must be as low as possible, or the signal will become buried in

noise after subsequent amplification.

The first low-loss SAW filters involved resonator structures [19]. In this case, the energy generated by the transducers is contained in an acoustic cavity by means of reflectors on either side of the transducer, as shown in Figure 1.5. Because the acoustic wave is elliptical with both longitudinal and transversal components which cannot both be reflected efficiently by a single line reflector, a distributed structure is employed. Unfortunately, such structures are only efficient over very narrow frequency bands (< 1%), and the resulting frequency response, while ideal for such uses as feedback components in oscillators, is too narrow band for many applications.

Soon thereafter, techniques involving multi-phase structures were studied [20]. Here, three or four phased signals are used to drive a transducer in such a way as to provide wave generation in the forward direction, and destructive interference in the opposite direction, as shown in Figure 1.6. While these devices provide excellent performance, they require separate matching and phasing circuitry for each input, and their construction is complicated by the required cross-overs. This leads to a considerable increase in cost.

Techniques based on using Multistrip Couplers (MSC) began to appear at about the same time [21]. The MSC is

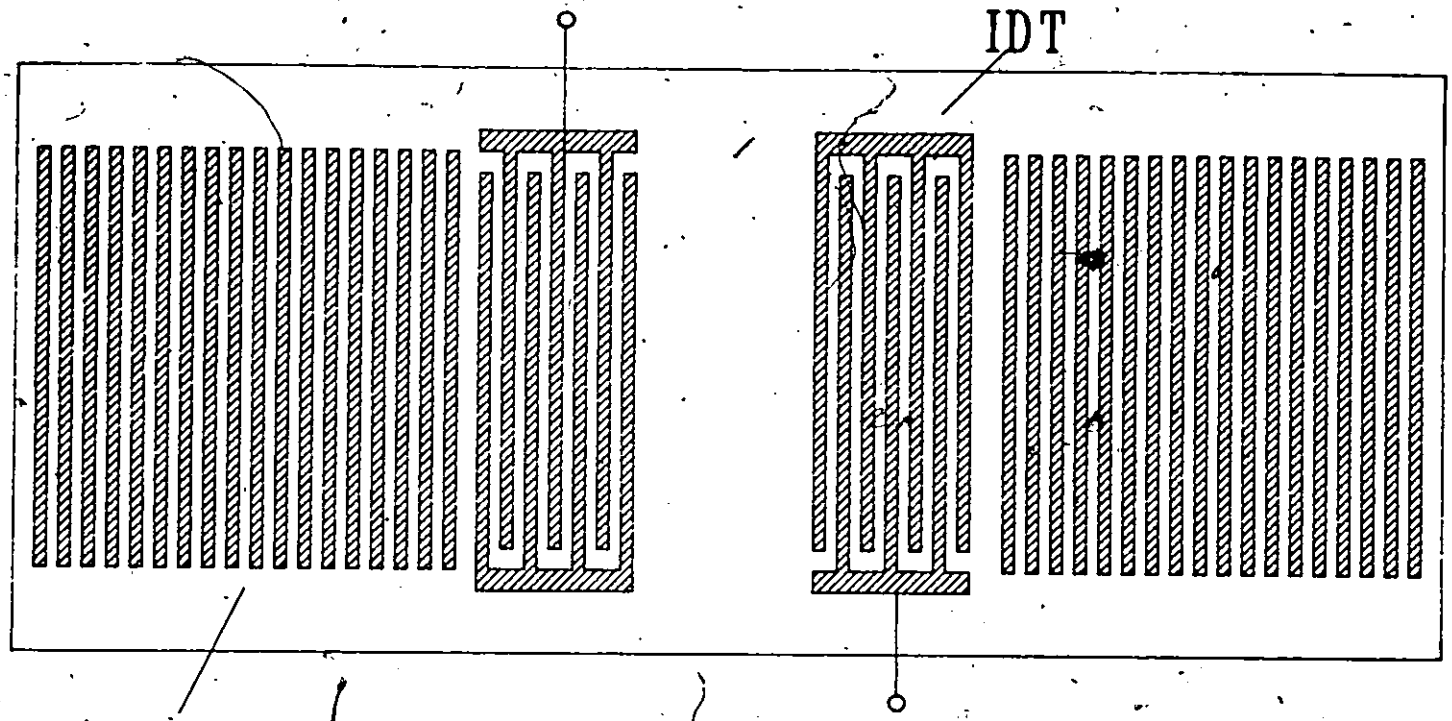

Figure 1.5: SAW resonator

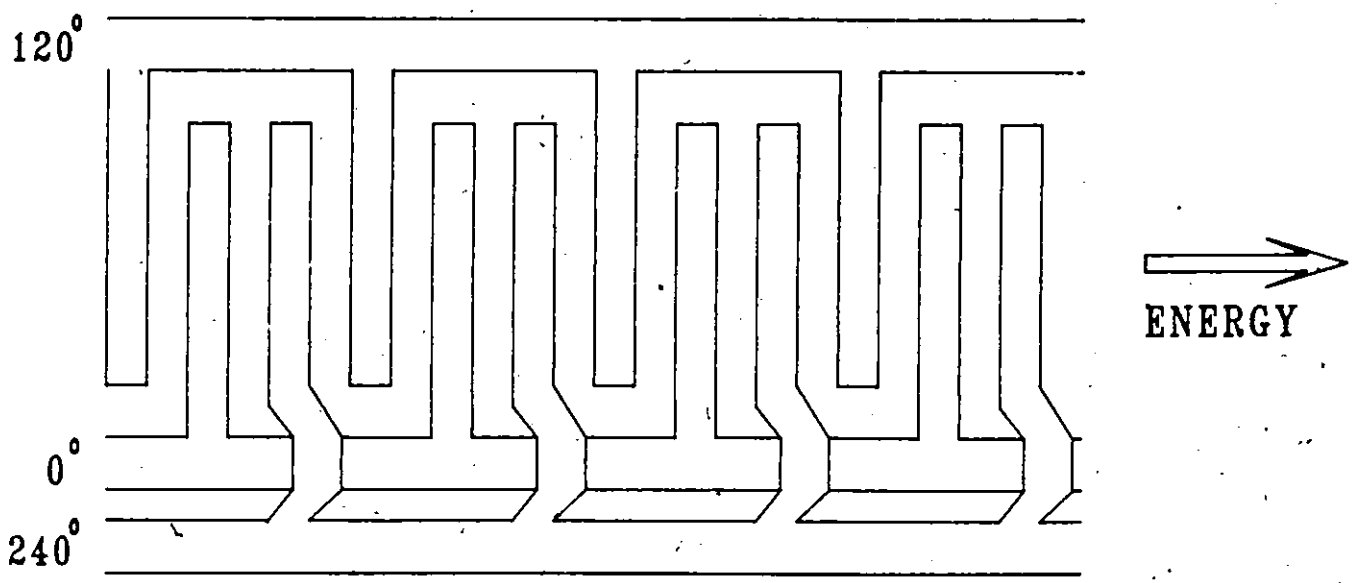

Figure 1.6: Three phase low-loss SAW transducer

usually used as a track changer to reduce the effect of bulk waves or to allow the use of two apodized transducers [22]. If the coupler is made to be half the length, it can also operate as a 3 dB power splitter. By folding one such splitter into a U shape, as shown in Figure 1.7, it can be used to redirect energy, which would otherwise be lost, towards the output transducer, without significantly reducing the bandwidth of the filter. Similar techniques use an MSC in a ring configuration [23]. These techniques, however, only work on substrates with a high electro-acoustic coupling constant and require a significantly larger substrate surface area.

More recently, techniques using finger reflections to promote unidirectionality have begun to appear [24]. By displacing centers of reflection, the reflected waves can be made to add to the generated waves in the forward direction and to partially cancel the waves in the reverse direction. These techniques have been shown to result in device losses of less than 4 dB and bandwidths of up to about 2%.

The last technique, and the subject of investigation in this Thesis, was suggested some years ago [25], and involves capturing the generated waves by placing an output transducer on either side of the input, as shown in Figure 1.8. To capitalize on the effect, several input and several output transducers can be used. In this latter case, all

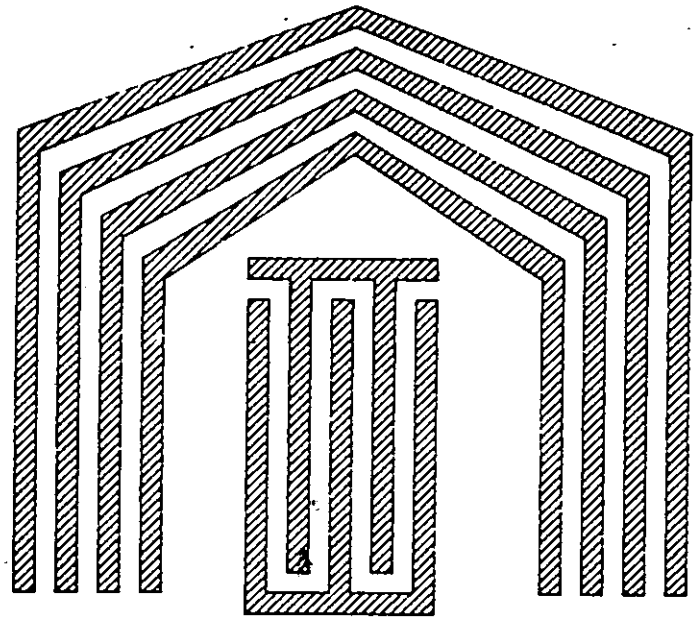

Figure 1.7: Multristrip coupler as a SAW reflector

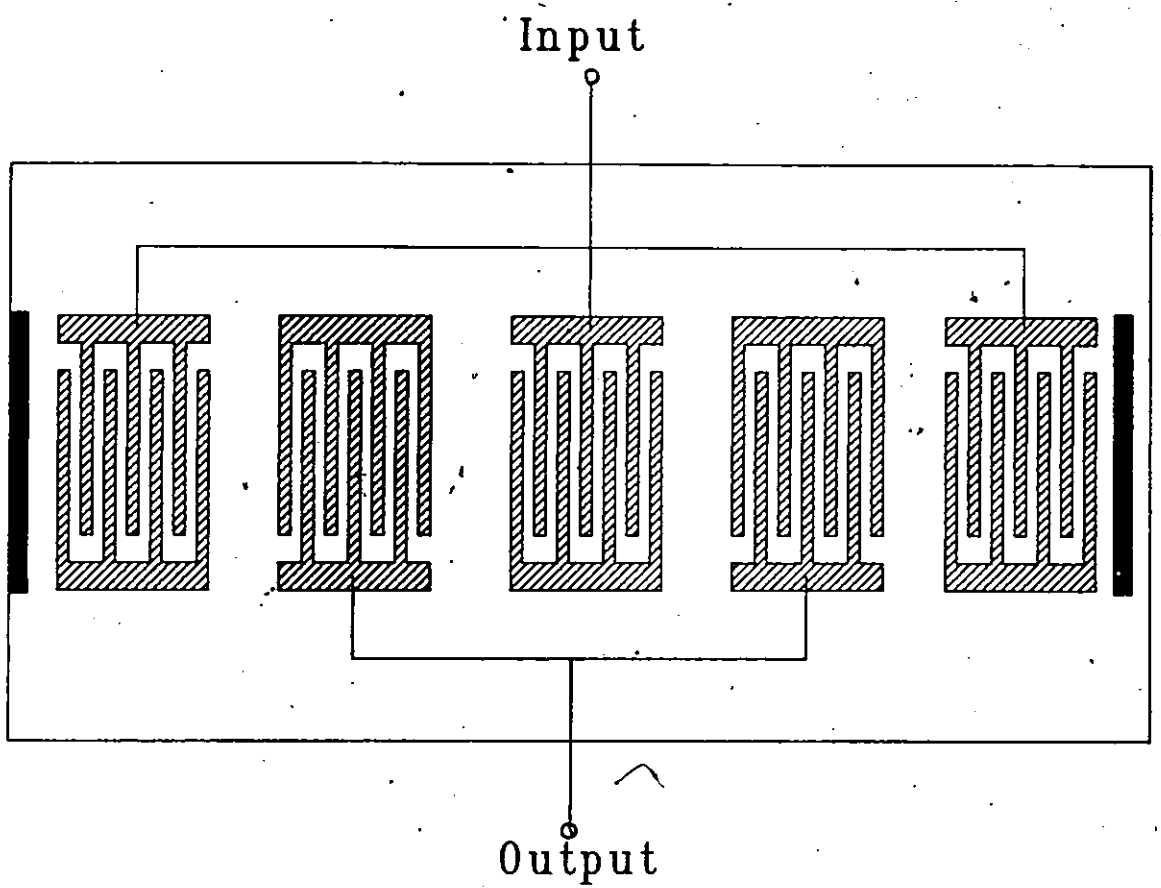

Figure 1.8: The Interdigitated Interdigital Transducer

output transducers are subject to waves coming into both acoustic ports, and, by reciprocity, should absorb all the energy if it is properly matched. The only energy lost therefore would be at the end input transducers, which lose half their generated energy. The theoretical minimum insertion loss of this Interdigitated Interdigital Transducer (IIDT) structure is

$$IL = 10 \log((N_{out} / N_{in}) \quad dB. \qquad (1.3.1)$$

where N_{in} in the number of input transducers and N_{out} is the number of output transducers.

1.4 Scope and Outline of the Thesis.

Very little work has been done on the Interdigitated Interdigital Transducer structure. While sample responses of filters based thereon have been published, no careful analysis and modelling has been done to date.

In the past, many models and analysis tools have been proposed in the literature. For the most part, however, a separate approach has been taken for each SAW device structure to be studied. This results in a multitude of analysis techniques, each of which must often be tailored

to the device currently under study.

It is felt by the author that a better approach would be to divide the SAW device into sections (IDTs, reflector arrays, spaces, etc...), each of which would be modeled for its effect on the surface waves. Given the structure to be investigated, a computer program would find the frequency response and display it, with no need for any programming code to be written.

Chapter 2 describes the theory that is used in the SAW device software package, the listing for which is given in Appendix C. It is based on a Coupling-of-Modes (COM) approach that models each component as a transmission matrix for the two counter-rotating waves travelling in opposite directions.

In Chapter 3, the theory is used to describe the operation of the Interdigitated Interdigital Transducer (IIDT) filter. While this has been proposed as a technique to achieve low losses, the author is not aware of any prior modeling done to explain its performance.

Chapter 4 describes experiments done on IIDT low loss filters as well as on IIDT comb filters and frequency hopping oscillator based thereon.

Finally, Chapter 5 presents the conclusions reached during the course of these studies and suggests future areas of investigation.

CHAPTER 2

COUPLING-OF-MODES THEORY

2.0 Introduction.

Coupling-of-Modes (COM) theory was originally developed to analyze the performance of general coupled systems [26]. Kogelnik [27] applied the theory to the study of thick hologram gratings. Yariv [28] subsequently showed that the theory could be used to study coupling between any two optical modes (whether of the same frequency or not) due to an arbitrary perturbation.

The similarities between integrated optics and SAW devices did not go unnoticed. In particular, COM theory was found to be very effective in the study of SAW reflector arrays used in resonators [16] and Reflective Array Compressors (RAC) [29]. More recently, Chen and Haus [30], in an excellent paper, developed expressions for all the required parameters from variational principles.

In all of these studies, only narrowband regions

were studied because many of the simplifications made during the derivation rendered the analysis invalid over wide ranges. This was of little concern because the studies were limited to those of narrowband resonator structures. More recently, the theory has been shown to be the best, if not the only, method of studying certain narrow band, non-resonant structures [31]. Much work is still needed to increase the bandwidth of low-loss SAW filters.

In this chapter, COM expressions will be derived for many of the structures encountered in SAW devices. An attempt will be made to follow a logical sequence in the derivations, beginning with SAW delay sections, followed by reflector arrays and ending with transducers. It will be seen that, in the case of transducers, a deviation from strict COM theory will be necessary. The expressions will be found to be very useful in analyzing many of the low-loss SAW structures.

2.1 Coupling of Modes Theory.

The basis of the theory involves the propagation of two waves, say S and R, in a medium. These waves could be of arbitrary frequencies and propagation direction, but for our purposes we will assume that the waves are propagating

in opposite directions and are of the same frequency. In this case, the waves could be written

$$R = R(x)\ e^{-j\beta x} \qquad (2.1.1)$$

$$S = S(x)\ e^{j\beta x} \qquad (2.1.2)$$

where an $e^{j\omega t}$ dependence is assumed. Here β is the propagation constant in the x direction.

In the absence of perturbations in the medium, these two waves, or modes, would propagate without incurring mutual interaction. Should there be a perturbation, such as a groove or an aluminium strip on the surface of a SAW substrate, there will be coupling of energy from one mode to the other (see Figure 2.1). Coupling-of-Modes theory is a formalism that describes these interactions.

The aim is to achieve a set of transmission matrices to describe the various SAW structures in a device. The waves on either side of the i-th section will be described by the equation

$$\begin{bmatrix} R \\ S \end{bmatrix}_{i-1} = T_i \cdot \begin{bmatrix} R \\ S \end{bmatrix}_i \qquad (2.1.3)$$

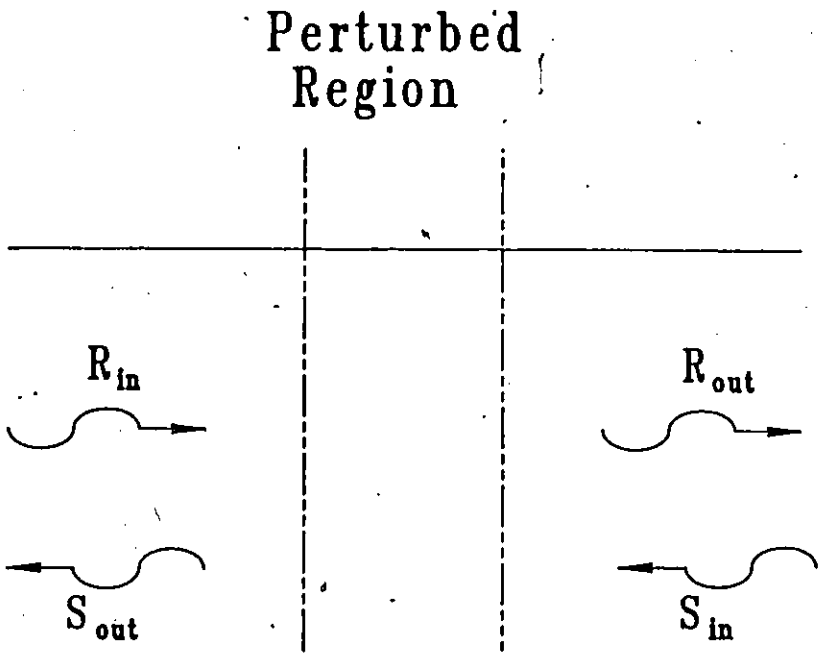

Figure 2.1: Coupling-of-modes in a perturbed medium

where T_i is the transmission matrix of the i-th section. By cascading all the transmission matrices, the SAW waves on either end of an N-section device as shown in Figure 2.2 can be described by

$$\begin{bmatrix} R \\ S \end{bmatrix}_0 = T \cdot \begin{bmatrix} R \\ S \end{bmatrix}_N \qquad (2.1.4)$$

where

$$T = \prod_{i=1}^{N} T_i \qquad (2.1.5)$$

2.2 Delay Sections.

In a lossless delay section, each wave incurs a phase shift, with no interaction between the two propagating waves. This leads directly to the transmission matrix

$$T_i = \begin{bmatrix} e^{j\beta d} & 0 \\ 0 & e^{-j\beta d} \end{bmatrix} \qquad (2.2.1)$$

where d is the length of the delay section.

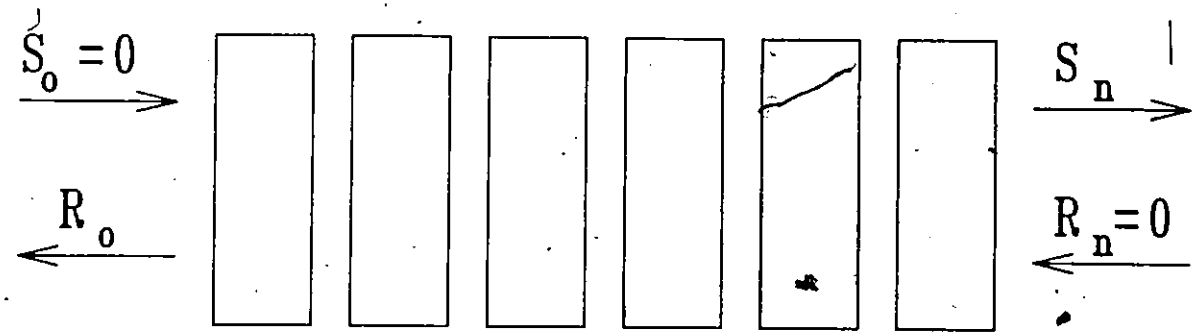

$$\begin{pmatrix} 0 \\ R_o \end{pmatrix} = \prod T_i \begin{pmatrix} S_n \\ 0 \end{pmatrix} \quad ($$

Figure 2.2: SAW device as a sequence of sections

2.3 Reflector Arrays.

This section will present the derivation of a closed form expression for reflector arrays. Unlike iterative techniques that traverse the arrays strip by strip, COM theory will allow the relationship of the waves at the both ends of the structure to be computed directly.

In order to understand the assumptions that are made in the COM formalism, it is best to derive the transmission matrix of a reflector array from first principles. In this case, we shall begin with the general wave equation

$$\partial^2 E/\partial x^2 + k^2 E = 0 \qquad (2.3.1)$$

where E is a wave propagating in the x direction and k is the propagation constant. If we now focus our attention on Surface Acoustic Waves (SAW) and assume a propagation loss α and a variation in the wave velocity of the form

$$v(x) = v_o + v_1 \cos(2\beta_o x) \qquad (2.3.2)$$

where

$$\beta_o = n\,\omega_o / v_o \qquad (2.3.3)$$

ω_o is the resonant angular frequency

v_o is the mean SAW velocity

v_1 is the SAW velocity variation

This corresponds to a periodic wave velocity variation in the propagation direction. If this velocity variation can be assumed to be small, i.e.,

$$v_1 << v_o \tag{2.3.4}$$

then it can be shown [27] that

$$k^2 = \beta^2 + 2j\alpha\beta + 4\kappa\beta \cos(2\beta_o x) \tag{2.3.5}$$

where the coupling coefficient κ

$$\kappa = \pi v_1 / \lambda_o \tag{2.3.6}$$

and λ_o is the resonant acoustic wavelength. Now assume that the total wave E(x) given in (2.3.1) is composed of the two waves R and S

$$E(x) = R(x)\ e^{-j\beta_o x} + S(x)\ e^{j\beta_o x} \tag{2.3.7}$$

near resonance. Then, replacing (2.3.7) into (2.3.1)

$$\partial^2 E/\partial x^2 + k^2 E = R'' e^{-j\beta_o x} - R' 2j\beta_o e^{-j\beta_o x} + R$$

$$(\beta^2 - \beta_o^2 + 2j\alpha\beta + 2\kappa\beta(e^{j2\beta_o x} + e^{-j2\beta_o x})) e^{-j\beta_o x}$$

$$+ S'' e^{j\beta_o x} + S' 2j\beta_o e^{j\beta_o x} + S$$

$$(\beta^2 - \beta_o^2 + 2j\alpha\beta + 2\kappa\beta(e^{j2\beta_o x} + e^{-j2\beta_o x})) e^{j\beta_o x}$$

$$= 0 \qquad \ldots(2.3.8)$$

where the prime symbol represents derivation with respect to distance. If it is assumed that the variations in R and S are slow (i.e., weak coupling), then we can ignore the R" and the S" terms. Further, if we consider only the terms containing $e^{j\beta_o x}$ and $e^{-j\beta_o x}$ separately, ignoring the terms with higher exponential powers, (2.3.8) can be reduced to the coupled equations

$$\begin{aligned} -R' (2j\beta_o) + R (\beta^2 - \beta_o^2 + 2j\alpha\beta) + S (2\kappa\beta) &= 0 \\ S' (2j\beta_o) + S (\beta^2 - \beta_o^2 + 2j\alpha\beta) + R (2\kappa\beta) &= 0 \end{aligned} \qquad (2.3.9)$$

This can be rewritten in a simpler form, putting $\beta/\beta_o \approx 1$,

$$\begin{aligned} -R' + (\alpha - j\delta)\ R &= j\kappa\ S \\ S' + (\alpha - j\delta)\ S &= j\kappa\ R \end{aligned} \qquad (2.3.10)$$

where

$$\delta = (\beta^2 - \beta_o^2)\ /\ 2\beta_o \qquad (2.3.11)$$

Uncoupling equation (2.3.10), we obtain

$$\begin{aligned} R'' - (\kappa^2 + (\alpha - j\delta)^2)\ R &= 0 \\ S'' - (\kappa^2 + (\alpha - j\delta)^2)\ S &= 0 \end{aligned} \qquad (2.3.12)$$

Solutions to (2.3.12) are of the form

$$\begin{aligned} R(x) &= r_1\ e^{\gamma x} + r_2\ e^{-\gamma x} \\ S(x) &= s_1\ e^{\gamma x} + s_2\ e^{-\gamma x} \end{aligned} \qquad (2.3.13)$$

where

$$\gamma^2 = \kappa^2 + (\alpha - j\delta)^2 \qquad (2.3.14)$$

is the propagation constant

r_1, r_2, s_1, s_2 are constants to be evaluated.

Disregarding the loss term α for the time being, equation (2.3.14) yields complex values for γ when $|\delta| > |\kappa|$, and real values otherwise. Recalling from equation (2.1.1) that R and S have an assumed $\exp(\pm j\beta x)$ term, equations (2.3.13) indicate that the waves propagate as $\exp(\pm(j\beta \pm \gamma)x)$. The plot of the imaginary part of the propagation constant, as given in Figure 2.3, indicates that there is a reflection band of width 2κ, centered at the Bragg frequency, for which γ is real. Outside this band, this dispersive behaviour disappears and the propagation constants approach those of unperturbed waves. This behaviour explains the relationship between κ and the reflection bandwidth of the reflector array.

This is intuitively satisfying because as κ is increased, each reflector becomes more efficient, and the reflection impulse response of the array becomes shorter. The Fourier transform of the latter corresponds to the frequency response of the reflection coefficient, which then contains a wider main lobe.

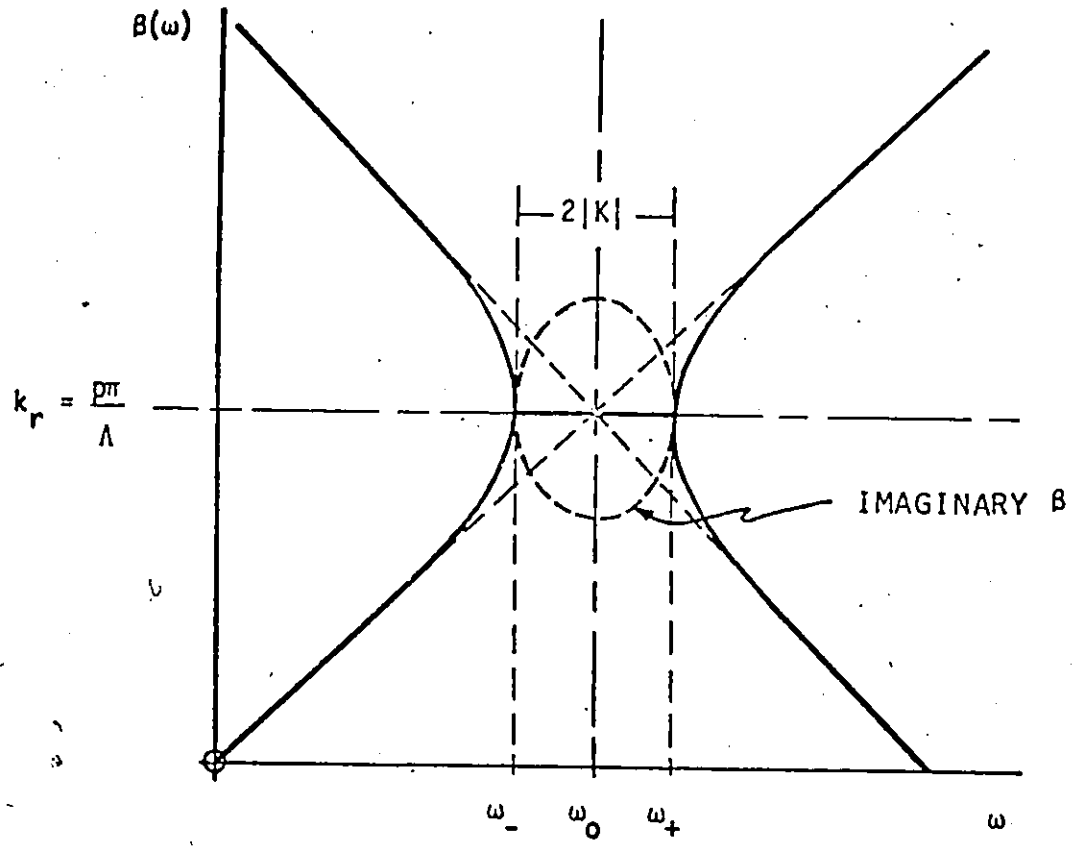

Figure 2.3: Dispersion of propagation constant in reflectors [29]

We are interested in the coefficients t_{ij} of the transmission matrix T , given by

$$t_{11} = R(d) \;/\; R(0) \quad \text{and} \quad t_{21} = S(d) \;/\; R(0) \qquad \text{for } S(0) = 0$$

$$t_{12} = R(d) \;/\; S(0) \quad \text{and} \quad t_{22} = S(d) \;/\; S(0) \qquad \text{for } R(0) = 0 \qquad (2.3.15)$$

where R(0), R(d), S(0) and S(d) are illustrated in Figure 2.4 and d is the array length. Replacing (2.3.13) into the first equation in (2.3.10) results in

$$-(\gamma r_1 e^{\gamma x} - \gamma r_2 e^{-\gamma x}) + (\alpha - j\delta)\,(r_1 e^{\gamma x} + r_2 e^{-\gamma x}) = j\kappa\,(s_1 e^{\gamma x} + s_2 e^{-\gamma x}) \qquad \ldots(2.3.16)$$

Collecting terms with the same exponentials gives

$$\begin{aligned} (\gamma - \alpha + j\delta)\; r_1 + j\kappa\, s_1 &= 0 \\ (-\gamma - \alpha + j\delta)\; r_2 + j\kappa\, s_2 &= 0 \end{aligned} \qquad (2.3.17)$$

Impose now the conditions S(0) = 0 and R(0) = 1 on (2.3.17), which correspond to an outgoing wave of magnitude 1 and no incoming wave at the end of the array, and solve for r_1

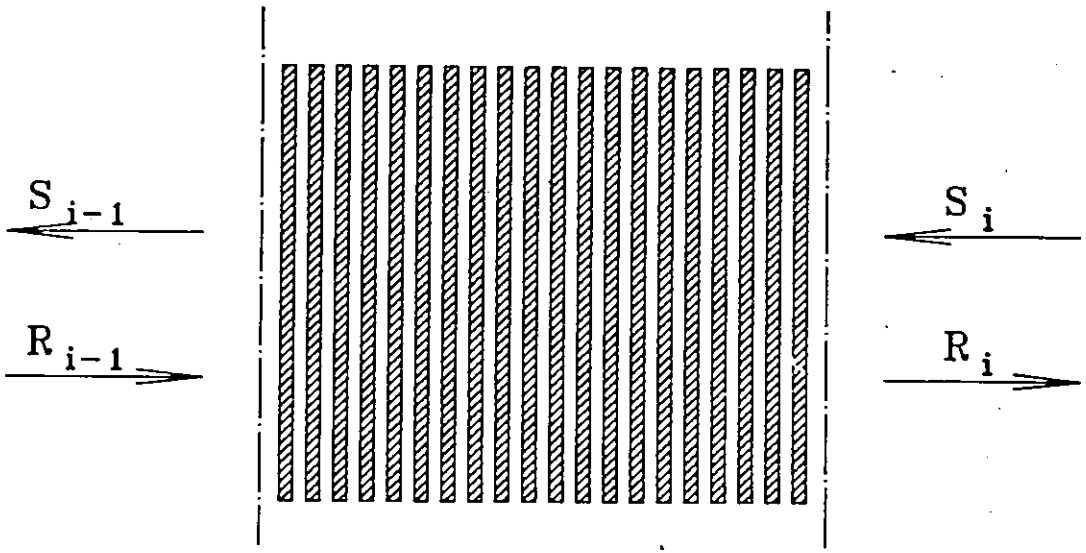

$$\begin{pmatrix} R \\ S \end{pmatrix}_{i-1} = \begin{pmatrix} & T_i & \end{pmatrix} \begin{pmatrix} R \\ S \end{pmatrix}_i$$

Figure 2.4: Waves at either end of reflector array

and r_2. This assumption results in

$$r_1 = 0.5 + \alpha/2\gamma - j\ \delta/2\gamma$$

$$r_2 = 0.5 - \alpha/2\gamma + j\ \delta/2\gamma \qquad (2.3.18)$$

so that applying (2.3.18) to (2.3.13) gives the desired result

$$t_{11} = R(d)/R(0) = \cosh(\gamma d) + (\alpha/\gamma - j\ \delta/\gamma)\ \sinh(\gamma d) \qquad \ldots(2.3.19)$$

If we solve (2.3.17) for s_1 and s_2,

$$s_1 = -\ s_2 = j\kappa/2\gamma \qquad (2.3.20)$$

and substitute in (2.3.13), we obtain

$$t_{21} = S(d)/R(0) = j\kappa/\gamma\ \sinh(\gamma d). \qquad (2.3.21)$$

If we impose now the conditions $S(0) = 1$ and $R(0) = 0$ on equation (2.3.17) and follow the same last few steps, we obtain

$$t_{12} = R(d)/S(0) = -j\kappa/\gamma\ \sinh(\gamma d) \qquad (2.3.22)$$

$$t_{22} = S(d)/S(0) = \cosh(\gamma d) - (\alpha/\gamma - j\,\delta/\gamma)\,\sinh(\gamma d) \quad \ldots(2.3.23)$$

All that is now required is to account for the phase shift due to the propagation through the structure. With this phase shift included, the total transmission matrix for a reflector array is given by

$$T = \begin{bmatrix} (\cosh(\gamma d) + (\alpha/\gamma - j\delta/\gamma)\,\sinh(\gamma d))\, e^{j\beta_o d} & -j\kappa/\gamma\,\sinh(\gamma d)\, e^{j\beta_o d} \\ j\kappa/\gamma\,\sinh(\gamma d)\, e^{-j\beta_o d} & (\cosh(\gamma d) - (\alpha/\gamma - j\delta/\gamma)\,\sinh(\gamma d))\, e^{-j\beta_o d} \end{bmatrix} \quad \ldots(2.3.24)$$

This agrees with the transmission matrix given by Cross and Schmidt [16] in a slightly different form. The values for κ and α are usually found experimentally, but Chen suggests a theoretical approach [30].

Throughout the derivation of the transmission matrix of the whole reflector array given above, it has been assumed that the frequency of operation is very close to synchronism. This allows a simplification of the expression to the point that a closed form expression is possible for

the whole array. It has also been assumed that the instantaneous SAW velocity is cosinusoidal in variation, while the physical structure would instead suggest a stepped velocity, with the step occurring at the boundary of metalized and non-metalized regions. In the case of reflector arrays, these assumptions are valid because the low coupling leads very narrow band operation.

It would be interesting to compare at this point the frequency response of the reflection coefficient of a reflector array as computed by this COM model to one based on an iterative process where the effect of each metal strip is considered. This would show how closely the narrow-band COM formulae match a more intuitive approach.

Probably the simplest method of visualizing the effect of a single reflector strip is to consider a section of transmission line of impedance Z_o (the unmetalized region) of length $\lambda_o/8$ followed by a section with impedance Z_m (the metalized region) of length $\lambda_o/4$, again followed by a length with impedance Z_o and length $\lambda_o/8$, as illustrated in Figure 2.5. At each boundary, part of the incident wave will be reflected. The reflection coefficient ρ in these cases would be

$$\rho = \pm(Z_m - Z_o) \; / \; (Z_m + Z_o) \qquad (2.3.25)$$

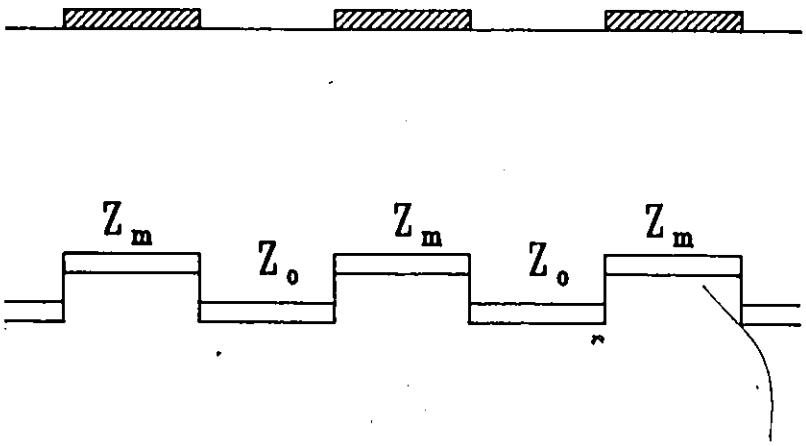

Figure 2.5: Reflector array modelled as a sequence of transmission lines

at the boundaries of the metalized region. The leading + sign in (2.3.25) corresponds to the unmetalized to metalized transition, while the - sign corresponds to the metalized to unmetalized transition.

By taking into account the appropriate phase shifts, and imposing conservation of energy, the total transmission matrix T_r for one reflector strip, including both boundaries, is given by

$$T_r = 1 / 1 - \rho^2 \begin{bmatrix} \rho^2 + e^{j\beta\lambda/2} & \rho - \rho\, e^{j\beta\lambda/2} \\ \rho - \rho\, e^{-j\beta\lambda/2} & \rho^2 + e^{-j\beta\lambda/2} \end{bmatrix} \quad \ldots(2.3.26)$$

where a metalization ratio of $\eta = 0.5$ is assumed.

A comparison of the frequency responses of the reflection coefficient based on these two models is illustrated in Figure 2.6. At frequencies close to resonance, both approaches agree with one another. As the frequency offset increases, the positions of the sidelobes begin to deviate, even though the relative magnitudes are quite similar. The closed form expressions obtained from COM theory are evidently more computationally efficient.

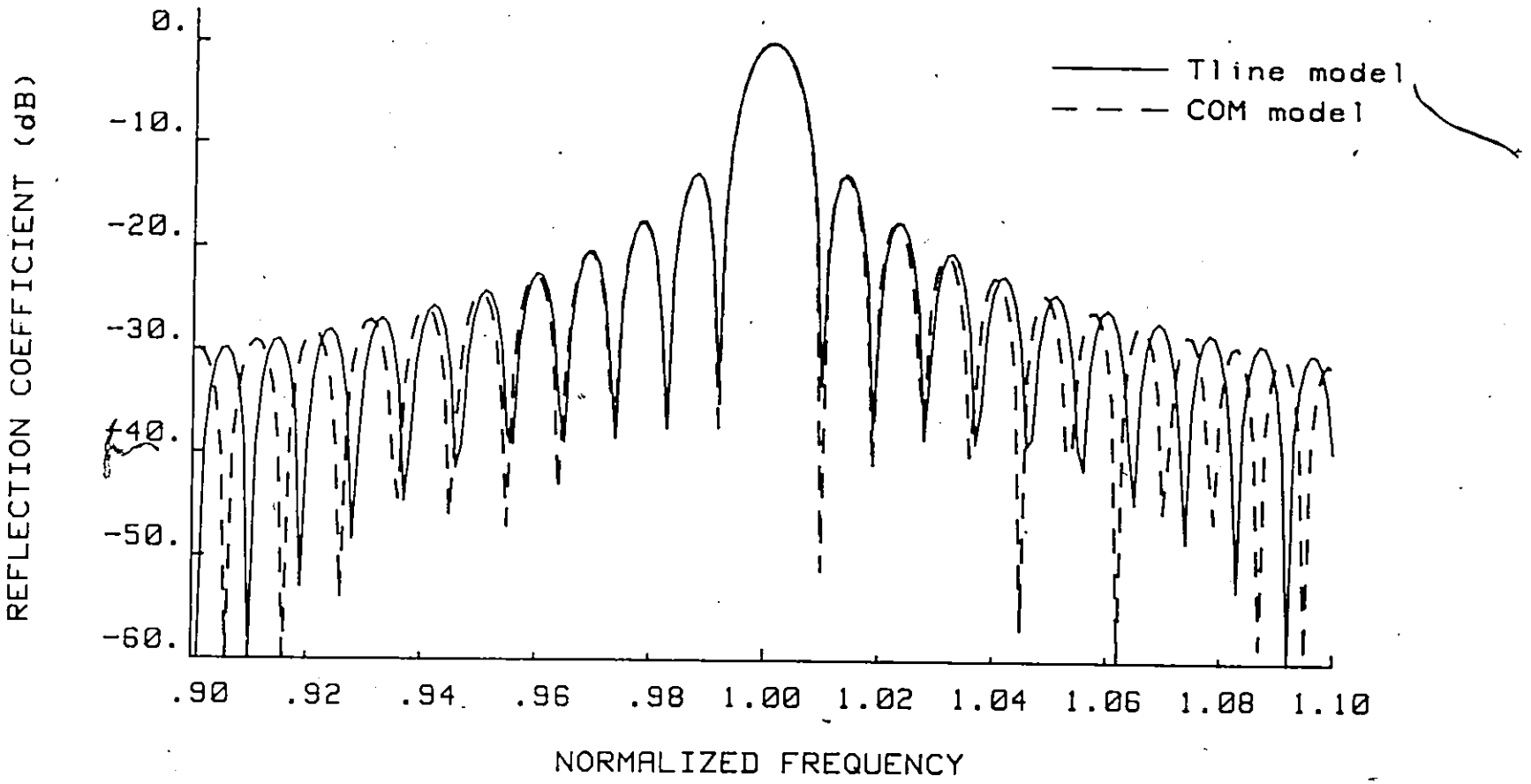

Figure 2.6: Comparison of transmission line model and COM model for reflector array reflection coefficient

2.4 Interdigital Transducers.

Interdigital transducers differ from reflectors in that, in addition to wave reflections, we now also have wave generation within the metal strip due to an applied voltage. Instead of a two-port structure, this results in a three-port one (two acoustic and one electric), and the transmission model thereby requires a 3 x 3 matrix.

The first approach that will be taken assumes that the IDT can be modeled as a superposition of a reflector array, accounting for any internal finger reflections, and a point generator positioned at the finger center, with a frequency response corresponding, as will be seen shortly, to the Fourier Transform of the charge distribution on a finger.

Consider the sketch of an IDT finger shown in Figure 2.7. For this case, the COM equations (2.3.10) become

$$\begin{aligned} -R' + (\alpha - j\delta)\, R &= j\kappa\, S + j\mu\, V \\ S' + (\alpha - j\delta)\, S &= j\kappa\, R + j\upsilon\, V \end{aligned} \qquad (2.4.1)$$

where V is the voltage applied to the electrode and μ and υ are coupling constants. Now if we let I' be the incremental current drawn from the electrode, then

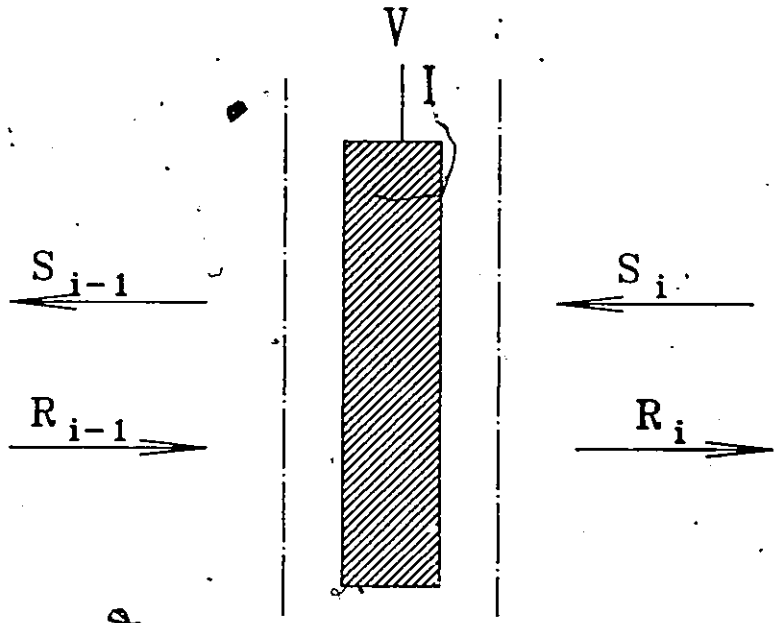

$$\begin{pmatrix} R \\ S \\ I \end{pmatrix}_{i-1} = \begin{pmatrix} \quad T_i \quad \end{pmatrix} \begin{pmatrix} R \\ S \\ V \end{pmatrix}_i$$

Figure 2.7: Matrix representation of IDT finger

$$I' = j\zeta R + j\chi S + j\omega C V \qquad (2.4.2)$$

where C is the incremental capacitance of the transducer and ζ and χ are two other coupling constants. The four unknown parameters μ, υ, ζ and χ are in fact related [32]. Applying conservation of energy [30], the net acoustic power increase must equal the induced electrical power

$$d|R|^2/dx - d|S|^2/dx = 1/2\ (V\ dI^*/dx + V^*\ dI/dx) \qquad ...(2.4.3)$$

where V is the root mean square voltage, I is the root mean square current, and the asterisk indicates the complex conjugate. Applying (2.4.3) to (2.4.1) and (2.4.2) requires that

$$\zeta = -2\mu^* \qquad (2.4.4)$$

$$\chi = -2\upsilon^*$$

If we assume that we are dealing with a lossless reciprocal system, we can time-reverse all signals by taking the complex conjugate of the variables in (2.4.1) and (2.4.2). The resulting excitations must also be solutions to the system of equations, which requires that

$$\upsilon = \mu^* \tag{2.4.5}$$

Chen showed that, in fact, μ is real [30], so that υ and μ are equal. Equations (2.4.1) and (2.4.2) can then be rewritten

$$\begin{aligned} -R' + (\alpha - j\delta)\, R &= j\kappa\, S + j\mu\, V \\ S' + (\alpha - j\delta)\, S &= j\kappa\, R + j\mu\, V \\ I' &= -2j\mu\, R - 2j\mu\, S + j\omega C\, V \end{aligned} \tag{2.4.6}$$

These equations can now be uncoupled in the same manner as before

$$\begin{aligned} R'' - (\kappa^2 + (\alpha - j\delta)^2)\, R &= (\kappa\mu - j\mu(\alpha - j\delta))\, V \\ S'' - (\kappa^2 + (\alpha - j\delta)^2)\, S &= (\kappa\mu - j\mu(\alpha - j\delta))\, V \end{aligned} \tag{2.4.7}$$

This is a nonhomogeneous form of equations (2.3.12) The solutions are

$$R = r_1 e^{\gamma x} + r_2 e^{-\gamma x} - (\kappa\mu - j\mu(\alpha - j\delta))/\gamma^2 V$$

$$S = s_1 e^{\gamma x} + s_2 e^{-\gamma x} - (\kappa\mu - j\mu(\alpha - j\delta))/\gamma^2 V \qquad (2.4.8)$$

Unfortunately, it is not possible to obtain closed form transmission matrices for the general case based on (2.4.8). Hartmann et al. [32] derived an expression for the input conductance of an unweighted transducer using a slightly different formulation but, for the purposes of this Thesis, a general form not restricted to unapodized IDTs was sought.

One approach that is conceptually simple is based on the alternate analysis given in Section 2.3 for reflector arrays and involves replacing the continuous coupling with points. Here an IDT finger is modelled as two centers of reflection at the edges and one center of transduction, all separated by transmission sections. This is illustrated in Figure 2.8. This approach allows control over metalization ratios in the model. To compute the transmission matrix of the finger, it can be divided into two cascaded sections of half the length. The scattering matrices S_1 of the left half of the finger and S_2 of the right half are easily seen to be

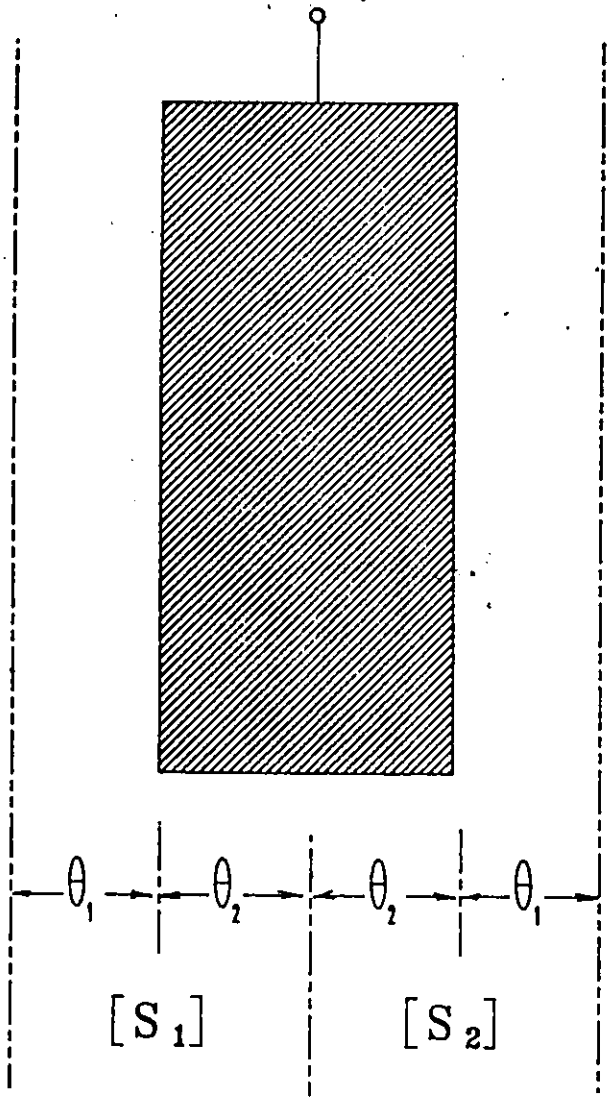

Figure 2.8: IDT finger with SAW reflections at edges and generation at center

$$S_1 = \begin{bmatrix} \rho\, e^{-j2\theta_1} & \sqrt{1-\rho^2}\, e^{-j(\theta_1+\theta_2)} & 0 \\ \sqrt{1-\rho^2}\, e^{-j(\theta_1+\theta_2)} & -\rho\, e^{-j2\theta_2} & 0 \\ 0 & 0 & 0 \end{bmatrix} \quad (2.4.9)$$

and

$$S_2 = \begin{bmatrix} -\rho\, e^{-j2\theta_2} & \sqrt{1-\rho^2}\, e^{-j(\theta_1+\theta_2)} & j\mu \\ \sqrt{1-\rho^2}\, e^{-j(\theta_1+\theta_2)} & \rho\, e^{-j2\theta_1} & j\mu\, e^{-j(\theta_1+\theta_2)} \\ -j2\mu & -j2\mu\, e^{-j(\theta_1+\theta_2)} & j\omega C \end{bmatrix}$$

...(2.4.10)

where θ_1 and θ_2 are as defined in Figure 2.8 and μ is the electrical to acoustic coupling coefficient. Any weighting associated with the finger can be included in this last parameter.

Converting these two scattering matrices to transmission matrices according to the formulae in Appendix A, and then multiplying them, results in the transmission matrix for one finger. Its coefficients are

$$t_{11} = 1/(1-\rho^2)\ (e^{j2(\theta_1+\theta_2)} - \rho^2\ e^{j2(\theta_1-\theta_2)})$$

$$t_{12} = -j2\rho/(1-\rho^2)\ \sin(2\theta_2)$$

$$t_{13} = j\mu/(1-\rho^2)(e^{j(\theta_1+\theta_2)} + \rho\sqrt{1-\rho^2}\ e^{j(\theta_1-\theta_2)} + \rho^2\ e^{j(\theta_1-3\theta_2)})$$

$$t_{21} = j2\rho/(1-\rho^2)\ \sin(2\theta_2)$$

$$t_{22} = 1/(1-\rho^2)\ (e^{-j2(\theta_1+\theta_2)} - \rho^2\ e^{-j2(\theta_1-\theta_2)})$$

$$t_{23} = j\mu/(1-\rho^2)(\rho e^{-j(\theta_1-\theta_2)} + \sqrt{1-\rho^2}\ e^{-j(\theta_1+\theta_2)} + \rho\ e^{-j(\theta_1+3\theta_2)})$$

$$t_{31} = -j2\mu/\sqrt{1-\rho^2}\ e^{j(\theta_1+\theta_2)}$$

$$t_{32} = j2\mu\ (-e^{-j(\theta_1+\theta_2)} + \rho/\sqrt{1-\rho^2}\ e^{-j(\theta_1-\theta_2)})$$

$$t_{33} = j\omega C - 2\mu^2/\sqrt{1-\rho^2}$$

...(2.4.11)

For design purposes, these expressions have been found to be computationally efficient, while providing useful information on the effect of changing design parameters. Their major limitation is due to the assumption that existing surface waves are sampled by the transducer, with no energy absorption. This will not allow an estimate of

the insertion loss of a SAW filter.

The value of the parameter μ will now be considered. In doing so, it will be seen that an alternate set of expressions will result that provide a more accurate description of SAW transducers.

A simple approach would be to approximate the applied voltage to a delta function at the electrode center, in a manner reminiscent of the impulse response model used some years ago by Hartmann et al. [14]. This would, of course, lead to an flat frequency response for each finger, and all that would need to be considered would be the array factor of the whole transducer.

This simplifying assumption, however, does not hold over fractional bandwidths of more than a few percent [34]. When charges of opposite polarity are applied to two adjacent electrodes, the charge on each finger will cover the whole width of the finger, with a concentration occuring at the finger edges due to the attraction from the other fingers. To understand the effect this has on the frequency response, consider a point at a certain distance from a finger with charge $\rho(x)$. The wave R due to this charge that will reach the point is

$$R(x) = \int \rho(x') \, e^{-jkx'} \, dx' \qquad (2.4.12)$$

which is just the spatial Fourier transform of $\rho(x)$.

Datta considered the effect of charge distributions on the scattering matrix of an IDT finger [34]. He showed that the charge distribution on a transducer finger due to an incident wave of magnitude $|R|$ is given by

$$\rho(x) = (2\pi/p)\ (\epsilon_p + \epsilon_o)\ e^{-js\theta}\ (s + N)\ |R|$$

$$\left(\sum_{m=0}^{N-1} a_m \quad \sum_{n=-\infty}^{\infty} P_{n+m-N-1}(\cos\Delta)\ e^{-jn\theta} \right) \qquad \ldots(2.4.13)$$

where

$$a_o = -1/2 \qquad (2.4.14)$$

$$a_i = -\sum_{m=0}^{i-1} a_m\ P_{i-m}(\cos\Delta) \qquad (2.4.15)$$

$$\theta = 2\pi x\ /\ p \qquad (2.4.16)$$

$$p = \lambda_o\ /\ 2 \qquad (2.4.17)$$

ϵ_p is the effective permittivity of the substrate

ϵ_o is the permittivity of free space

s is the fractional part of $(f/2f_o)$

N is the integer part of $(f/2f_o)$

$$\Delta = \eta\pi \qquad (2.4.18)$$

η is the metalization ratio

P_n is the n-th Legendre polynomial

$(P_n = P_{-n-1}$ for $n < 0)$ (2.4.19)

This function is illustrated in Figure 2.9 for a

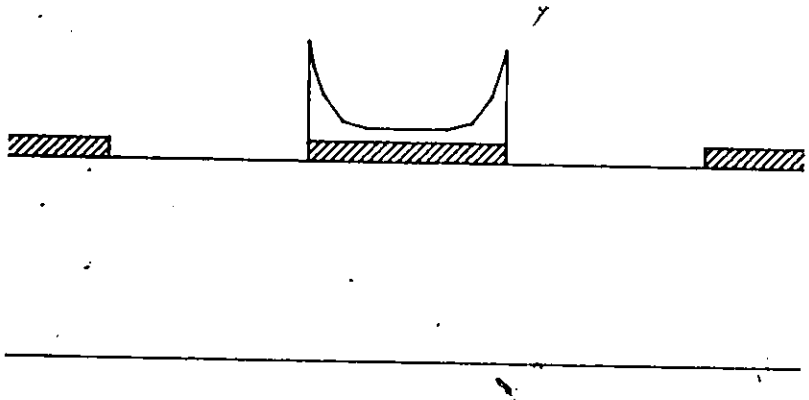

Figure 2.9: Charge distribution on excited IDT finger

metalization ratio of 0.5. From this charge distribution, the mixed scattering matrix, defined by

$$\begin{bmatrix} S_{i-1} \\ R_i \\ I_{i-1} \end{bmatrix} = \begin{bmatrix} m_{11} & m_{12} & m_{13} \\ m_{21} & m_{22} & m_{23} \\ m_{31} & m_{32} & m_{33} \end{bmatrix} \begin{bmatrix} R_{i-1} \\ S_i \\ V_i \end{bmatrix} \qquad (2.4.20)$$

can be obtained [34]. The parameters $m_{11} = m_{22}$, $m_{12} = m_{21}$ and $m_{13} = m_{23}$ are dimensionless, while $m_{31} = m_{32}$ and m_{33} have units of mhos. Their values are

$$m_{11} = j\,|\Delta v/v|\,2\pi(s+N) \sum_{m=0}^{N} a_m \{P_{2N+2s-m}(\cos\Delta) + (-1)^{N-m} P_{N-m+s}(-\cos\Delta)\, P_{N+2s-1}(\cos\Delta)\} / P_{s-1}(-\cos\Delta) \qquad \ldots(2.4.21)$$

$$m_{12} = 1 + j\,|\Delta v/v|\,2\pi(s+N) \sum_{m=0}^{N} a_m \{P_{m-1}(\cos\Delta) + (-1)^{N-m} P_{N-m+s}(-\cos\Delta)\, P_N(\cos\Delta)\} / P_{s-1}(-\cos\Delta) \qquad \ldots(2.4.22)$$

$$m_{13} = j\,|\Delta v/v|\,2\sin(\pi s)\, P_N(\cos\Delta) / P_{s-1}(-\cos\Delta) \qquad \ldots(2.4.23)$$

$$m_{31} = j\omega(\epsilon_p + \epsilon_o)\ W\ 2\pi(s + N) \sum_{m=0}^{N} a_m \left(P_{N-m+s}(\cos\Delta) + (-1)^{N-m} P_{s-1}(\cos\Delta)\ P_{N-m+s}(-\cos\Delta) / P_{s-1}(-\cos\Delta)\right) \quad \ldots(2.4.24)$$

$$m_{33} = j\ 2\omega\ (\epsilon_p + \epsilon_o)\ W \sin(\pi s)\ P_{s-1}(\cos\Delta) / P_{s-1}(-\cos\Delta) \quad \ldots(2.4.25)$$

where

$\Delta v/v$ is half the piezoelectric coupling constant

ω is the normalized angular frequency

W is the acoustic beamwidth

C_p is the capacitance per electrode pair.

These parameters have been modified in this Thesis to take into account device symmetry. The non-integer form of the Legendre polynomials (those containing s in their subscripts) in the above equations is defined as [35]

$$P_\nu(\cos\Delta) = \sin(\nu\pi)/\pi \sum_{n=0}^{\infty} (-1)^n \left(1/(\nu-n) - 1/(\nu+n+1)\right) P_n(\cos\Delta) \quad \ldots(2.4.26)$$

The functions defined by equations (2.4.21) to (2.4.25) are plotted in Figure 2.10.

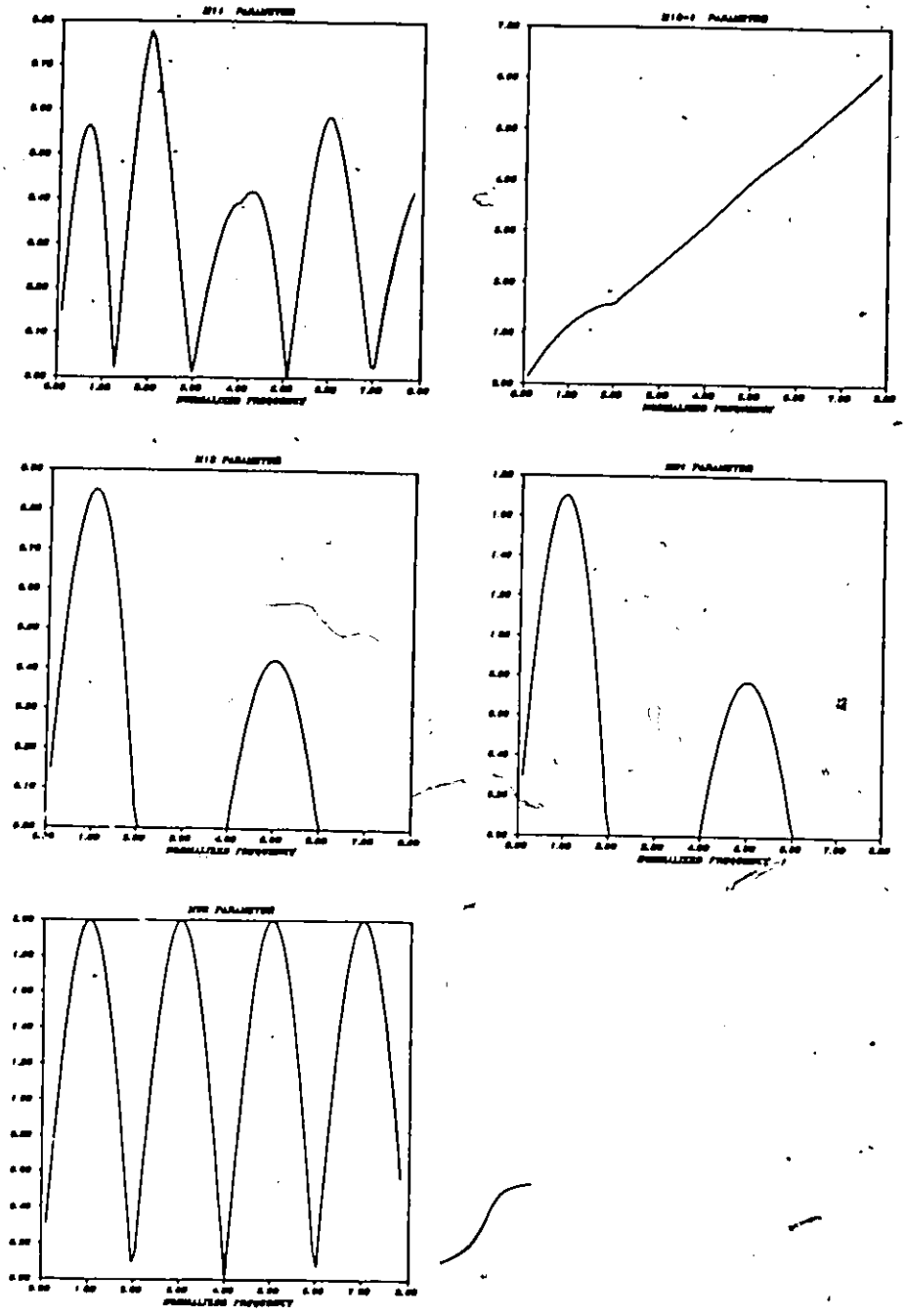

Figure 2.10: IDT finger's mixed scattering parameters for metallization ratio of 0.5. Plots have been normalized to remove dependence on substrate.

It is evident that the parameter $j\mu$ used in equation (2.4.11) is the same as m_{13}. It allows the computation of the coupling for all metalization ratios and for all frequencies, including the harmonics.

Close inspection of the functions reveals that these results do not strictly observe reciprocity or conservation of energy. In subsequent work by Panasik [33], some modifications were proposed to the mixed scattering parameters to correct the problem. A simplified version of these new scattering parameters is

$$m'_{11} = m'_{22} = m_{11}\, e^{j(\theta_{12} \pm \pi/2)}\, e^{-j\pi f/f_o} \qquad (2.4.27)$$

$$m'_{21} = m'_{12} = (1 - |m_{11}|^2)^{1/2}\, e^{j\theta_{12}}\, e^{-j\pi f/f_o} \qquad (2.4.28)$$

$$m'_{13} = m'_{23} = m_{13}\, e^{-j\pi f/2f_o} \qquad (2.4.29)$$

$$m'_{31} = m'_{32} = m_{31}\, e^{-j\pi f/2f_o} \qquad (2.4.30)$$

$$m'_{33} = 2\, m'_{13} m'^{*}_{31} / Z_o + j\omega C_p \qquad (2.4.31)$$

where

Z_o is the characteristic impedance of the substrate.

The mixed scattering matrices derived by Datta and

Panasik provide an alternate expression for the behaviour of an IDT. To make the latter compatible with the approach used for reflector arrays, the parameters can be converted to a transmission matrix of the form

$$\begin{bmatrix} R \\ S \\ I \end{bmatrix}_{i-1} = \begin{bmatrix} t_{11} & t_{12} & t_{13} \\ t_{21} & t_{22} & t_{23} \\ t_{31} & t_{32} & t_{33} \end{bmatrix} \begin{bmatrix} R \\ S \\ V \end{bmatrix}_{i} \qquad (2.4.32)$$

where the t_{ij} values are given in Appendix A. While these expressions require considerably more computation than the simpler ones described by equation (2.4.11), they give a more comprehensive model of the transducer.

It is probably worthwhile at this point to review what has been done so far in this section. The Coupling-of-Modes equations were derived in the first part, but it was seen that they did not lead to the desired closed form solution in the general case. An alternative iterative approach, based on point reflections at finger edges and point sources at finger centers was proposed instead, but was found to be lacking in some respects. Finally, the formulae derived by Datta on one hand, and Panasik on the other, were adapted for the current purpose. They provide a

full description of the SAW transducer finger and can be cascaded to calculate the frequency response of an IDT.

To make the model complete, the effect of external circuitry must be taken into account. To do this, superposition can be applied, so that the total voltage across the transducer pads is the vector sum of the applied voltage and the acoustically induced voltage. This allows Triple-Transit-Interference (TTI) to be included in the model. The scattering matrix must be modified according to

$$
\begin{aligned}
m''_{11} &= m'_{11} - m'_{13}m'_{31} / (Y_L + m'_{33}) \\
m''_{12} &= m'_{12} - m'_{13}m'_{32} / (Y_L + m'_{33}) \\
m''_{13} &= m'_{13}\, Y_L / (Y_L + m'_{33}) \\
m''_{21} &= m'_{21} - m'_{23}m'_{31} / (Y_L + m'_{33}) \\
m''_{22} &= m'_{22} - m'_{23}m'_{32} / (Y_L + m'_{33}) \\
m''_{23} &= m'_{23}\, Y_L / (Y_L + m'_{33}) \\
m''_{31} &= m'_{31}
\end{aligned}
\qquad (2.4.33)
$$

$$m''_{32} = m'_{32}$$

$$m''_{33} = m'_{33}\ Y_L\ /\ (Y_L + m'_{33})$$

where Y_L is the load admittance, assumed equal for both input and output transducers. To get these results, the IDT finger is represented by its equivalent circuit in Figure 2.11. In part (a) of the figure, it is seen that a voltage division occurs between the applied voltage and the voltage across the transducer pads. This accounts for the modifications in the m_{x3} parameters. In part (b), the effect on regeneration of the induced current can be evaluated. This leads to the change in the m_{11}, m_{12}, m_{21} and m_{22} parameters.

2.5 Computer Implementation of COM Theory.

There has been a lack, in the past, of a general purpose tool to study the response of an arbitrary SAW structure available in the open literature. Previous techniques relied, in the most part, on the assumption of single input and output transducers, and provided no support for reflector arrays. An ideal simulator would allow the user to specify a structure and it would provide the

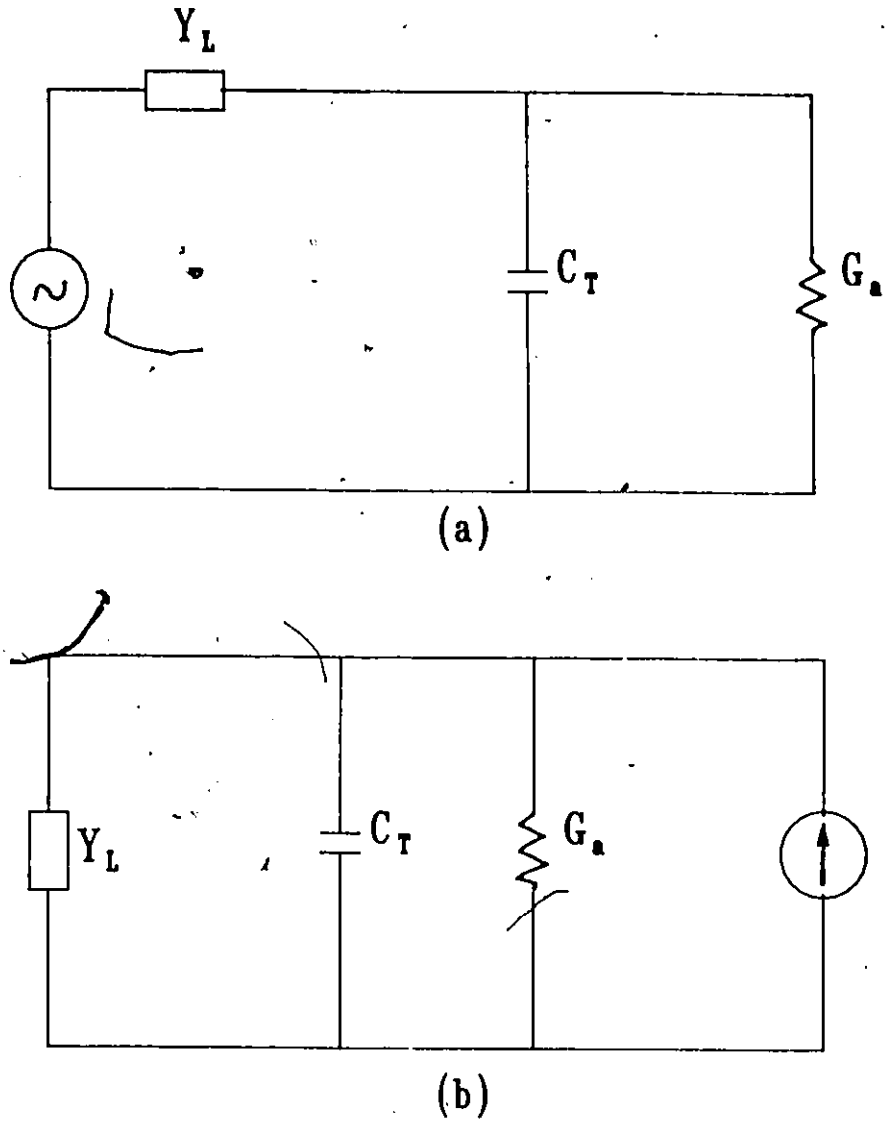

Figure 2.11: Equivalent circuits
for IDT finger
(a) as a transmitter
(b) as a receiver

corresponding frequency response. A menu driven computer program, based on the theory given above, was developed by the author with such an aim.

The package is listed in Appendix C and consists of five modules. This division limits the amount of data that must be handled at a time by the editor and the compiler. For ease of maintenance, the routines were written in FORTRAN which, though slower than some alternatives, allows the several thousand lines of code to be handled.

The main program, called COM, assigns default values to variables and displays a menu giving the user the choice of functions that he can invoke. These include saving or recalling device specifications, entering new specifications, computing the associated responses, and plotting the latter.

The next module, called EDIT, allows the specification of a device structure composed of transducers (single or split fingers, apodized or not), reflector arrays, and delay sections. Here, the substrate, the load impedance as well as the simulation frequency and time ranges can be assigned.

The third module, CMPUTE, evaluates the frequency and impulse responses of the SAW structure. It begins by assigning device parameters according to the specified structure. It then computes the transmission matrix for

each section in the structure (defined as an IDT, a reflector array or a delay section). For the reflector array, the COM transmission matrix is used, and for the delay section, a frequency dependent phase shift is added to each of the two counter rotating waves. The computation of the transmission matrix for each IDT is somewhat more complicated since apodization must be accommodated, which excludes the use of the simplified COM theory. The program first computes the mixed scattering matrix parameters for each finger as given by equations 2.4.21 - 2.4.31. These are then modified according to equations 2.4.33, and converted to transmission parameters as given in equations 2.4.32. Using this matrix for an individual finger, it is then cascaded to form the transmission matrix for each IDT in the structure.

At this point, the program has all the required transmission parameters to compute the frequency response. For a outgoing wave amplitude at the far end of the structure of 1 (and assuming no ingoing wave at this point), the structure is traversed and a scaling factor calculated for the input voltage. With this input voltage known, the structure is traversed a second time and the output voltage is evaluated. The ratio of input and output voltages is then taken.

The procedure is repeated for each frequency. Once

all points are evaluated, the routine performs an inverse Fourier transform on the response to evaluate the corresponding impulse response for time domain analysis.

The impulse response could be calculated using a inverse Fast Fourier Transform (FFT) routine. If the number of points were be made to be a power of 2, this would in fact be very efficient. Unfortunately, the FFT transforms a set of N points into another set of N points, giving the user little choice in the time ranges that result. For this reason, it was decided to use the less efficient Discrete Fourier Transform (DFT) computation.

The fourth module, PLOT, plots the frequency and time domain responses that were computed by CMPUTE on the computer screen. If a hardcopy is desired, a screen dump can then be performed. Sample plots, for a SAW resonator and for a delay line, are illustrated in Figure 2.12. The last module, called STORAGE, allows the user to save and recall device specifications and responses, if the latter are available.

The program was written for use on a Texas Instruments Business-Pro micro-computer. Much of the listing involves graphics which are host dependent. The CMPUTE module, on the other hand, is for the most part transportable and will therefore probably be of most interest to the reader.

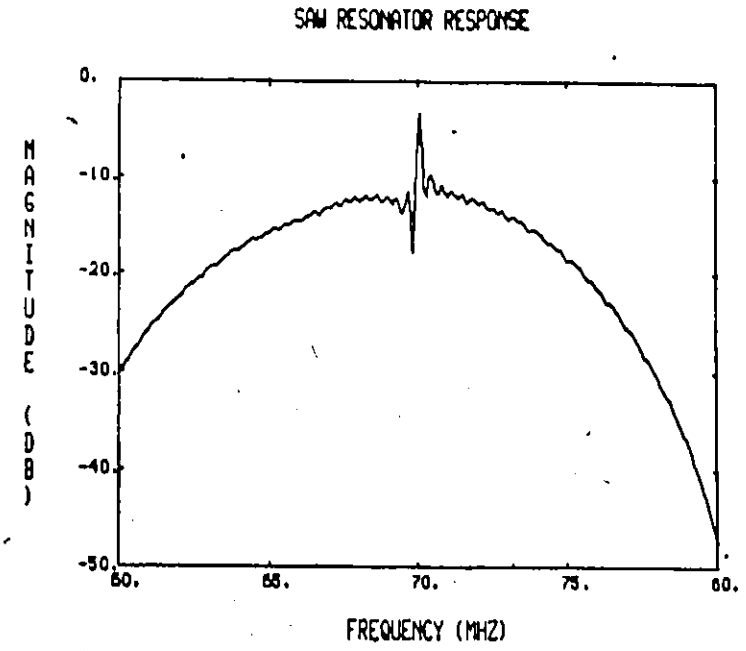

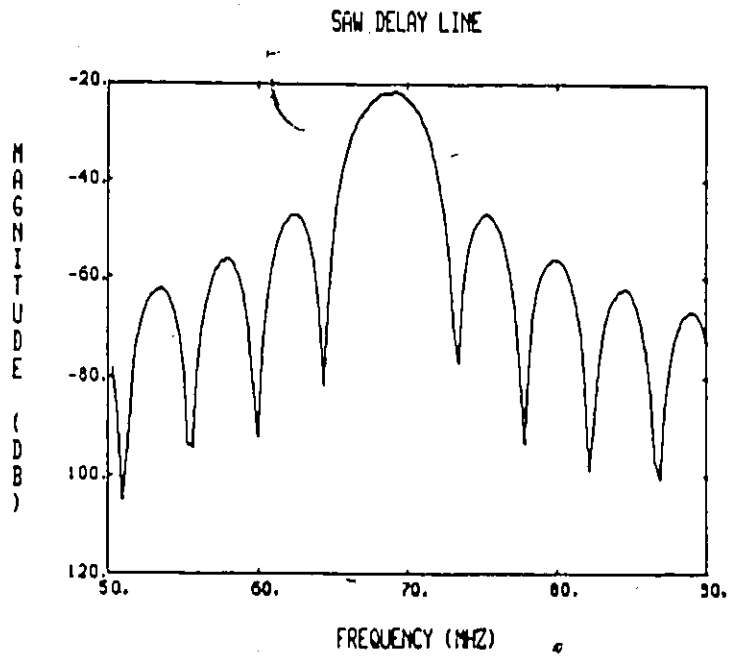

Figure 2.12: Sample theoretical frequency responses
(a) SAW resonator response
(b) SAW delay line response

CHAPTER 3

THEORY OF INTERDIGITATED/INTERDIGITAL TRANSDUCERS

3.0 Introduction.

The inability to match a reciprocal three port transducer at all ports simultaneously [10] has meant that, in the past, users of SAW filters have had to accept high losses in order to get high performance filters. Triple-transit-echo, the level of which in these bidirectional filters is [1]

$$TTI(dB) \simeq 6(dB) + 2\ IL(dB) \qquad (3.0.1)$$

below the carrier, requires device losses of over 20 dB in many cases in order to be suppressed to acceptable levels.

Recent attempts to reduce losses have concentrated on modifying the transducer in such a way as to make it a two-port device over the band of interest. Included in this

category are multi-phase devices [19] and those employing internal reflections within the transducer [24]. Unfortunately, the former require considerable supporting circuitry, while the latter are only effective over very narrow bands, never exceeding 3%. Other techniques involve veering unwanted waves in the desired direction, and thereby achieve low-loss at the expense of additional crystal surface area. These include the use of reflector arrays [22] and multistrip couplers [20].

In this chapter, a theoretical study of a device employing the three port nature of the IDT to reduce losses will be done. First proposed by Lewis [25], it involves interlacing input and output transducers so that all output transducers receive energy at both acoustic ports simultaneously, and all but the end input transducers radiate energy towards two output transducers, one on either side. It will be seen that, because of reciprocity, a inherently low-loss and wideband ($\geq$ 5%) frequency response will be achieved. In Chapter 4, experimental results on these devices will be described.

3.1 Device Description.

The basic SAW Interdigitated Interdigital Transducer (IIDT) structure is illustrated in Figure 1.8. It consists of N_{in} input transducers and $N_{out} = N_{in} - 1$ output transducers placed alternatively along the direction of SAW propagation. All input transducers have the same number of fingers and are connected by means of thin film metal strips. The same is done for all the output transducers. At each end of the structure, an absorber attenuates any outgoing surface waves, thus avoiding reflections from the edge of the crystal.

Each input transducer is excited by the same signal and generates acoustic waves propagating in both forward and backward directions. Half the energy produced by the two end transducers will be lost in the absorber. For all other input transducers, all generated acoustic energy will propagate towards output transducers.

Each output transducer, on the other hand, has an input IDT on either side. By reciprocity, if equal acoustic energy enters both of the output transducer's acoustic ports in phase, all energy should be absorbed, assuming perfect match at the electric port. All energy lost can therefore be attributed to the end input transducers [25]. The

proportion of energy lost is $1 / N_{in}$, so that the ratio of energy leaving the device to that entering is

$$E_{out} / E_{in} = 1 - 1 / N_{in} = N_{out} / N_{in} \qquad (3.1.1)$$

For this case, the insertion loss would be

$$IL = 10 \log(N_{out} / N_{in}) \text{ dB.} \qquad (3.1.2)$$

It is of interest to note that if perfect match could be achieved for all frequencies, the substrate used for the device would not affect the insertion loss. This is a distinct advantage of IIDTs over other low-loss structures, since in their case high coupling substrates are critical to their operation. Future applications, on gallium arsenide for example, may find this property very useful. In current situations, however, lithium niobate is preferred over quartz because the latter requires much larger apertures for a given input impedance.

Matching will affect the shape of the response as well as the minimum insertion loss. Under perfect match, all energy generated by the input transducers should be absorbed by the closest output IDTs, and the response of the device will just be a $(\sin(x)/x)^2$, which is the product of the input and output transducer responses, assumed to be

equal. If, on the other hand, the output is not perfectly matched, then only some of the energy will be absorbed by the closest output IDTs, and the rest will continue to propagate until it reaches other transducers, where it will again be partially absorbed. This process of sampling the waves at constant intervals leads to a comb frequency response.

It is clear, therefore, that the matching circuitry is critical to both low insertion loss and to a smooth frequency response. The reason for putting the input transducers at the end of the structure also becomes evident at this point. With an ideally matched filter, all energy will be absorbed by the output IDTs only if they receive equal energy, in phase, from both acoustic ports. Placing an output IDT at the end of the structure would not satisfy this condition and would result in regeneration. By placing the input transducers at the end, half the energy that they convert will be lost, but no spurious regeneration occurs.

3.2 Device Modelling.

The IIDT structure results in waves propagating in the forward and reverse directions, with interactions occurring in the transducers. The techniques derived in

Chapter 2 would therefore seem ideal for the analysis of the structure. The electrical signal to each input transducer is the same, while the output from the structure is the vector sum of the signal from each output transducer. It is important to acknowledge, however, that the model does not include diffraction, electromagnetic interference, bulk wave interference, reflections at finger edges, or resistive losses within the fingers. Some of these could, of course, be accounted for with further theoretical development.

For the design process, a physical feel for the operation of the structure would be helpful if optimum designs are to result. The key to such an understanding is the realization that we are dealing with a standing wave problem. Consider the example of the 3 transducer structure in Figure 3.1. The two input transducers generate waves travelling in phase, but in opposite directions. The forward-going wave generated by the leftmost IDT is

$$w^{+} = C \cdot e^{j(\omega t - \beta x)} \qquad (3.2.1)$$

and the backward-going wave generated by the rightmost IDT is

$$w^{-} = C \cdot e^{j(\omega t - \beta(d-x))} \qquad (3.2.2)$$

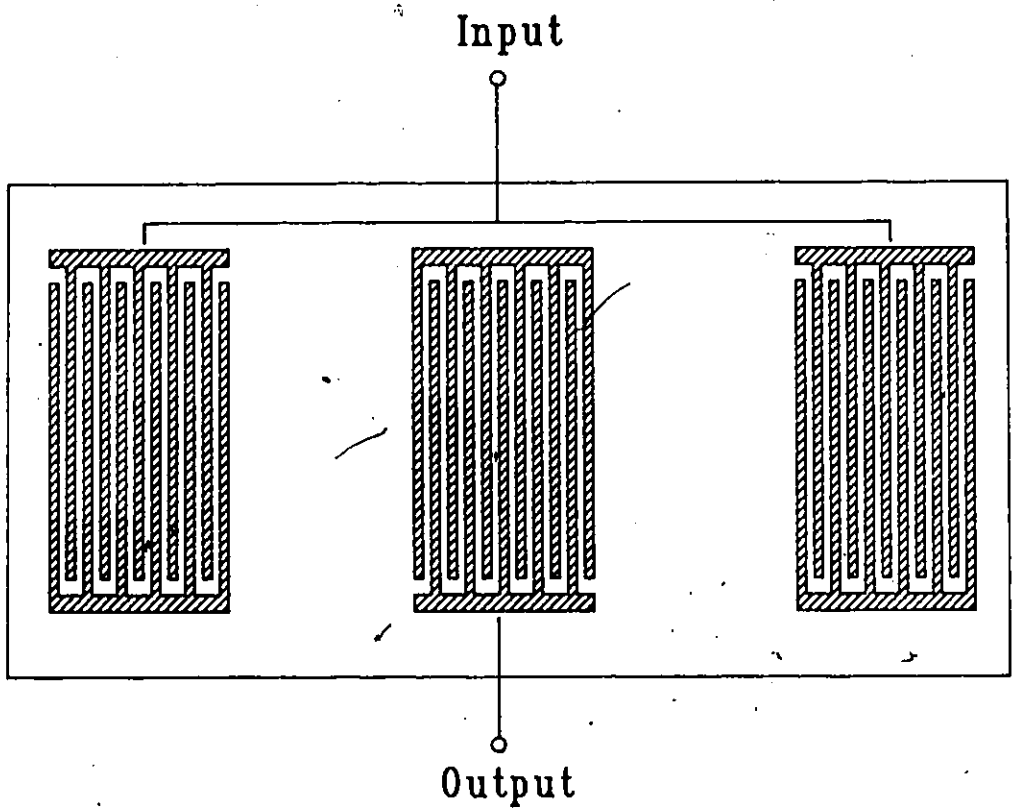

Figure 3.1: 2:1 IIDT structure

where d is the distance between the centers of the transducers, β is the propagation constant, and C is a constant. The sum of these waves between the two transducers is therefore

$$w = C \cdot e^{j\omega t} \left(e^{-j\beta x} + e^{-j\beta(d-x)}\right) \qquad (3.2.3)$$

If $d = n\lambda$, where λ is the wavelength of the acoustic wave, then

$$w = 2C \cdot e^{j\omega t} \cos\beta x \qquad (3.2.4)$$

This corresponds to a standing wave, where w is zero at points $x = (2n+1)\lambda/4$. Placing sampling points at these locations would result in a null at center frequency, while placing the sampling points at positions $x = n\lambda/2$ results in a peak at center frequency. This is illustrated in Figure 3.2. Similar conclusions are obtained for other values of d. As a consequence of this simple calculation, the spacing between adjacent IDTs must be precisely controlled if an efficient device is to result.

Other conclusions can also be reached from a simplified analysis. For instance, a N_{in}:N_{out} device can be divided into "cavities" operating in parallel, each consisting of two input transducers separated by an output

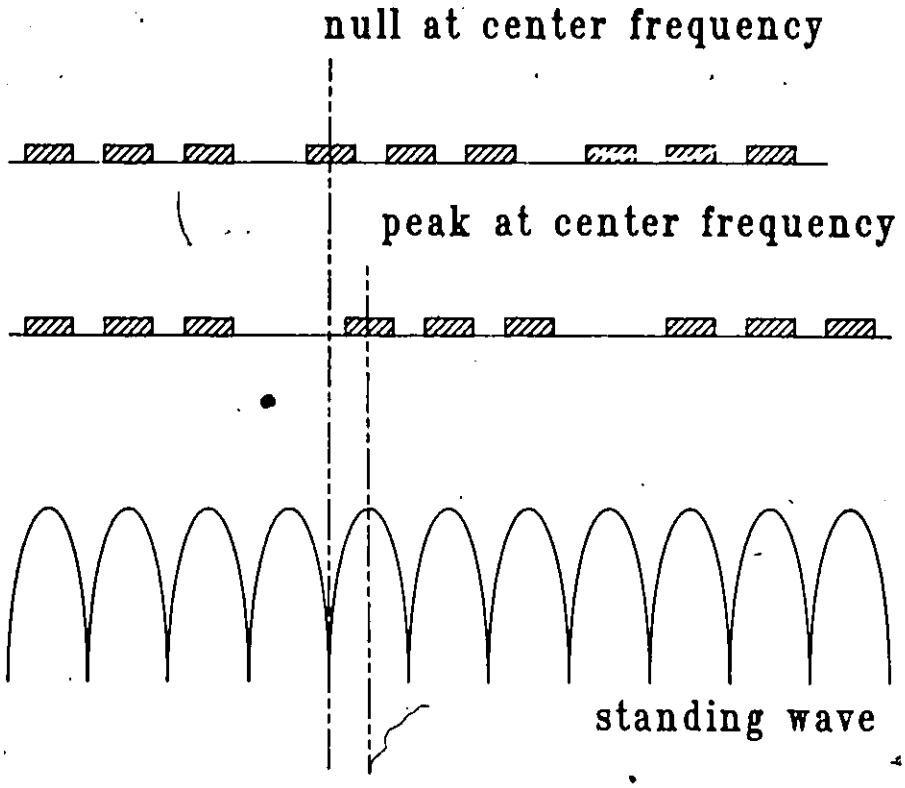

Figure 3.2: Effect of the position of the output IDT on the frequency response of a 2:1 IIDT

IDT. Reciprocity would then require that, to achieve independence, the two transducer spacings within this cavity be identical. Failure to satisfy this requirement would mean that the two waves would reach the center transducer out of phase with each other at most frequencies. This would inhibit full energy absorption.

If this requirement is met, and full energy absorption is possible, then each of these cavities is independent from all others. Inter-transducer distances can therefore be varied from cavity to cavity, should the designer so wish. However, if the requirement is not met, inter-cavity coupling will result, and the transducers cease to operate in parallel and the response becomes considerably more complicated. In this case, the transducers begin to operate in a serial fashion and simulating the device, using the theory in Chapter 2, is the best approach to take in the analysis.

3.3 IIDT Filters.

The IIDT offers the promise of a low-loss filter with a bandwidth comparable to that in conventional high-loss filters. This would allow the use of the filter in many applications where these latter filters cannot be

used, such as in the front-end of receivers, where insertion loss directly affects the signal to noise ratio of the signal. Since subsequent amplification cannot recover the lost signal, high-loss SAW filters have only found wide use in Intermediate Frequency (IF) sections of receivers, where signal power is of less concern.

The aim in designing an IIDT filter for such an application is to minimize the level of ripple in the passband, while also minimizing the insertion loss of the device. The key to meeting these requirements is to carefully match the device over the band of interest, so that the acoustic "cavities" operate independently.

This can, however, be very difficult to do because, in the case of IIDTs, input impedance of the device can vary significantly over the passband. While ideally this should not be the case, in practice coupling always occurs between the "cavities". This produces ripple in the frequency response, which translates to large variations in input and output impedances. Designing a matching circuit that performs as desired over all frequencies of interest can therefore be difficult, if not impossible, at costs that would be acceptable to manufacturers. Inductive matching can be used to tune out the reactive part of the input admittance at center frequency, while the aperture can be chosen to match the radiation impedance to the source and

load impedances. This provides an economical solution to the problem, but will result in an increasing degradation in performance at increasing frequency offsets. In particular, sidelobe suppression will suffer to some degree, and ripples will begin to appear in the passband.

When compared to other low-loss SAW filters, the underlying characteristics of the IIDT structure become apparent. In most other structures, any mismatch will increase the insertion loss, but will not usually degrade the shape of the passband.

In the case of transducers using internal reflections and multiphase transducers, a mismatch will result in some energy loss, but in general the latter will propagate away from the transducers, and thus will not affect the shape of the passband. With resonators, the transducers are normally mismatched, and low loss is achieved by energy containment at the resonant frequency. Since the bandwidth is usually very narrow, ripples do not appear. In the case of IIDTs and, to some degree, of techniques using multistrip couplers, a mismatch will increase insertion loss, but this is now accompanied with a dramatic increase in ripple.

A comparison of attainable bandwidth, insertion loss and sidelobe suppression, along with an indication of resulting passband ripple, is given in Table 3.1. In

	% Fractional BW	IL	Sidelobes	Ripples
Multiphase IDTs	>25%	2 dB	>60 dB	low
MSC-Based	<10%	3 dB	>60 dB	high
Resonators	<.1%	2 dB	>20 dB	--
SPUDT	< 3%	4 dB	>35 dB	--
IIDT	<10%	3 dB	>20 dB	high

Table 3.1: Comparison of low-loss SAW technologies.

general, low-loss is easily achieved with narrow-band structures, but cost increases and performance decreases as the 2% bandwidth is surpassed.

3.4 IIDT Comb Filters.

The previous section described an attempt to control the inherent ripple in the frequency response of the Interdigitated Interdigital Transducer structure. There are many applications, however, for which a comb response is desirable. These include multimode oscillators which permit oscillations at one of the many frequencies that obey the loop gain and phase shift requirements.

All sampling structures exhibit a comb response. The basic SAW IDT, for example, samples the incoming wave at the centre of the electrodes, and this results in an infinite number of passbands (harmonics) in the frequency domain, each separated by $2f_o$, where f_o is the center frequency of the transducer.

By grouping sets of transducer fingers, it is possible to sample at the group level in addition to the finger level. This is analogous to antenna theory [36], where the overall radiation pattern of a multiple element antenna is controlled by both the element and the array

factors.

A common SAW comb filter is shown in Figure 3.3. Here, the incoming wave is sampled by a group of transducer fingers, delayed, and sampled again. At frequencies for which the delay between the two sampling points will be such that they are phased by $2n\pi$, the signal will add in phase, leading to a comb passband. At others, they will be phased by $(2n+1)\pi$ and will cancel, leading to a null. The separation between two peaks will be

$$\Delta f_{peak} = v_o / d \qquad (3.5.1)$$

where d is the distance between phase centres of the two IDT groups, and v_o is the phase velocity of the SAW.

Increasing the number of these sampling groups to N will narrow the peaks, while introducing (N - 2) sidelobes, similar once again to the radiation sidelobes observed in antennas. Their existence is most easily explained by means of phasors, as illustrated in Figure 3.4 for the case of N = 3 sampling groups. At frequencies corresponding to comb peaks, each of the three samples is phase shifted by $-2\pi n$ from each other, and all three phasors add constructively. At nulls, each sample is shifted by $2\pi n/3$, causing destructive interference. At sidelobe peaks, the phasors are $\pi(2n+1)$ radians apart, so that the sum is in phase with

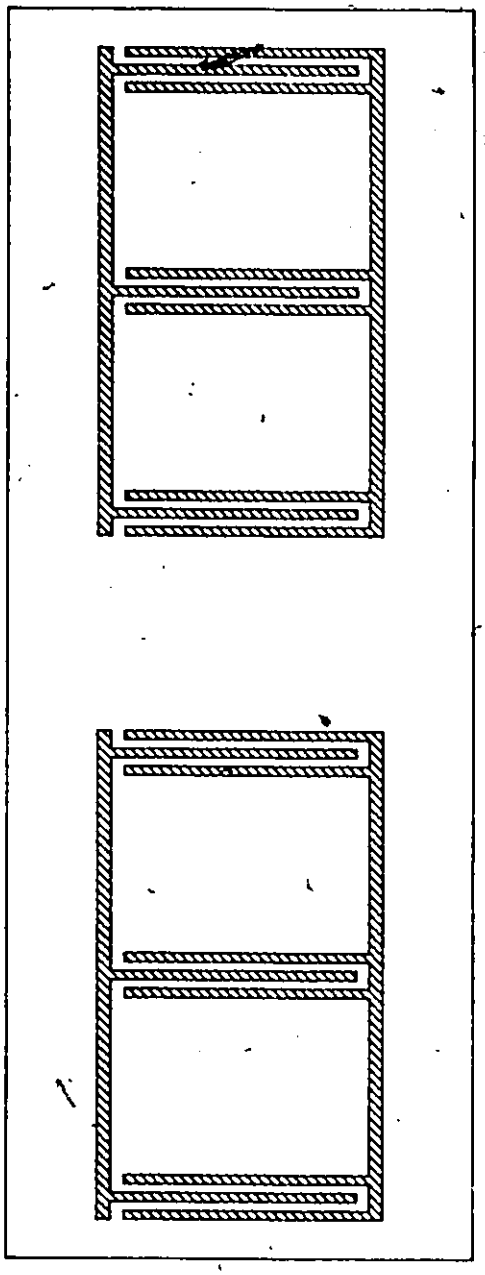

Figure 3.3: Traditional SAW comb filter

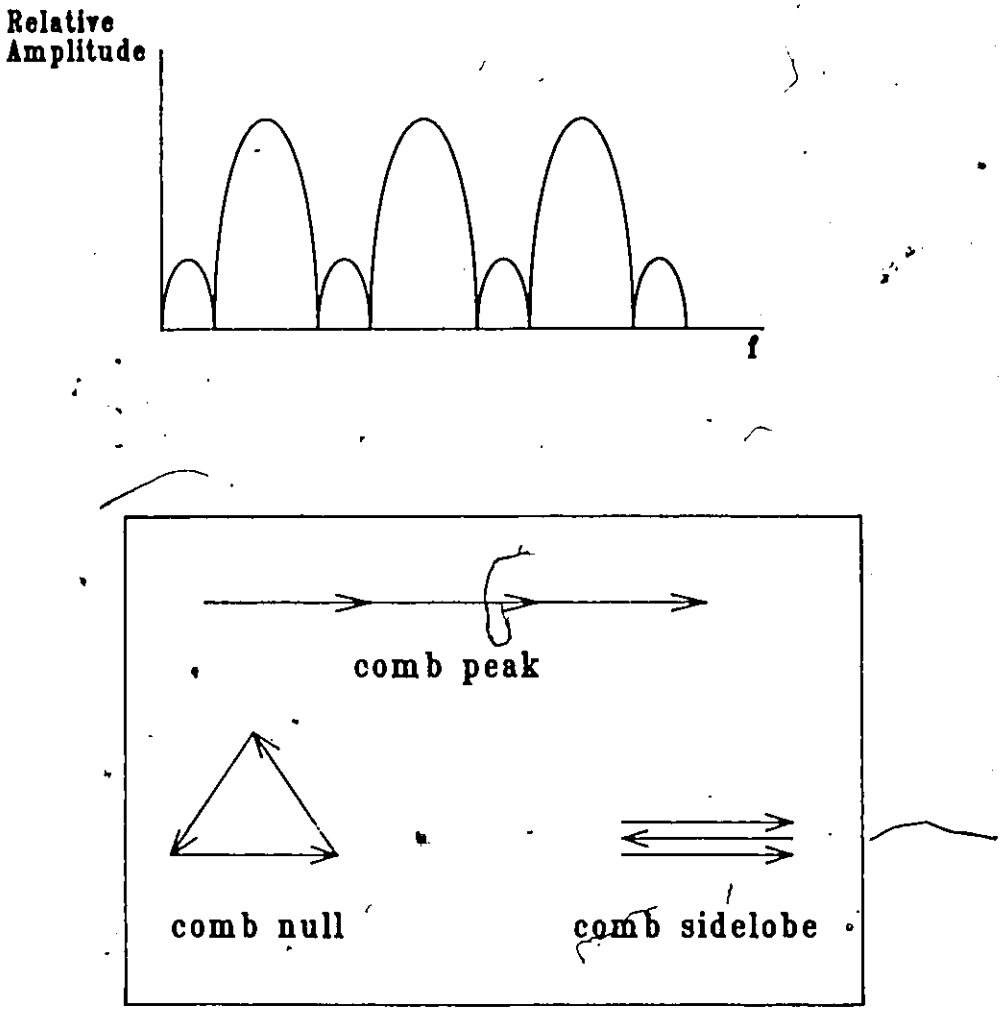

Figure 3.4: Phasor analysis of comb response

the output at the major peaks, but exhibits an amplitude of 1/3 the latter.

The overall response will also contain an underlying sinc response due to the response of the individual sampling groups. This can be compensated for by weighting the elements in these groups in order to flatten the response about the frequency of interest. Here, all the usual weighting techniques should apply, including apodization, finger withdrawal as well as phase weighting. In the case of apodization, any attempt to apodize the input as well as the output transducers would, of course, lead to the same problems as for other SAW filters.

Now, by moving the input and output transducers of this comb filter until they are superimposed, one ends up with the IIDT structure. The major difference in the response of these two related devices is apparent in the time domain. As seen in Figure 3.5, the conventional comb impulse response is symmetric, while the IIDT comb filter has an impulse response that corresponds to the second half of the former. As a consequence of this, the IIDT will not have a linear phase response, but this is of little concern, since its main application is in oscillators. In these applications, non-linear phase is often an advantage, since steep phase changes will narrow the range of frequencies at which the oscillator phase shift requirements are met, and

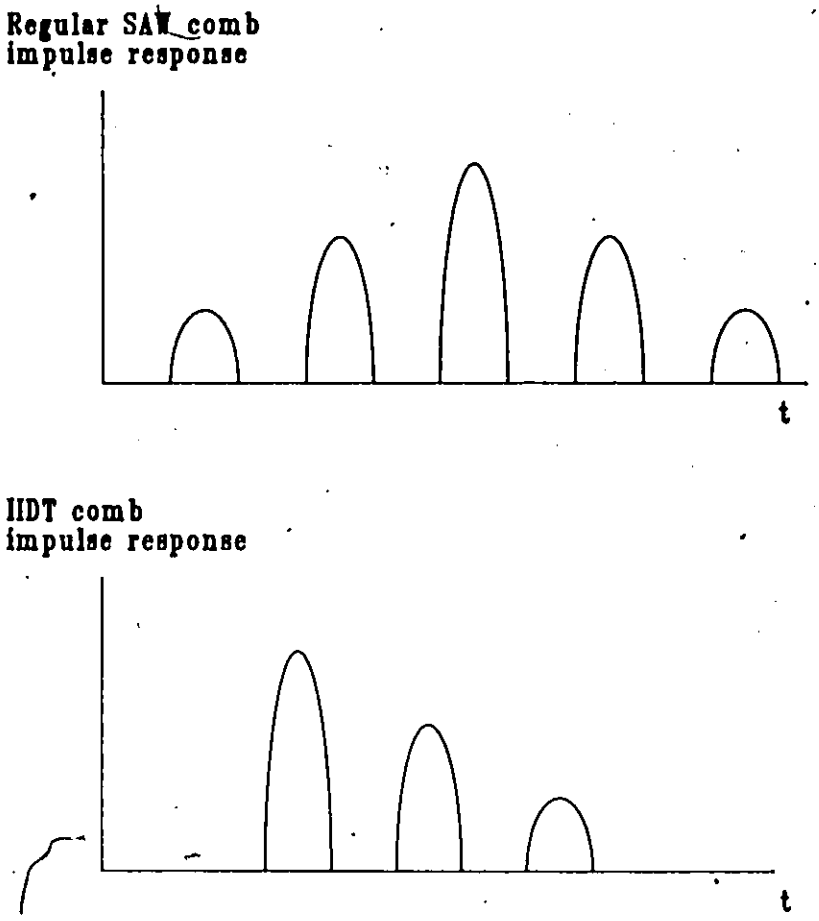

Figure 3.5: Comparison of impulse response of regular SAW comb filter and IIDT comb

thus stability will be increased.

The fundamental advantages of this comb structure are its compact size and its lower insertion loss. Conventional comb filters separate the input transducers from the output, so that the device is at least twice as large. This translates to twice the cost, since crystal real estate is the determining factor in device cost. The lower insertion loss lowers the amount of required amplification in an oscillator, and phase noise can thereby be decreased [37].

These advantages are not achieved without some cost. Because the number of impulse response peaks is about half the number found in conventional comb filters, the number of corresponding phasors will be smaller, and the comb sidelobes will not be as attenuated. This will make the design of an oscillator more difficult, since loop gain is now more critical.

CHAPTER 4

EXPERIMENTAL RESULTS ON INTERDIGITATED INTERDIGITAL TRANSDUCERS

4.0 Introduction.

All SAW devices to be described in this section were fabricated on 128° rotated YX-lithium niobate. The transducer patterns consisted of 1000 Å of Aluminium deposited by means of evaporation. The metallization ratio was approximately η=0.5. A brief description of the fabrication and testing procedure is given in Appendix B. The device measurements were made on a Hewlett Packard 8505A Network Analyzer connected to an HP 9816 computer running time-domain analysis software [38].

4.1 Device Geometry.

Various experiments have been performed by the author to determine the optimum interconnecting geometry for IIDTs. By alternating the orientation of the transducers, as shown in Figure 4.1, a ground line can be made to meander between them. This reduces the number of required ground connections to one. Similarly, this allows a single input and a single output connections. The ground line, while in the path of the acoustic waves, should not affect them by any significant amount.

Experiments show, however, that this configuration results in excessive "cross-talk" between the input and output IDTs occurring through the ground line. This causes a degradation in stopband suppression in a similar way as electromagnetic radiation. By separating the input and output ground lines, as shown in Figure 4.2, this problem can be solved to some degree. The two ground lines are then connected to the package.

Further attempts to control the level of feedthrough have involved placing ground planes between the transducers, as illustrated in Figure 4.3. The effect of these planes on the frequency response of the device is shown in Figure 4.4. As seen in the figure, these planes cause a degradation in sidelobe performance of approximately 4 dB. It is believed

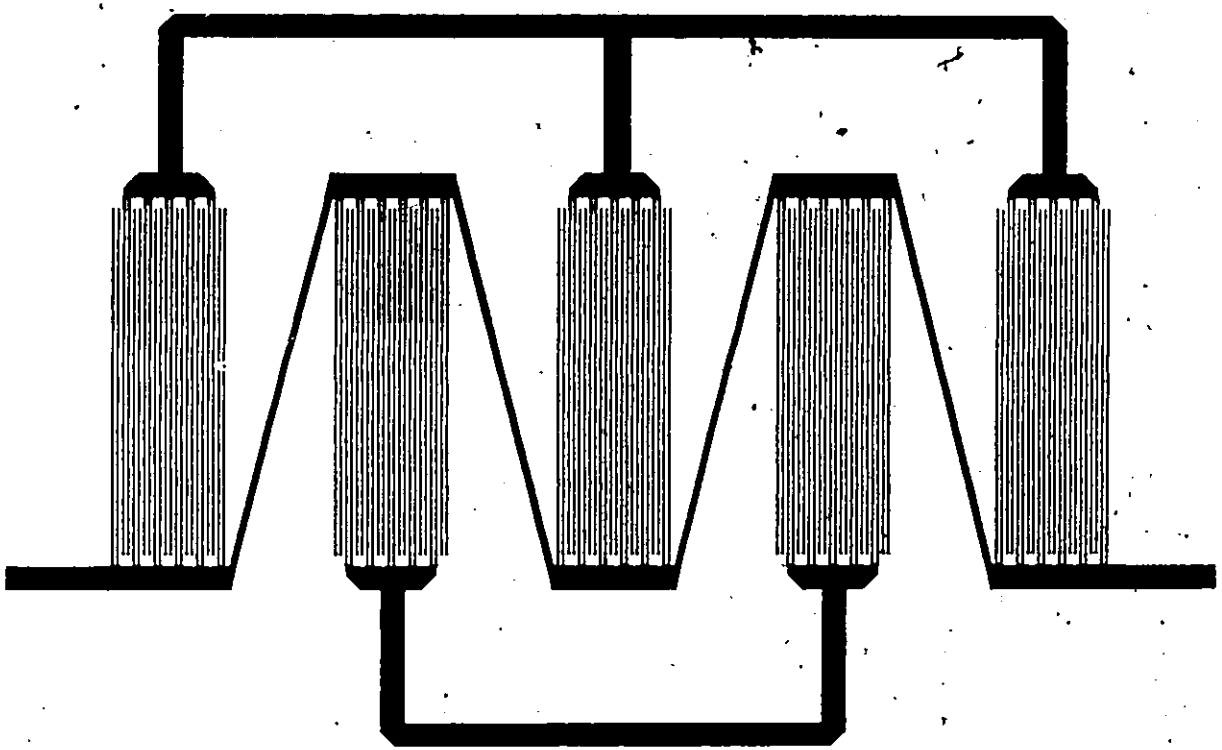

Figure 4.1: IIDT configuration with common ground to all IDTs

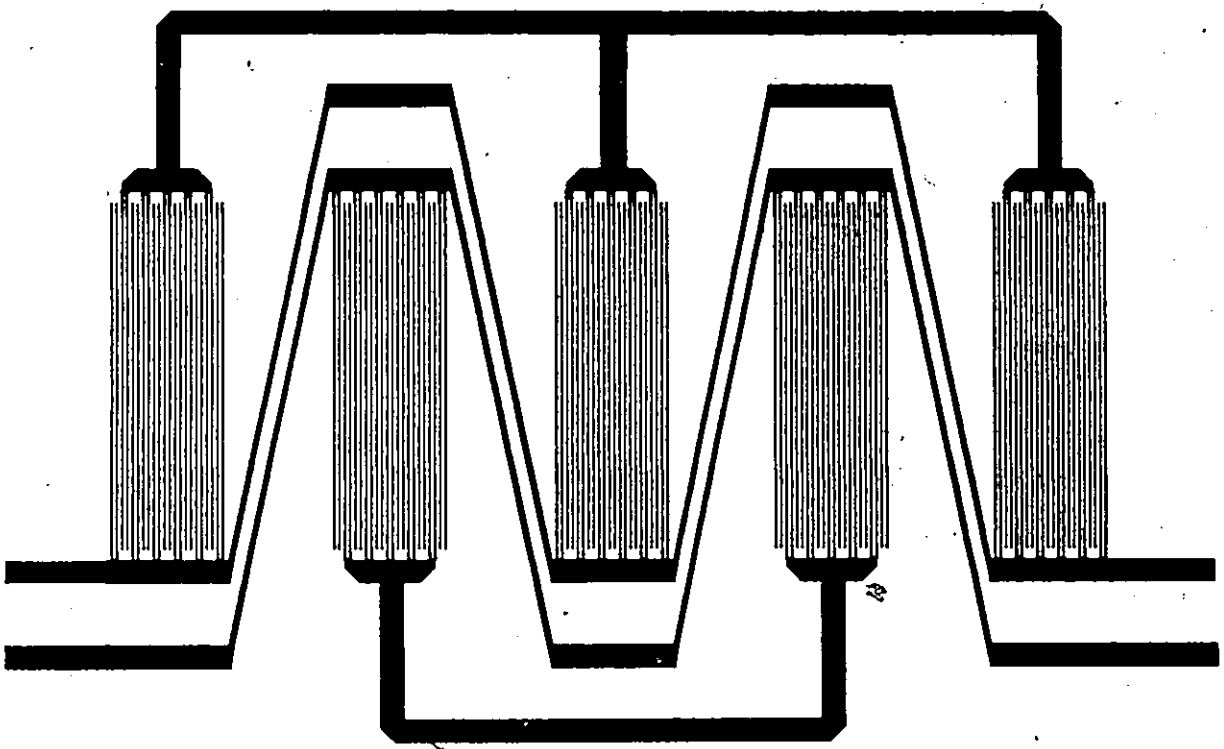

Figure 4.2: IIDT configuration with separate ground lines to input and output IDTs

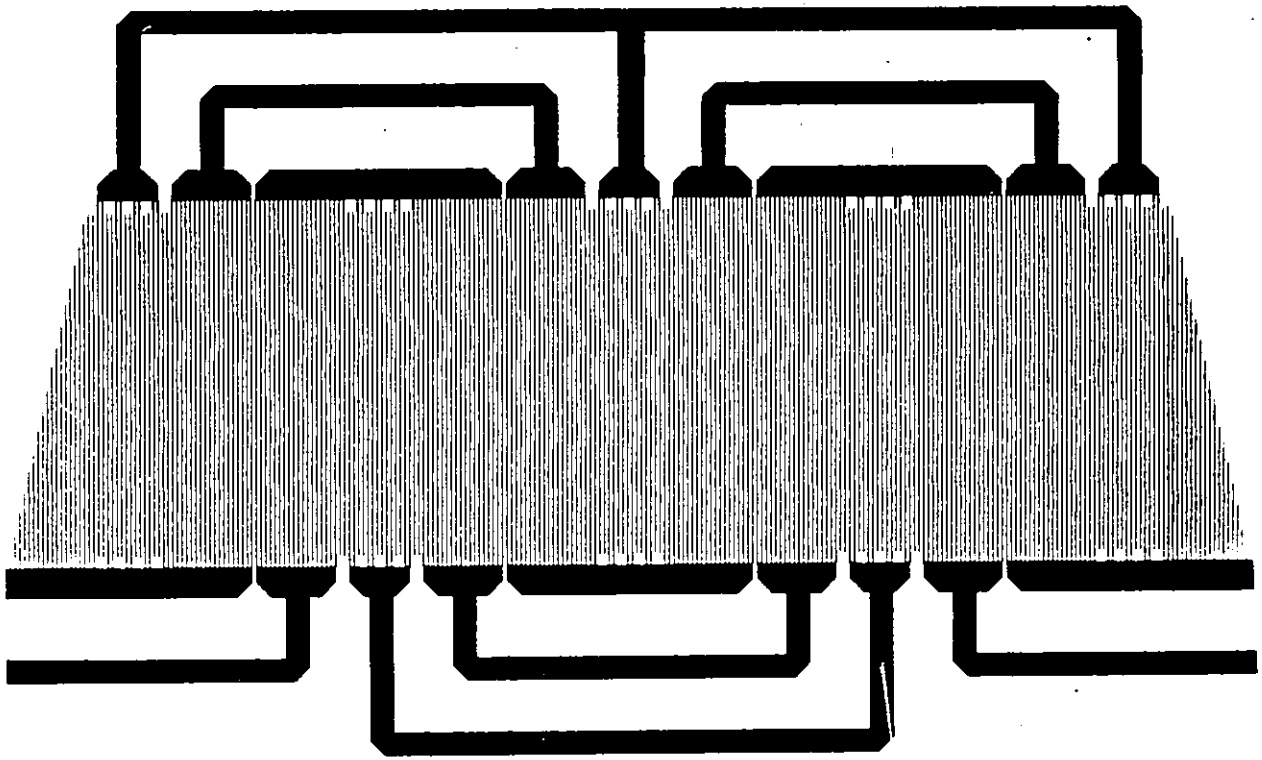

Figure 4.3: IIDT with ground planes between transducers

Figure 4.4: Effect of ground planes on electromagnetic feedthrough

(a) Experimental frequency response of IIDT without ground planes (Horizontal sweep 500 kHz to 130 MHz, vertical scale 5 dB/div, mkr -5.8 dB)

(b) Experimental frequency response of IIDT with ground planes (Horizontal sweep 500 kHz to 130 MHz, vertical scale 5 dB/div, mkr -5.1 dB)

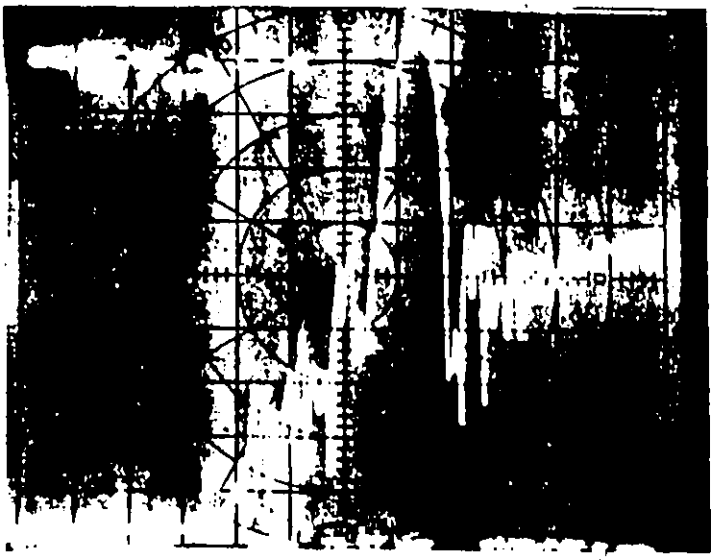

(a)

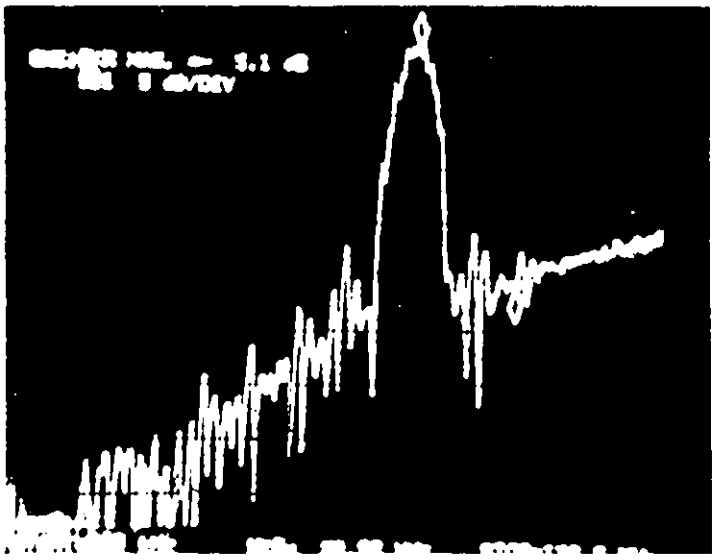

(b)

that this is due to coupling between the two ground planes which become very close in the modified structure. Had it been possible to connect these planes to separate grounds, instead of using grounds common to the transducers, an improvement might be possible. The lack of facilities has not permitted such an experiment.

Finally, all corners on the transducer pads and their connecting lines have been rounded as is often done in microstrip circuits to minimize radiation. The effect of this approach cannot be determined accurately because of the variation in observed feedthrough from device to device. It is felt, however, that this change can only have a positive effect.

4.2 IIDT Filters.

Designing a low-loss IIDT filter requires smoothing the passband while minimizing losses. Unlike conventional bidirectional SAW filters, where these requirements are conflicting, this new structure should, in theory at least, achieve both objectives simultaneously.

4.2.1 2:1 IIDT Filter.

As a first step, a 2:1 IIDT was fabricated with 29 split fingers in each of the two outer input transducers, and 41 in the inner output transducer. Using Smith's [15] expression for acoustic radiation admittance at centre frequency f_o

$$G_o = 2 k^2 C_s f_o (N_t - 1)^2 \qquad (4.2.1)$$

where k^2 is the electromechanical coupling constant, C_s is the capacitance per electrode pair, and N_t is the number of fingers in the transducer, an electrical impedance of approximately 50 Ω required an aperture of .32 mm. The spacing between transducer centres was set at 39 λ_o. The predicted frequency response, using the software package in Appendix C, for a device matched at center frequency is shown in Figure 4.5. Note that large ripples are evident in the response.

This result can be explained by two mechanisms. The output transducer could be regenerating some of the incident acoustic power in spite of the attempt made to equate the two waves. This would cause triple-transit in the conventional sense, with a portion of the waves returning to the transducer that generated them. In addition, the output

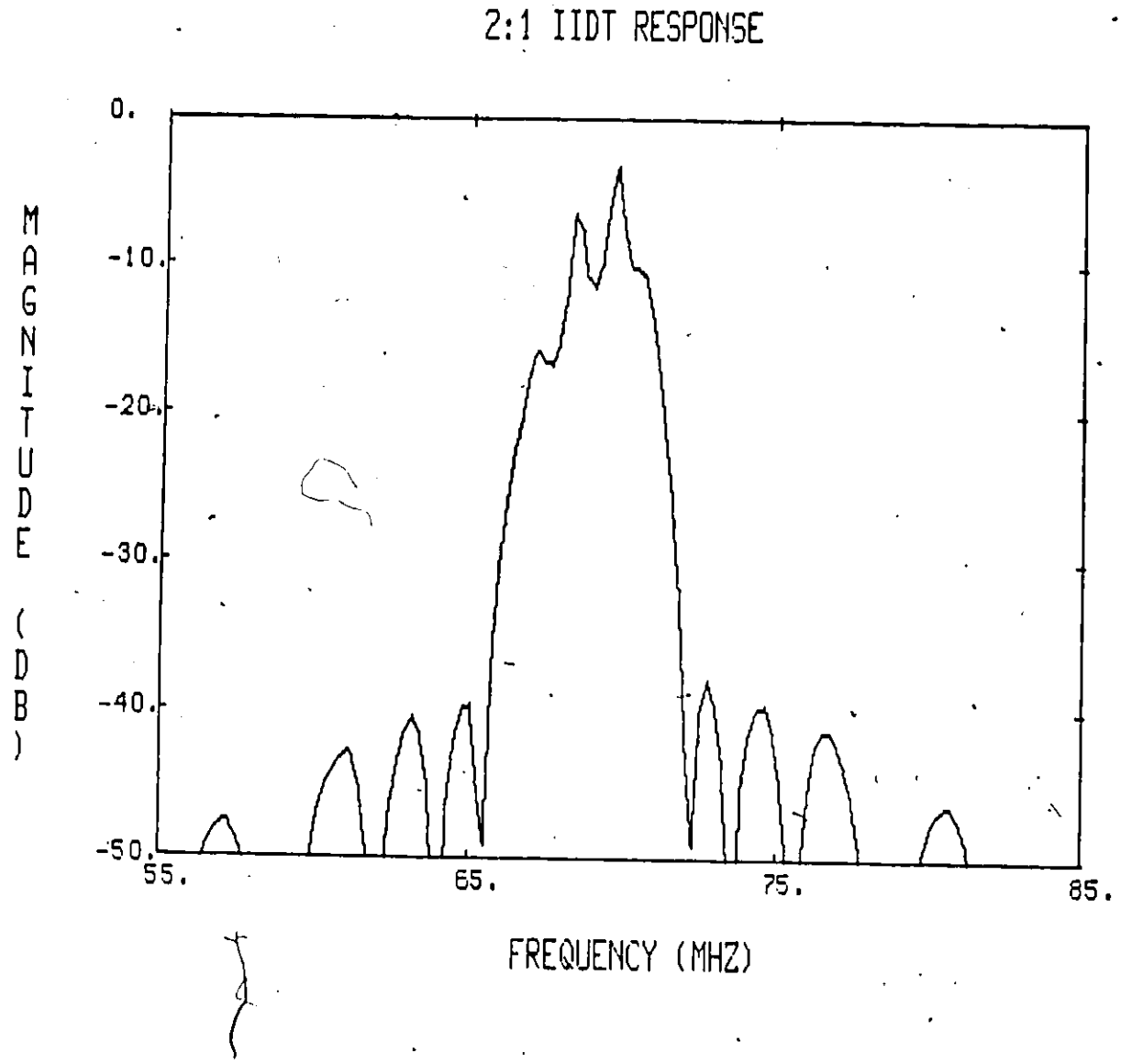

Figure 4.5: Predicted frequency response of 2:1 IIDT device

transducer may not be absorbing all the power that is incident, but instead allowing a significant portion to propagate onto the other input transducer which, due to its three port nature, will regenerate a fraction. It is the opinion of the author that both effects are present.

There are two reasons for this conclusion. The first is that the devices are assumed to be matched only at center frequency. The input and output impedances vary significantly over the band of interest, and the possibility of matching over the whole band is unlikely. The second reason is that true reciprocal operation of a SAW transducer is not possible, since it would involve applying all the spurious waves (bulk waves, diffracted waves, sideward propagating waves, etc...) to the receiving transducer. Simply controlling the plane surface waves incident onto the two "conventional" acoustic ports is not sufficient to cause absorption of most of the incident acoustic power. These non-ideal conditions will cause both regeneration and energy propagation to be present.

The frequency response of the unmatched device is shown in Figure 4.6 (a). As can be seen, large ripples are evident in the passband. The impulse response in Figure 4.6 (b) shows that the main source of this ripple is triple- and quintuple-transit interference. The level of TTI is 11 dB below the main signal. Some of this is expected because the

Figure 4.6: Responses of unmatched 2:1 IIDT device

(a) Experimental frequency response

(Horizontal sweep 55 to 85 MHz,

vertical scale 5 dB/div, mkr -9.4 dB)

(b) Experimental impulse response

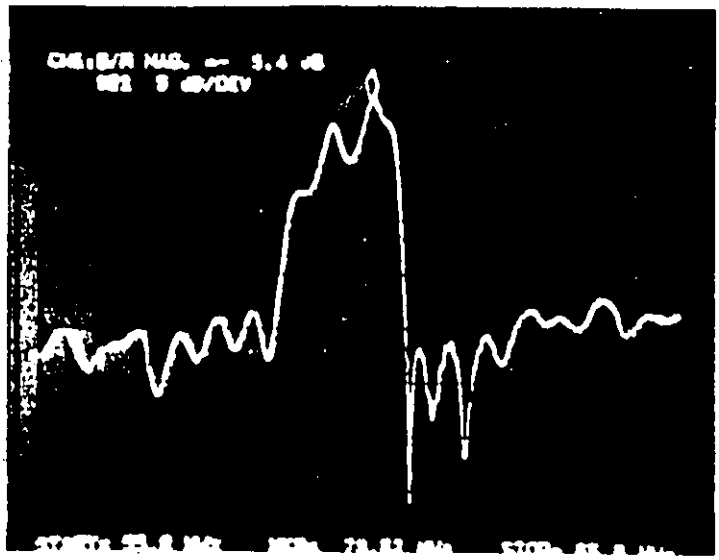

(a)

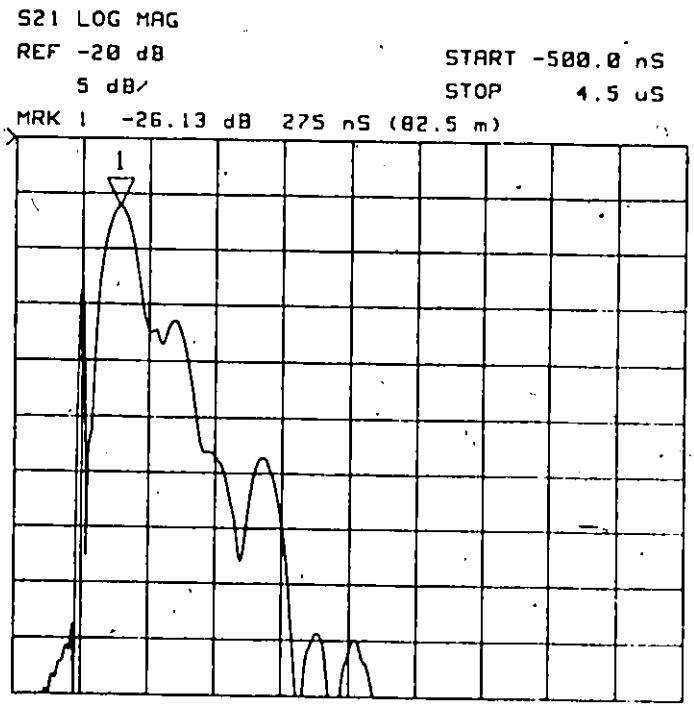
S21 LOG MAG
REF -20 dB
5 dB/
START -500.0 nS
STOP 4.5 uS
MRK 1 -26.13 dB 275 nS (82.5 m)
1

(b)

reactive part of the transducer impedance has not been tuned out. Also evident in the impulse response is the electromagnetic feedthrough, seen as an impulse at time 0, which is caused by direct coupling between input and output transducers. In fact, this interference appears to be more prevailing in the interdigitated structure than in conventional SAW devices, probably because of the number and the close proximity of input and output transducers. It translates in the frequency domain as a flat degradation in sidelobe performance of the IIDTs.

Figure 4.7 (a) shows the frequency response of the same device with transducers matched at centre frequency to the source and load impedances. Matching was achieved on the HP 8505 Network Analyzer by observing the S_{11} parameter on a Smith Chart while varying short circuit stub lengths. This was done until the center frequency reflection coefficient was centered on the screen. The same was done for the S_{22} parameter when matching the output. It is clearly seen that insertion loss has decreased to 7.7 dB, but, contrary to expectations, the magnitude of the ripple in the passband has increased. This is confirmed by the impulse response in Figure 4.7 (b), which shows the TTI to be 9 dB below the main signal. Note that now the septuple transit level has been considerably enhanced over that in Figure 4.6 (b). This degradation is caused by the improved

Figure 4.7: Responses of matched 2:1 IIDT device
(a) Experimental frequency response
(Horizontal sweep 55 to 85 MHz,
vertical scale 5 dB/div, mkr -7.7 dB)
(b) Experimental impulse response

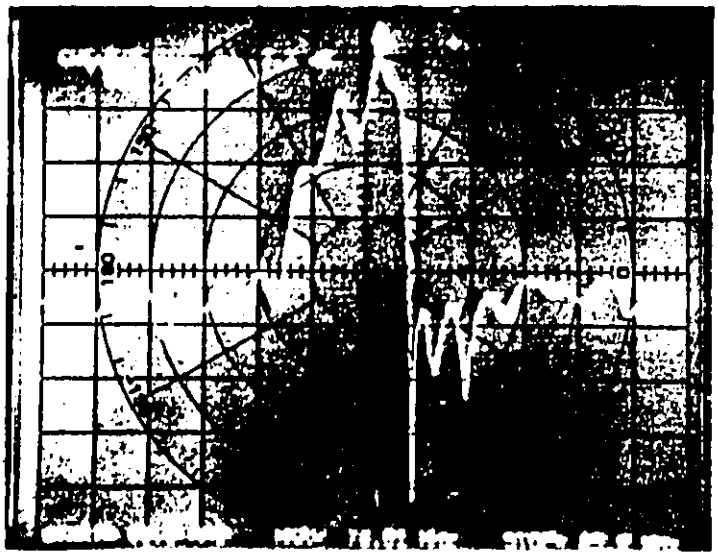

(a)

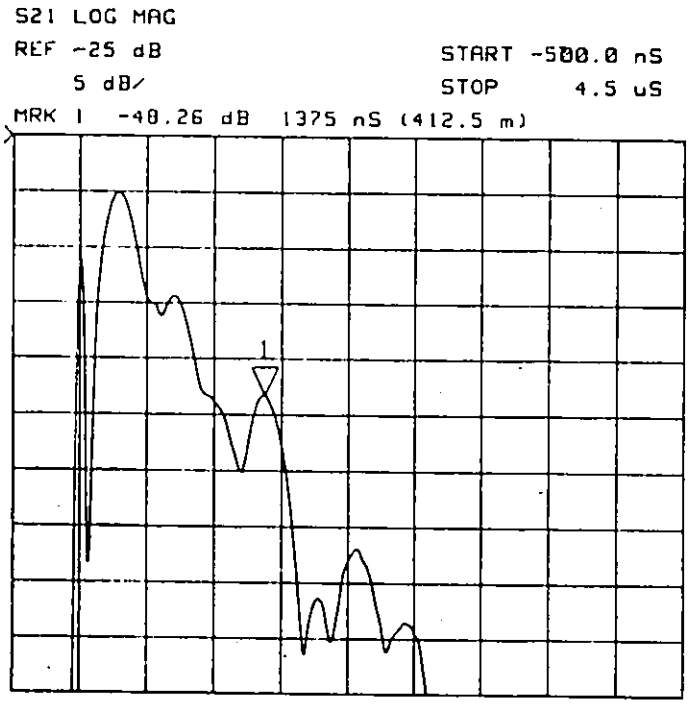
S21 LOG MAG
REF -25 dB
5 dB/
START -500.0 nS
STOP 4.5 uS
MRK 1 -48.26 dB 1375 nS (412.5 m)
1

(b)

matching on the input transducers, which causes them to regenerate any incident waves more efficiently.

The ripple separation is inversely proportional to the spacing between transducers. By moving the latter as close as possible, while maintaining a distance of $(n/2 + 1/4)\lambda$ between their phase centers, it is possible to control the ripple by placing a trough at center frequency and a peak at each band edge. When superimposed with the transducer's sinc response, this has the effect of flattening and widening the passband of the filter, as seen in Figure 4.8. This device has 57 fingers in each input transducer and 81 in the output. The aperture is .8 mm and the transducer separation is 46.25 wavelengths.

These observations indicate a possibility of building wideband low-loss filters using IIDTs. To reduce the amount of ripple, it is however necessary to purposely mismatch the input transducers while matching the output. In this manner, the waves that reach the end input transducers are not regenerated efficiently. As seen in Figure 4.9, this can decrease the amount of ripple to tolerable levels.

Figure 4.8: Experimental frequency response of 2:1 IIDT with ripples placed at band edges (Horizontal sweep 59 to 79 MHz, vertical scale 5 dB/div, mkr -8.2 dB)

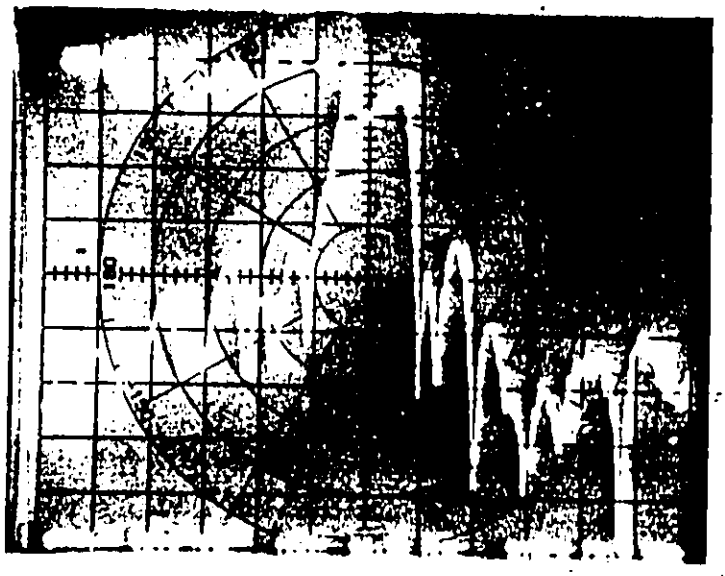

Figure 4.9: Experimental frequency response of 2:1 IIDT with output matched and input mismatched (Horizontal sweep 59 to 79 MHz vertical scale 5 dB/div, mkr -7.9 dB)

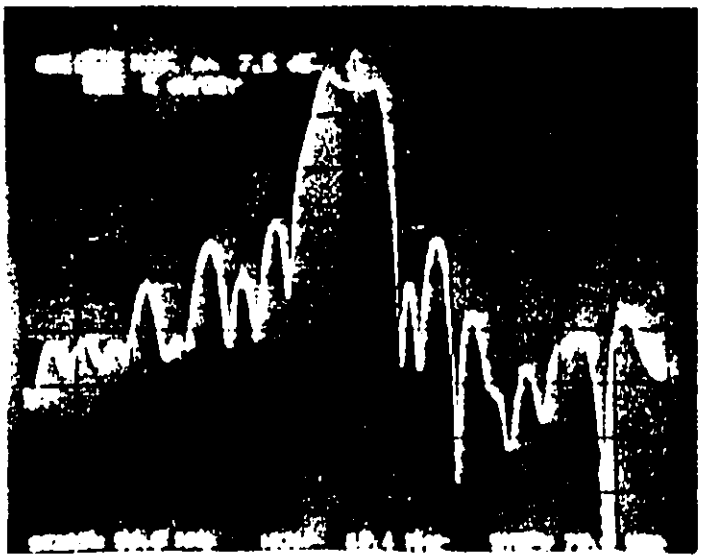

4.2.2 3:2 IIDT Filter.

Interdigitated filter with more than three transducers, while allowing lower insertion losses, exhibit very much the same degradation in performance. A 3:2 transducer device with 81 fingers in each output transducer and 57 in each input transducer has a predicted response shown in Figure 4.10. Here the IDT separation is 46.25 wavelengths at center frequency and the aperture is set at .4 mm. The experimental responses are shown in Figure 4.11. It can be seen that, once again, mismatching the input transducer reduces the peak to peak ripple at the expense of increased insertion loss, which increases from 5 dB to 8 dB. The number of ripples has increased since, in addition to ripples caused by regeneration, there are now ripples caused by the sampling of the acoustic waves done by the several output IDTs. The difference between the theoretical and the experimental responses is attributed to a misalignment introduced when, because of the device length, the mask had to be cut in half and the two halves joined together after photo reduction.

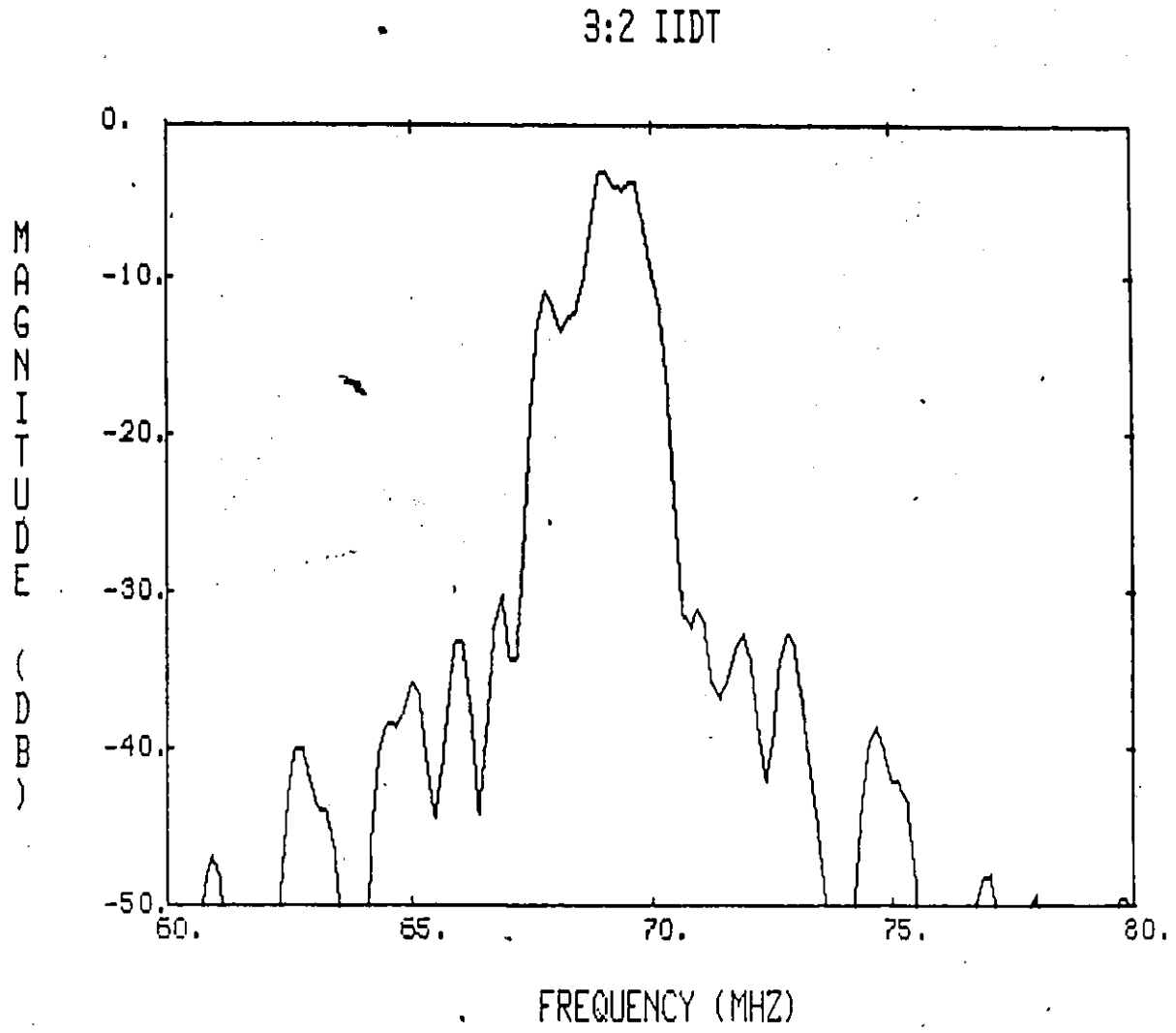

Figure 4.10: Predicted frequency response of 3:2 IIDT device

Figure 4.11: Experimental frequency responses of 3:2 IIDT

(a) with matched input

(Horizontal sweep 59 to 79 MHz, vertical scale 5 dB/div, mkr -5.0 dB)

(b) with mismatched input

(Horizontal sweep 59 to 79 MHz, vertical scale 5 dB/div, mkr -8.8 dB)

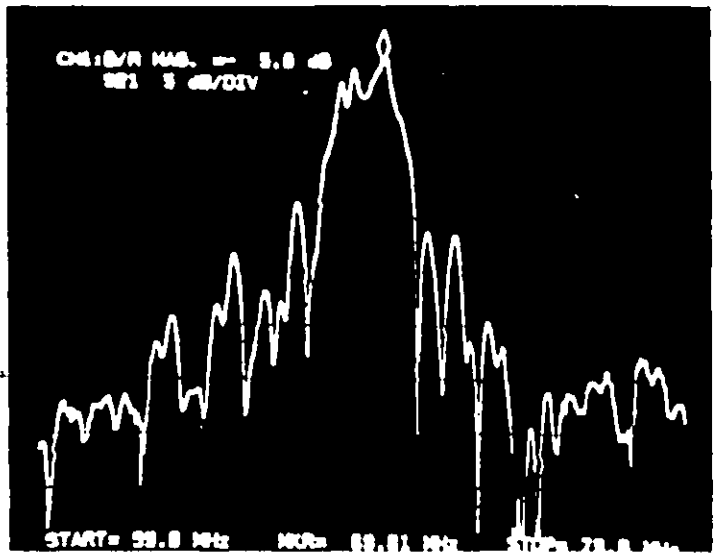

(a)

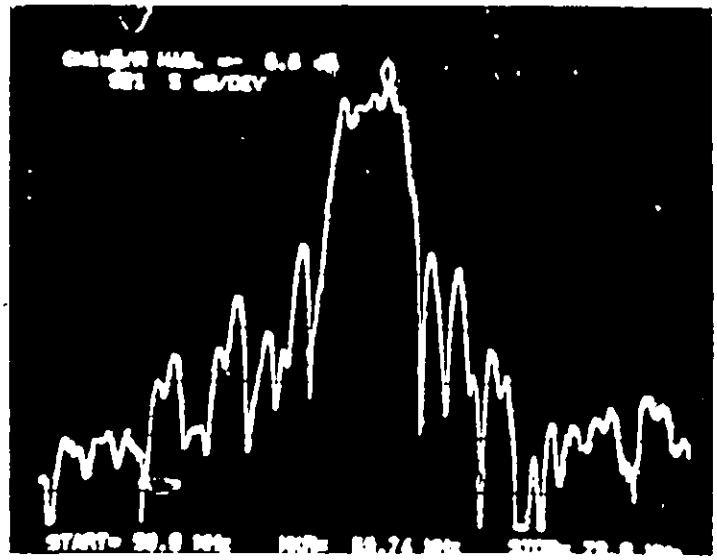

(b)

4.2.3 5:4 IIDT Filter.

Further increasing the number of transducers causes a further degradation of the in-band performance. Figure 4.12 predicts the frequency response of a 5:4 device, which corresponds to the maximum mask size allowed by the photo reduction equipment. All transducers have 21 fingers and are separated by 20 wavelengths. The aperture is set at 1 mm. Figure 4.13 (a) shows the experimental frequency response of the filter. Mismatching the input of this device does not appreciably reduce the amount of ripple, since regeneration by the end input transducers has a much smaller relative effect. Most of the ripple is now caused by the generated waves propagating under all the output transducers. This is clearly visible on the impulse response in Figure 4.13 (b) where, following the peak at time 0 due to electromagnetic feedthrough, there are 5 distinct peaks. The fifth peak on a 4 output IDT device indicates that regeneration is still present to some degree.

4.2.4 IIDT With Slanted Fingers.

The IIDT structures defined thus far have all possessed some degree of ripple. The periodicity of the

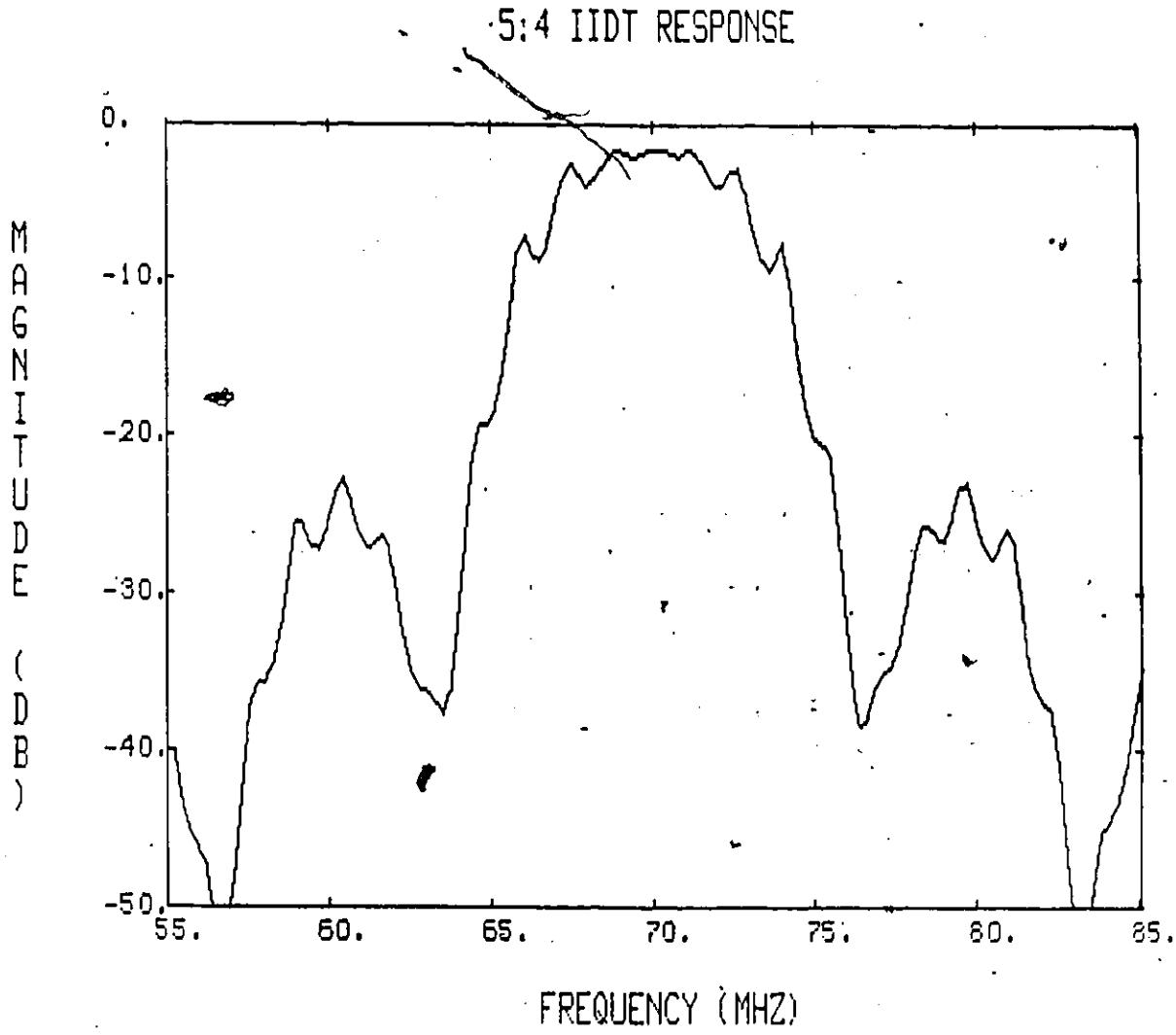

Figure 4.12: Predicted frequency response of 5:4 IIDT device

Figure 4.13: Responses of 5:4 IIDT device
(a) Experimental frequency response
(Horizontal sweep 55 to 85 MHz,
vertical scale 5 dB/div, mkr -4.9 dB)
(b) Experimental impulse response

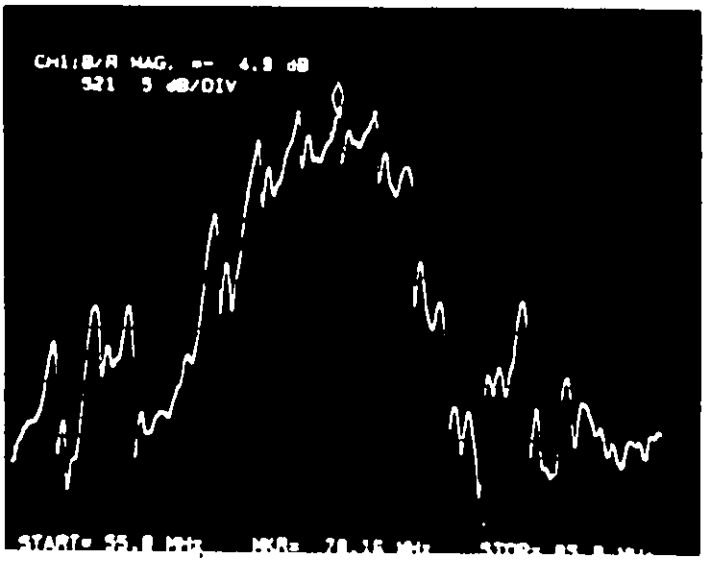
CH1:B/R MAG. 4.8 dB
S21 5 dB/DIV

(a)

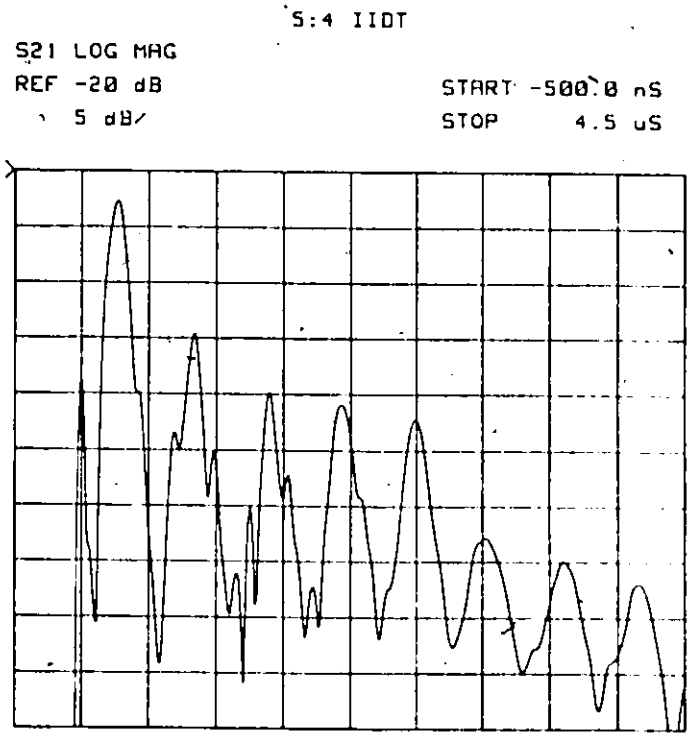
S:4 IIDT
S21 LOG MAG
REF -20 dB
5 dB/
START -500.0 nS
STOP 4.5 uS

(b)

ripple is determined by the distance between the centers of the transducers. This opens the interesting possibility of varying these distances in some way, so that the superposition of all the peaks produces an overall smoothing effect. This is similar to the technique used in [39] for SAW resonators.

The most promising approach involves sloping the transducers as shown in Figure 4.14. In this case, the distance between the transducers in their upper portion is less than the distance in their lower portion, with a smooth transition in between. Note that the finger spacings are constant, and that the slope increases as the edge of the structure is approached. When the contribution of each infinitessimal part of the aperture is vector summed, the desired smoothing effect should result. This technique will only work on auto-collimating substrates which tend to steer the beam towards the other transducers located along the preferred SAW propagating direction. The tilt angle should not exceed 9 degrees from the propagating axis in the case of lithium niobate [40].

A slanted transducer IIDT has been fabricated by the author using a 3:2 structure in an attempt to smooth the passband. Each IDT has 21 fingers, an aperture of 1.8 mm, and a slant designed so that inter-transducer distances vary

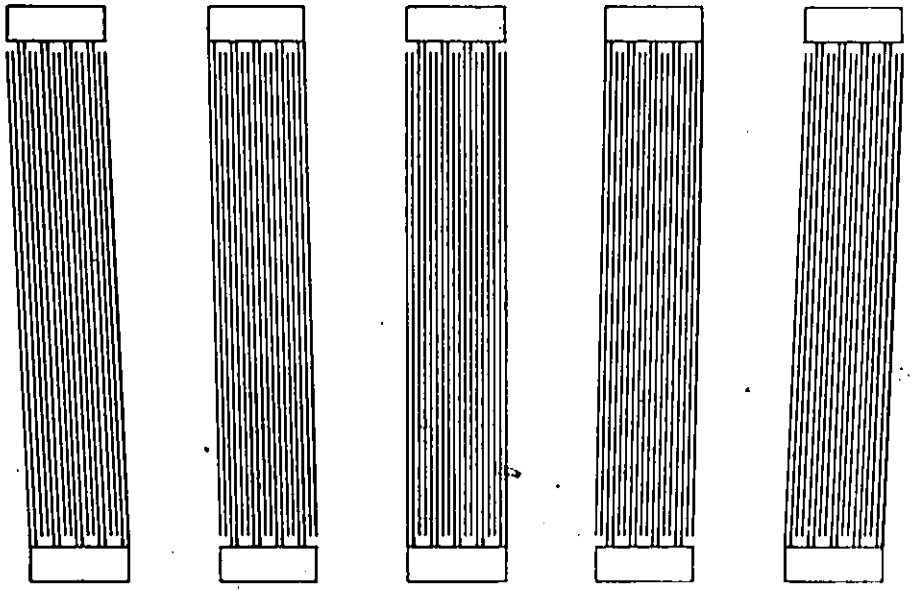

Figure 4.14: IIDT using slanted fingers

from 18 to 18.5 λ_o across the aperture. The resulting experimental frequency response is shown in Figure 4.15, along with the impulse response. The bandwidth is approximately 10%, and insertion loss is 5.9 dB. It can be seen that the filter passband has been smoothed somewhat, and low insertion loss is not sacrificed in the process. The ripple to the left of the passband is a remnant of those seen in the previous devices.

Increasing the transducer slopes beyond the amount used above does not result in any improvement in performance since the standing waves that exist within the structure repeat every half wavelength. In fact, if the slope is increased, destructive interference begins to occur within the passband, and notches appear.

4.2.5 Band Shaping.

In the conventional ideal IIDT, the sidelobes of the filter are 26 dB below the main peak. In practice, since matching is not possible at all frequencies, sidelobes are usually considerably higher than this level, mostly in the 13 to 17 dB range. To improve the suppression, some form of transducer weighting is necessary.

The simplest form involves apodization. By applying

Figure 4.15: Responses of 2:1 slanted IIDT

(a) Experimental frequency response
(Horizontal sweep 50 to 90 MHz,
vertical scale 5 dB/div, mkr -5.9 dB)

(b) Experimental impulse response


S21 5 dB/DIV
START= 50.0 MHz
MKR= 69.5 MHz
STOP= 90.0 MHz

(a)

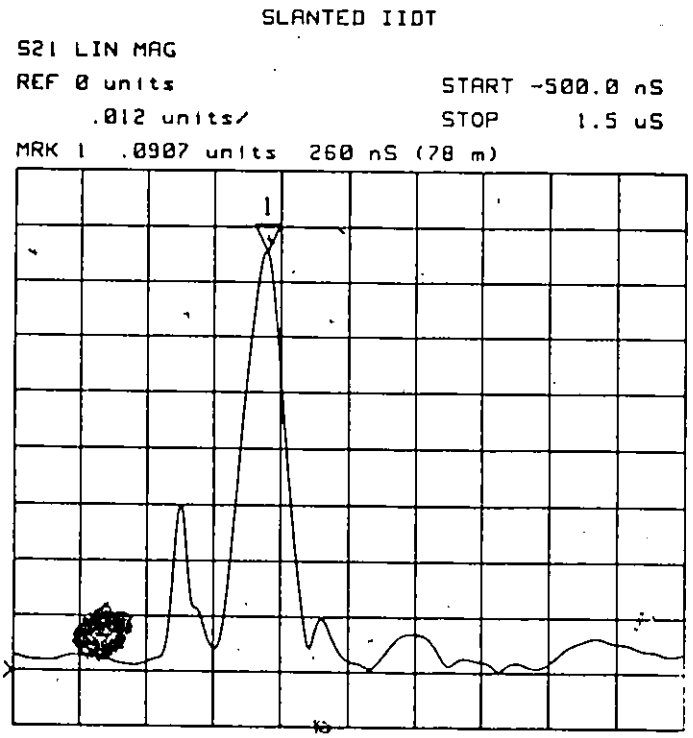
SLANTED IIDT
S21 LIN MAG
REF 0 units
.012 units/
START -500.0 nS
STOP 1.5 uS
MRK 1 .0907 units 260 nS (78 m)
1

(b)

a window function [17] to either the input or the output transducers, the sidelobe suppression can be improved to over 20 dB, as shown in Figure 4.16. To better demonstrate the effect of tap weighting, the frequency responses have been modified by "gating out" the electromagnetic feedthrough which tends to obscure the device's inherent sidelobe level. Both of these devices are 3:2 structures. The unapodized IIDT has 19 fingers in each transducer, while the apodized device has 19 fingers in the input IDTs, and 27 fingers weighted with a Hamming function in the output. The number of fingers has been increased in this case to compensate for the lower coupling efficiency of the apodized transducer. Spacing between transducers is 22 wavelengths in both cases.

Apodization would not work on the slanted transducer IIDT because each portion of the cross-section has a different delay associated with it. Withdrawal weighting would be an alternative, but only for long transducers.

4.3 IIDT Comb Filters.

The inherent comb response of the IIDT structure can be enhanced quite easily by purposely mismatching the input and output transducers so that energy is not absorbed

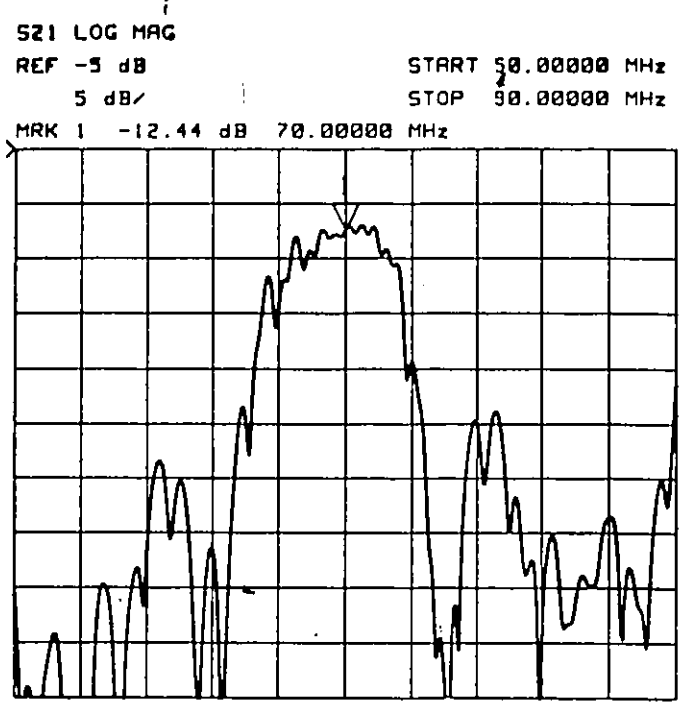

(a)

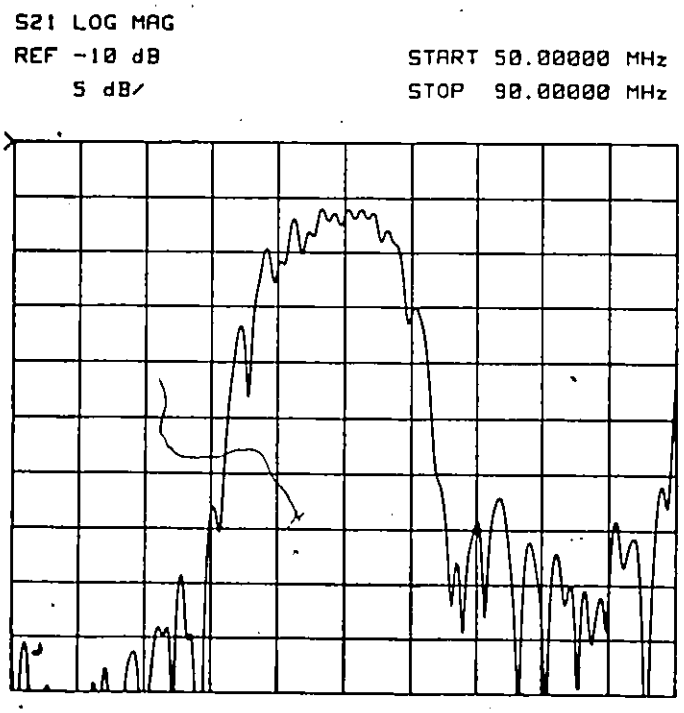

(b)

Figure 4.16: Experimental frequency responses
(a) of unweighted IIDT
(b) of weighted IIDT

efficiently, but tends instead to freely propagate through the whole structure, where it is sampled at discrete points.

Figure 4.17 shows the predicted frequency response of a 5:4 IIDT comb filter. Each of the 9 transducers has 7 fingers, is separated from the next by 10.5 wavelengths, and has an aperture of .8 mm. The device exhibits the classical comb superimposed on a sinc response, where the peaks are roughly 15 dB over the comb sidelobes. It can also be seen that there are two sidelobe peaks between major comb peaks, as is expected for a four tap sampler.

In Figure 4.18, the experimental responses for the IIDT comb can be seen to agree very well with the predicted ones. In particular, the comb peaks and the comb sidelobes can be clearly seen in the frequency response in part (a) of the figure. The impulse response, in part (b), corresponds precisely to the second half of the response of conventional SAW comb filters, as was predicted in Section 3.4. Also evident is a small amount of regeneration, which is indicated by the fifth major peak on a four tap device, and some electromagnetic feedthrough, corresponding to the peak at time 0.

An interesting property of the IIDT comb can be seen in Figure 4.19, which shows its experimental phase response. The non-symmetric impulse response results in a nonlinear phase, as seen in the figure. In particular, the group

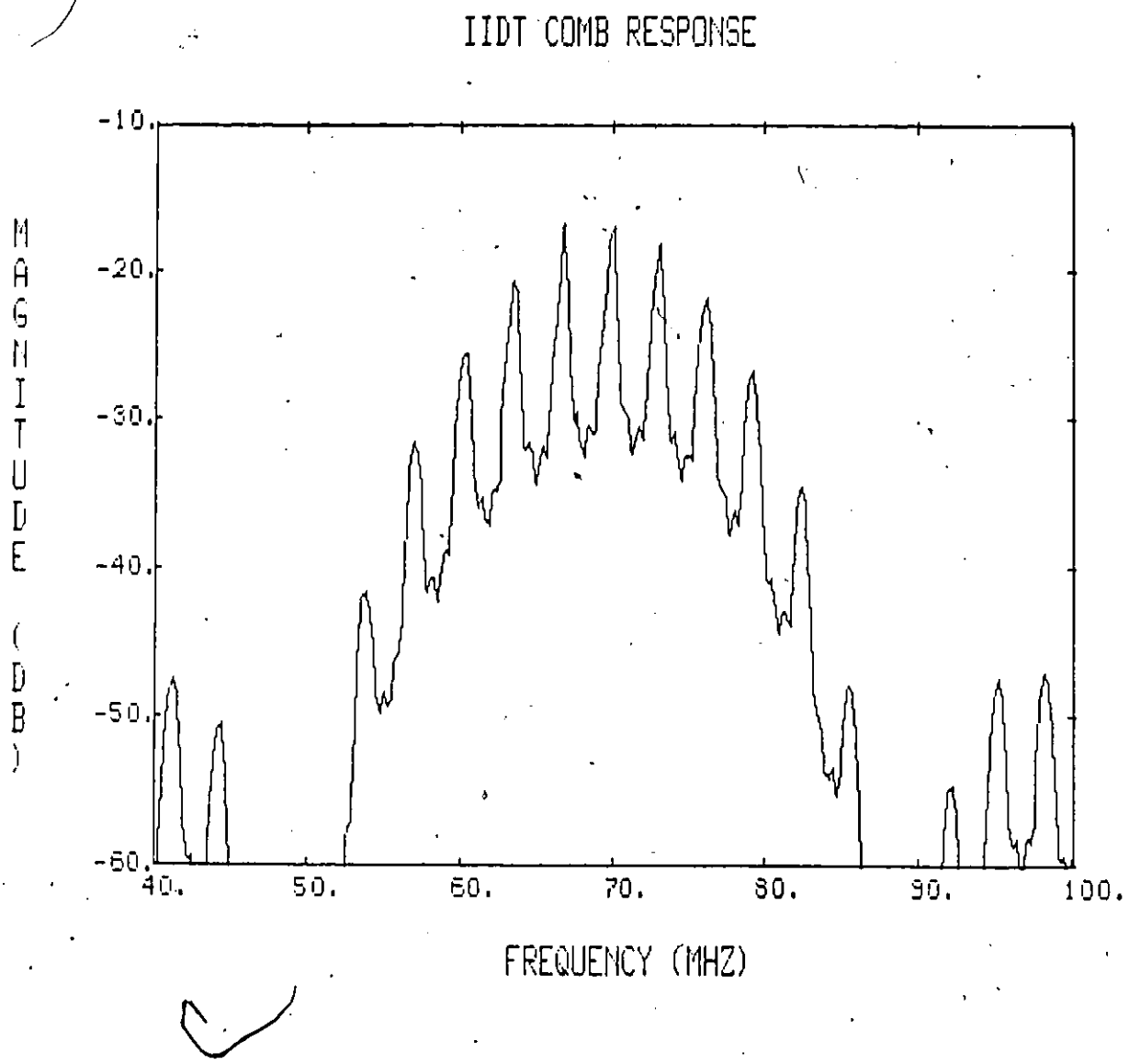

Figure 4.17: Predicted frequency response of IIDT comb

Figure 4.18: Responses of IIDT comb filter

(a) Experimental frequency response
(Horizontal sweep 40 to 100 MHz,
vertical scale 5 dB/div, mkr -13.8 dB)

(b) Experimental impulse response

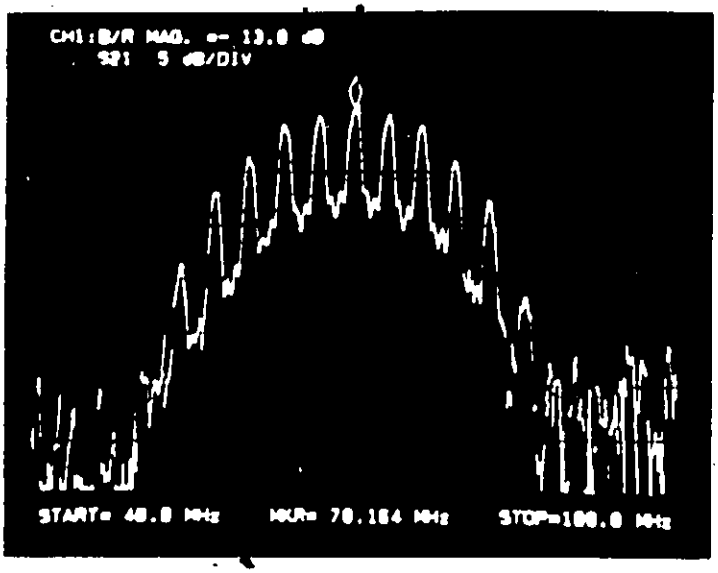
CH1:B/R MAG. -- 13.0 dB
S21 5 dB/DIV
START= 40.0 MHz
MKR= 70.184 MHz
STOP=100.0 MHz

(a)

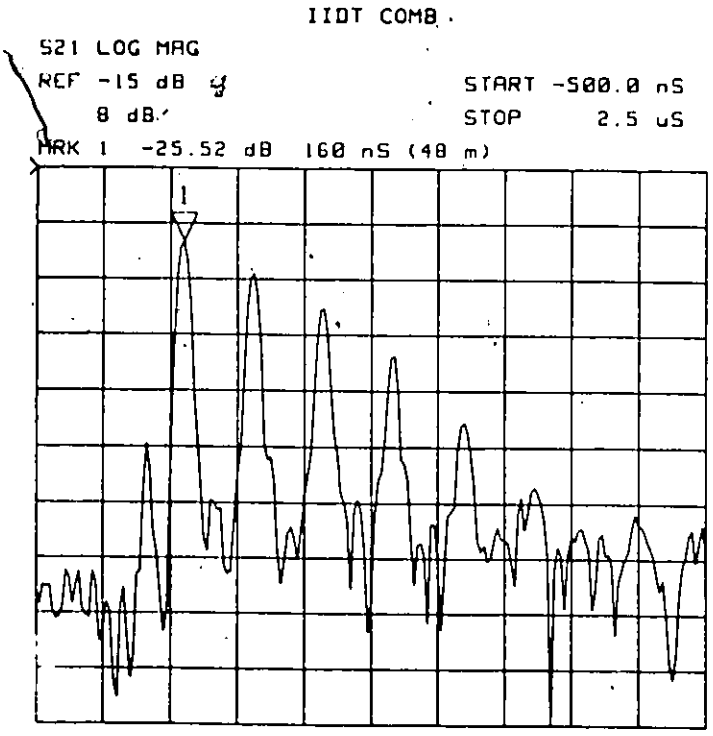
IIDT COMB
S21 LOG MAG
REF -15 dB
8 dB/
START -500.0 nS
STOP 2.5 uS
MRK 1 -25.52 dB 160 nS (48 m)
1

(b)

Figure 4.19: Experimental phase response of IIDT comb (Horizontal sweep 49.9 to 90 MHz, vertical scales 10 dB/div for magnitude, 90^{o}/div for phase)

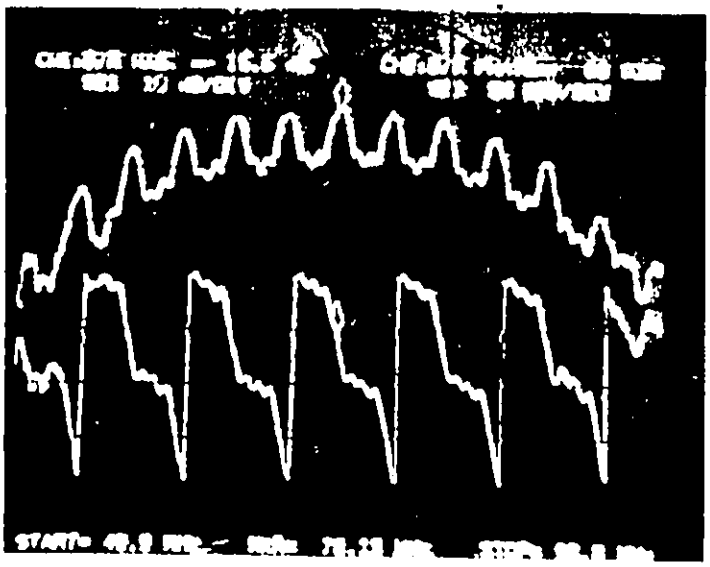

delay, which is defined by

$$\tau = -1/2\pi \ (\partial\phi(f)/\partial f) \qquad (4.3.1)$$

where $\phi(f)$ is the phase shift through the device, increases significantly at the comb peaks. This will enhance the IIDT comb's performance in low-noise oscillator applications [37], where both the loop gain and the loop phase shift conditions must be met.

4.4 IIDT Comb Oscillator.

Figure 4.20 shows the circuit diagram of a multimode oscillator. It involves a loop consisting of the IIDT comb and a 20 dB amplifier. Line lengths are adjusted to satisfy the phase requirements. The mode of oscillation can then be selected by applying a brief injection signal at the desired frequency to the loop. When this external signal is removed, the oscillator will continue to operate at the same frequency.

Figure 4.21 shows the spectrum of the oscillator operating at each of the five central modes. It is clearly seen that when operating in one mode, it is at the total exclusion of all others. In this case, an HP 8662A

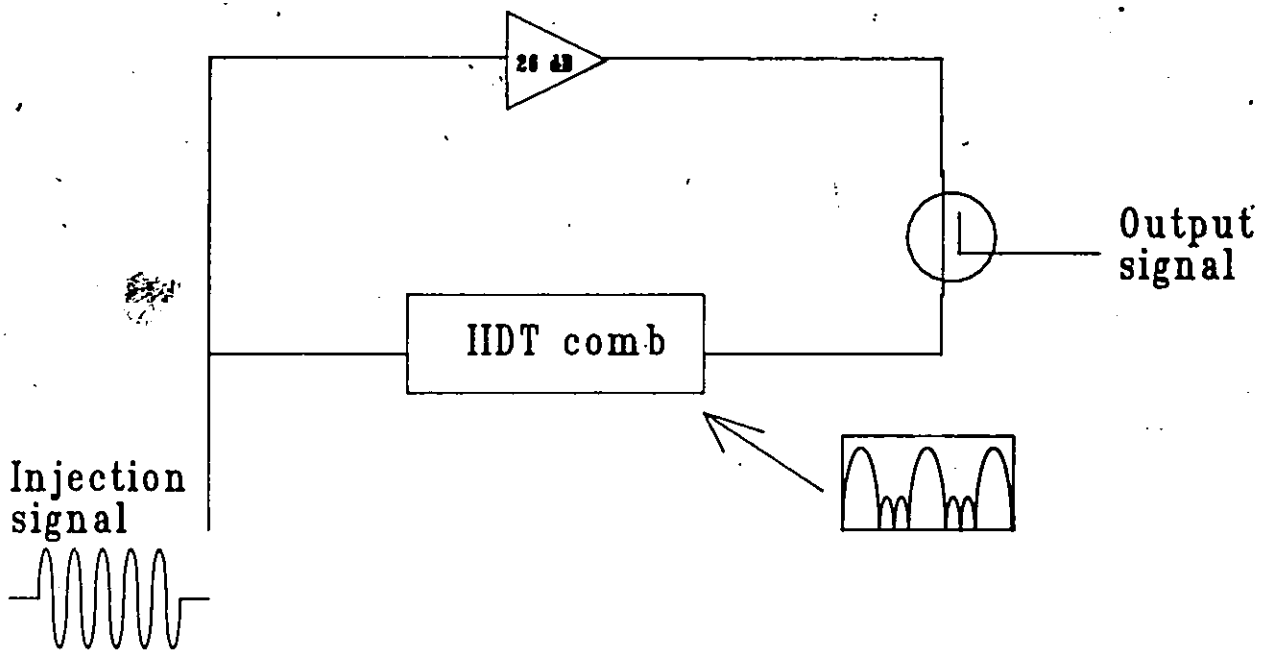

Figure 4.20: Multimode oscillator circuit

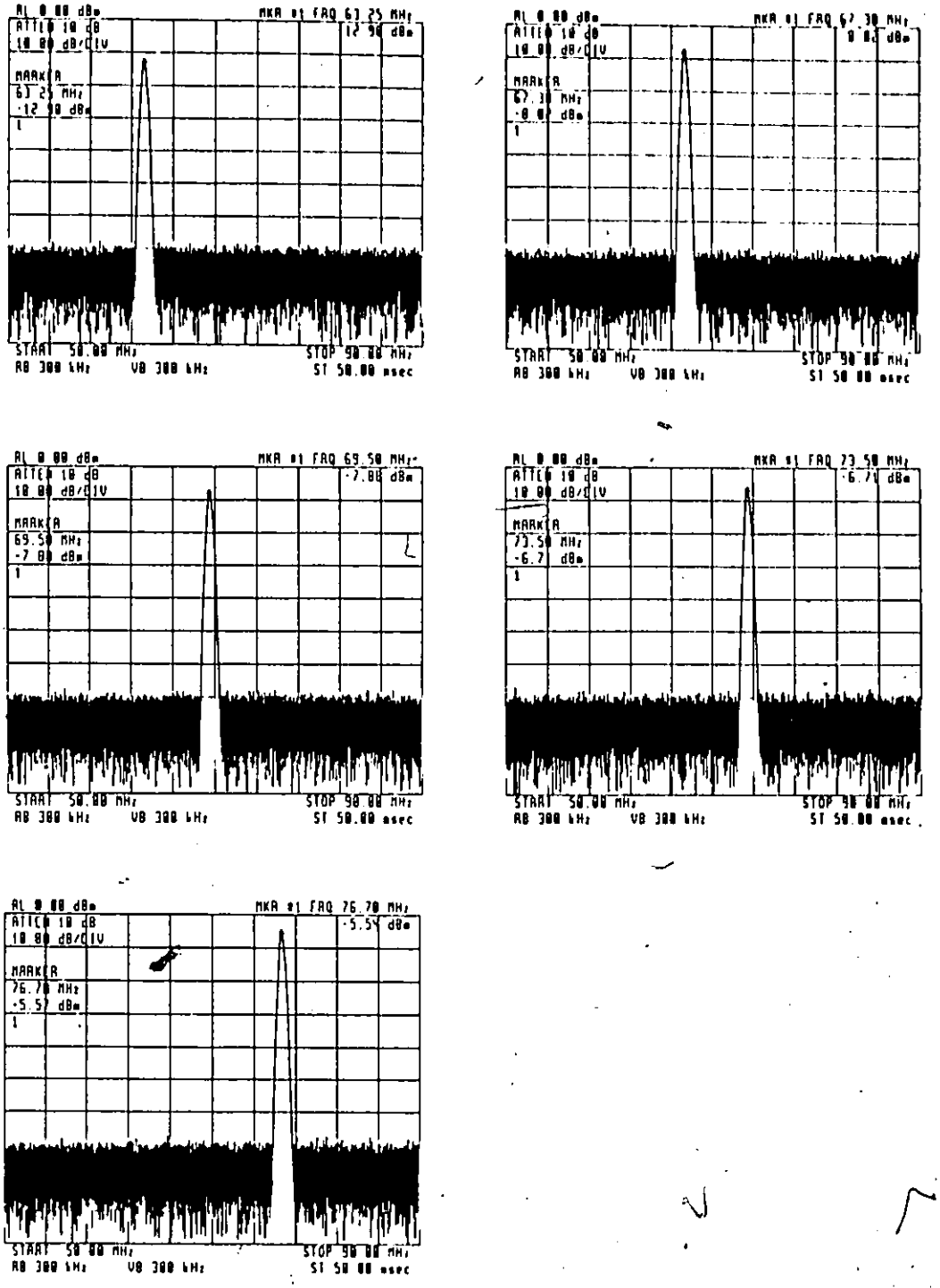

Figure 4.21: Spectrum of oscillator at each of five central modes

synthesizer was used as the injection source. Under the control of the HP 9816 computer, the synthesizer changed frequency to the desired new mode, output power was increased to 0 dBm, and, as quickly as the instruction could be executed, reduced to -120 dBm. At this level, the injection signal had no effect on the oscillator. While this technique is useful in testing the operation of the oscillator, it does not give much information on switching speeds.

For this, much narrower injection pulses are required. Figure 4.22 sketches the setup used. It consists of two pulse generators (HP 222A and HP 8008A), with the first triggering the second. The outputs of each is then mixed with signals coming from two separate sources, each dialed into one of the oscillator modes. The output of these mixers are then summed by means of a hybrid, and this is then used as the injection signal. In this way, the oscillator will switch back and forth between two modes, and measurements can be made on an oscilloscope. Figure 4.23 shows a photograph of the switching in progress. Each of the two RF pulses, in this case with frequencies of 67.3 and 73.5 MHz, is approximately 100 ns long, and, after about 50 ns, the oscillator is seen to continue oscillating at the new frequency. Full settling does not occur until the injected signal has propagated around the loop, which takes

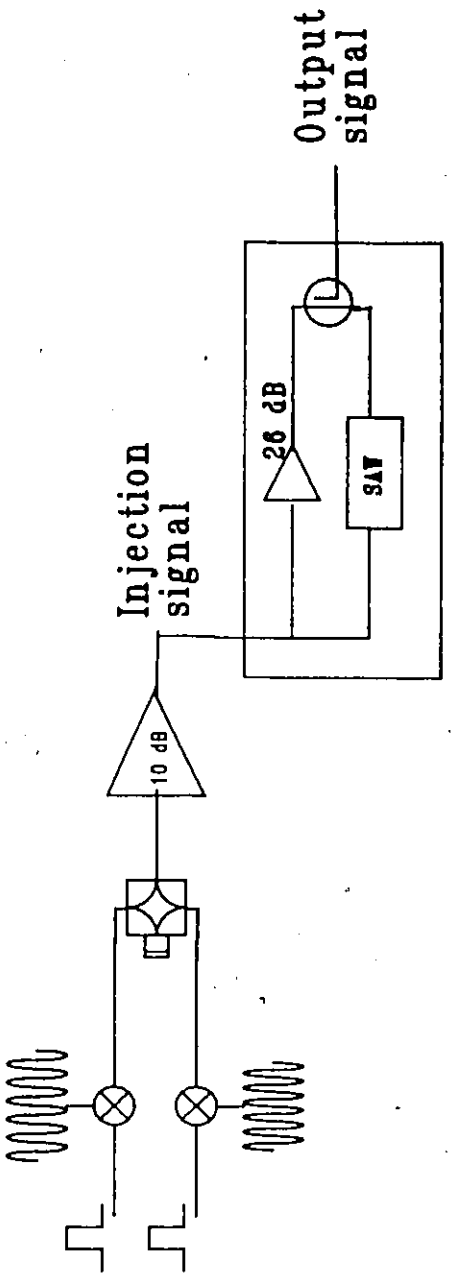

Figure 4.22: Circuit used to measure switching time of multimode oscillator

Figure 4.23: Oscillator output during switching

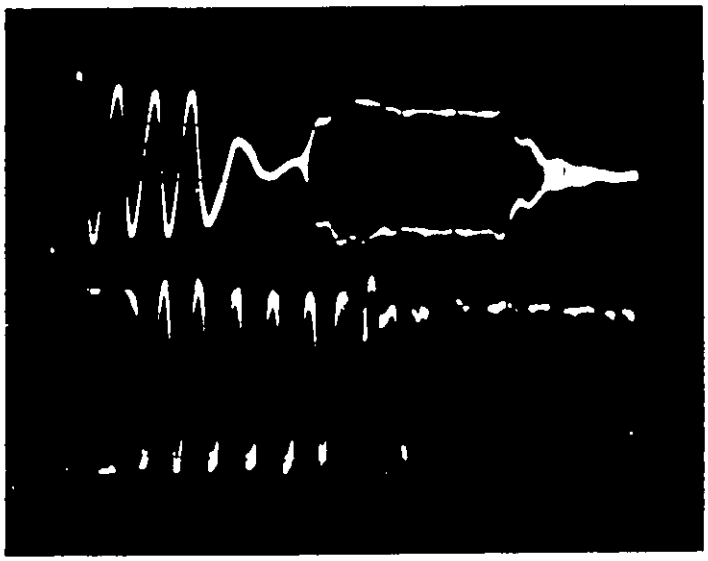

close to 1 μs.

Oscillator stability is usually measured in terms of phase noise [37], which is expressed in dBc/Hz, meaning dB below the carrier in a 1 Hz bandwidth. Following the analysis by Leeson [41], the phase noise exhibits varying characteristics at different frequency intervals, depending on the underlying slope. These include random walk (f^{-4}), flicker frequency (f^{-3}), white frequency (f^{-2}), flicker phase (f^{-1}), and white phase (f^{0}) noise. The last two are due to noise sources external to the oscillator loop, while flicker frequency and white frequency represent their effects within the loop [8].

The phase noise of the IIDT comb while operating at one of the modes is plotted in Figure 4.24, as measured on an HP 5390A frequency stability analyzer using Hadamard techniques [42]. At low frequency offsets, random walk prevails. This is expected, since the oscillator is not phase locked to a stable reference and, in the long term (corresponding to small frequency offsets), the frequency of oscillation will vary with time. Flicker frequency is not observed in this oscillator, and for offsets of 200 to 1000 Hz, white frequency noise is dominant. Beyond 1 kHz, flicker phase noise is seen. If larger frequency offsets were observed, white phase noise would also be visible.

While not matching the performance of some resonator

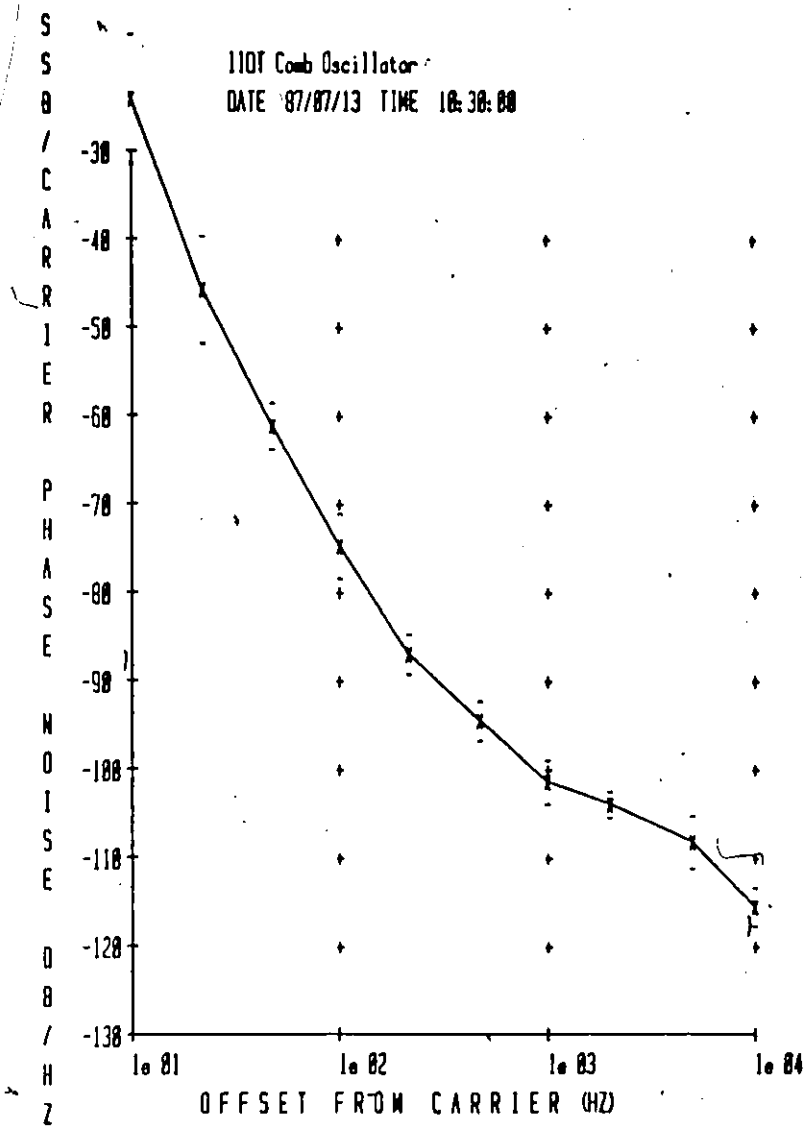

Figure 4.24: Oscillator phase noise plot

based systems, this performance is sufficient for many applications. In fact, at offsets of 10 kHz, the phase noise is seen to approach the limits of the measurement system, indicated by a ")" on the plot. This performance can be attributed to a great extent to the IIDT comb, where the relatively low loss, as compared to other SAW comb filters, and the large group delay tend to improve performance [37]. Further improvements would be expected if the system were temperature stabilized.

The reason for injection locking becomes obvious at this point. A very cheap signal source can be used to switch the oscillator from one mode to another, and, once the injection is removed, the system takes on the low noise characteristics of the SAW oscillator.

The external source can be of many types beyond the admittedly expensive synthesizers used in the above experiments. One, which has been used in a similar context [43] uses two chirp filters with group delay slopes of equal magnitude, but of opposite signs. As illustrated in Figure 4.25, if both chirps are impulsed with delayed pulses, and the outputs are mixed, the output of the mixer will be an rf pulse of constant frequency. The latter will depend only on the relative delay of the two pulses.

While this chirp-synthesizer can generate a range of frequencies, it is not able to maintain them for long, since

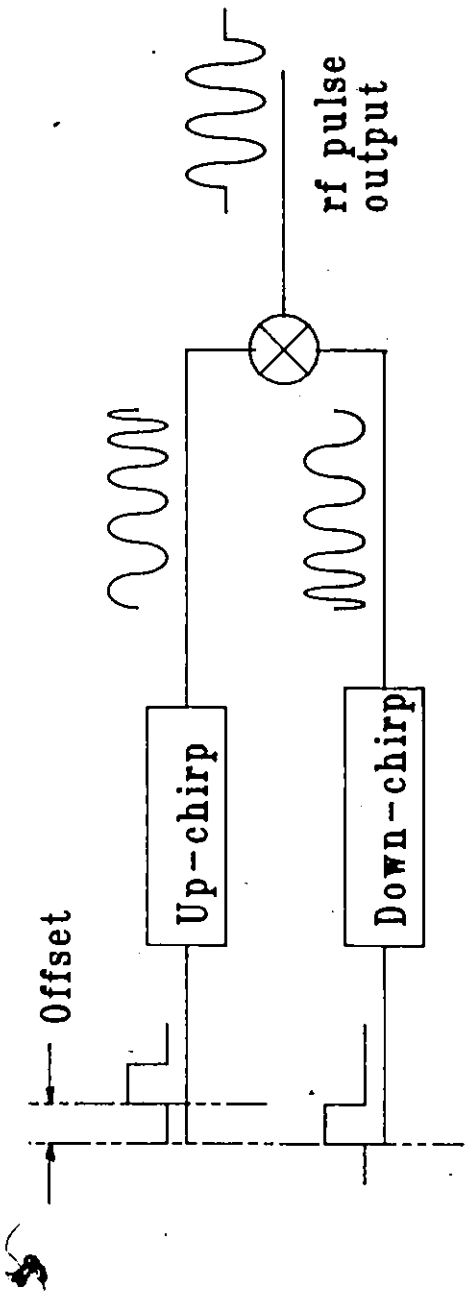

Figure 4.25: Chirp-synthesizer circuit

the duration of the rf pulse depends on the overlap period of the impulsed chirps. Not only does the duration vary with the output frequency, but it will never exceed the total impulse duration of the chirps. By using these outputs to force a mode change, on the other hand, the signal can be maintained indefinitely at one of the modes.

Other external frequency sources could include Voltage Controlled Oscillators (VCOs) using varactor diodes. These are widely available, but by themselves do not provide low noise operation.

A multimode oscillator system based on the IIDT comb filter could be used in frequency agile radar applications where fast switching over a few frequencies is required. It could also be used in a high capacity modem using a small signal set, or in a television channel selection circuit.

CHAPTER 5

CONCLUSIONS

This Thesis reports on a search for knowledge on the subject of Interdigitated Interdigital Transducers (IIDT) SAW filters. Previous work has only provided some limited experimental results, with no effort made to model such structures [25].

Chapter 2 provides a detailed model to analyze most SAW structures. Based on transmission matrices derived from Coupled Mode theory, it allows arbitrary combinations of transducers, reflectors and spaces to be studied with no additional programming required. This solves the problem of having to rewrite analysis tools for each device configuration.

Chapters 3 and 4 provide theoretical and experimental evidence to the validity of the model. They also describe many of the problems encountered in the implementation of the IIDT structures which have not previously been adequately portrayed. The most important of

these is the difficulty in achieving full, or even significant, energy absorption by the output transducers. This causes acoustic energy to propagate under several output transducers, which leads to ripple in the filter passband.

Techniques are then proposed to limit the degradation that results therefrom. These include purposely mismatching the input transducers to reduce regeneration at the expense of an increase in insertion loss, and positioning the ripples in such a manner as to benefit from their presence. Slanting the transducers by a small amount is a novel technique shown to also result in an improvement in ripple suppression by interleaving the ripples in order to achieve a smoothing effect.

When the ripple can be controlled, the IIDT device provides an excellent approach to achieve relatively wideband ($\approx$ 10%), low loss ($<$ 6 dB) filters with sidelobe levels exceeding 20 dB. In particular, its small size should make it very cost competitive. Other low-loss SAW filters either cannot compete in bandwidth, require much more crystal surface area or use costly external matching and phase shifting circuitry.

Enhancing the ripples gives us a comb structure that shows great promise. It has lower insertion loss than the conventional comb structures and is considerably more

compact. Its application to frequency hopped oscillators leads to switching times of well under 1 μs, which is as fast as any other technique known to the author. The short term stability is also excellent, though the sensitivity of lithium niobate to temperature changes could affect long term performance.

A lot of work could still be done to the computer program to improve the rudimentary interface between user and model. While presenting the user with softkeys as a means of making choices is sufficient for the current purpose, a pointing device would be more convenient.

The SAW device model itself could be extended to include multistrip couplers and multiphase transducers. Computational speed could be improved by writing time-critical sections in assembly language as well as recognizing and making use of common transfer matrices between sections instead of recomputing them. These solutions might then allow placing the computations in an optimization loop and applying the program to automated device synthesis.

The IIDT structure seems destined to exhibit some degree of ripple in the passband. Slanting the transducers leads to the most promising results, but this does not allow any apodization. Investigations to further reduce the ripples by varying transducer separations independently, in

order to achieve a smoothing effect, might be worthwhile.

Finally, response degradation due to electromagnetic feedthrough, a common problem in all SAW devices, has yet to find a solution. Its effect is particularly pronounced in the case of IIDT filters and, while the techniques described in Chapter 4 lead to some improvements, further work is necessary.

APPENDIX A

SCATTERING AND TRANSMISSION PARAMETERS

A.0 Definition of Paramenters.

The scattering and the transmission matrices are defined in terms of Figure 2.1 as

$$\begin{bmatrix} S_{i-1} \\ R_i \\ V_{out} \end{bmatrix} = \begin{bmatrix} s_{11} & s_{12} & s_{13} \\ s_{21} & s_{22} & s_{23} \\ s_{31} & s_{32} & s_{33} \end{bmatrix} \begin{bmatrix} R_{i-1} \\ S_i \\ V_{in} \end{bmatrix}$$

and

$$\begin{bmatrix} R_{i-1} \\ S_{i-1} \\ V_{out} \end{bmatrix} = \begin{bmatrix} t_{11} & t_{12} & t_{13} \\ t_{21} & t_{22} & t_{23} \\ t_{31} & t_{32} & t_{33} \end{bmatrix} \begin{bmatrix} R_i \\ S_i \\ V_{in} \end{bmatrix}$$

A.1 Scattering to Transmission Conversion.

$$t_{11} = 1/s_{21} \qquad t_{12} = -s_{22} / s_{21} \qquad t_{13} = -s_{23} / s_{21}$$

$$t_{21} = s_{11}/s_{21} \qquad t_{22} = s_{12}-s_{11}s_{22}/s_{21} \qquad t_{23} = s_{13}-s_{11}s_{23}/s_{21}$$

$$t_{31} = s_{31}/s_{21} \qquad t_{32} = s_{32}-s_{22}s_{31}/s_{21} \qquad t_{33} = s_{33}-s_{23}s_{31}/s_{21}$$

A.2 Transmission to Scattering Conversion.

$$s_{11} = t_{21}/t_{11} \qquad s_{12} = t_{22}-t_{12}t_{21}/t_{11} \qquad s_{13} = t_{23}-t_{13}t_{21}/t_{11}$$

$$s_{21} = 1/t_{11} \qquad s_{22} = -t_{12}/t_{11} \qquad s_{23} = -t_{13}/t_{11}$$

$$s_{31} = t_{31}/t_{11} \qquad s_{32} = t_{32}-t_{12}t_{31}/t_{11} \qquad s_{33} = t_{33}-t_{13}t_{31}/t_{11}$$

APPENDIX B

SAW DEVICE FABRICATION

B.0 Introduction.

All device fabrication is done within the Microwave Acoustics Laboratory at the University. The process begins with a crystal wafer and progresses through to the SAW device. It allows device sizes ranging up to about 2 cm, with resolution limiting line widths to 5 μm. The lack of clean room facilities, however, usually precludes attempting line widths of less than 10 μm because of contamination.

The next four sections provide a very brief overview of the fabrication procedures used at McMaster University to build a SAW device. The intention is not to give a full description of SAW device fabrication techniques, but to inform the reader of the general steps that are followed.

B.1 Mask Preparation.

The mask is generated using a Hewlett-Packard 9836 desktop computer driving an HP 7586B drafting plotter. A menu driven program was written that accepts a reduced set of the same input data as the simulation program described in this Thesis. It allows the generation of masks for apodized and non-apodized transducers, slanted finger transducers, stepped finger transducers, shorted and open-circuited reflector arrays, stepped reflector arrays, multistrip couplers and spaces. A photograph of the setup is given in Figure B.1.

The source patterns are drawn on size E Polyester film using drafting pens filled with Indian ink. The pens tips come in .18 mm, .35 mm, .5 mm, .7 mm and 1 mm sizes. To obtain the correct line thickness, a second pass is made with the pen offset by a computed amount. The whole plot is repeated 3 times for improved contrast.

These patterns are then reduced 100X in a two-step process. In the first, the mask is reduced 5X onto a 5 x 7 inch Kodalith sheet of film. For this, a camera with a 135 mm f1.8 lens is used, capable of 10 lines/mm resolution. In the second, the photograph is reduced a further 20X onto a Kodak 2 x 2 inch high resolution glass plate using a camera with a 75 mm f4.0 lens, capable of 200 lines/mm. This slide

Figure B.1: Mask generating equipment

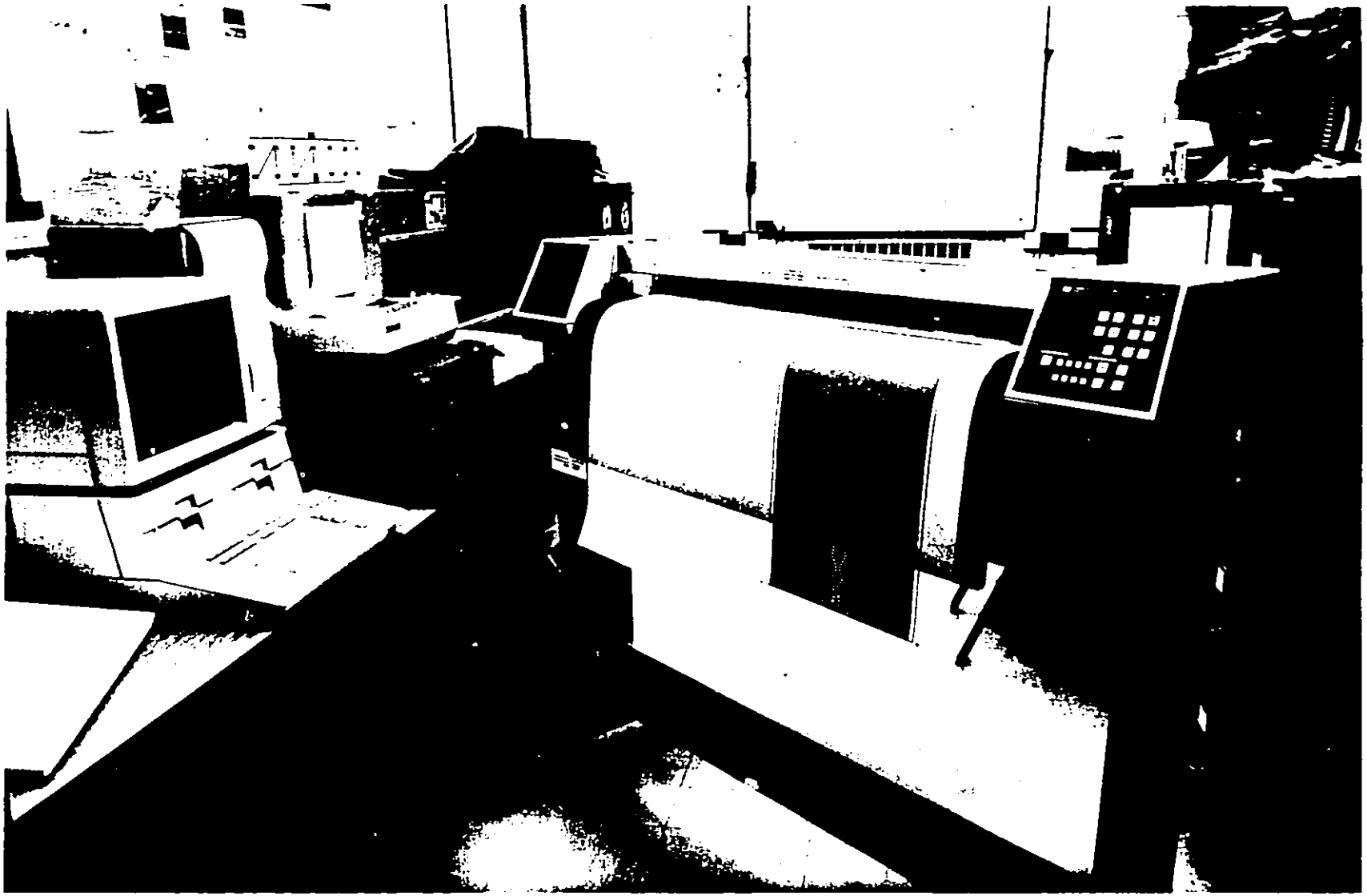

is then used in the device fabrication.

B.2 Substrate Preparation.

The substrates are usually purchased as 3 inch wafers. These are cut using a circular high speed saw into .5 X 1 inch sections. These are usually reused many times for the sake of economy.

The substrate is first etched to remove any remaining aluminium from previous devices. Then it is cleaned using acetone, then trichloroethylene and lastly methanol the remove any contaminants. Once clean, they are placed in an Edwards vacuum unit which is pumped down to 10^{-6} mbar. Aluminium is then evaporated to a thickness of 1000 Å by heating a tungsten coil containing a 1 cm piece of Aluminium wire. The thickness is controlled by exposing an oscillator crystal to the aluminium vapor and recording the resulting frequency change.

The substrates are removed from the unit and coated with Shipley Microposit Photo Resist type 1400-17 and spun at 4000 rpm for a minute. Baking them at 80^{o}C for 30 minutes hardens the resist.

B.3 Device Fabrication.

The coated substrate is selectively exposed to Ultra Violet (UV) light using a Kasper Instruments type 2001 mask aligner (resolution: 1.5 μm) and the mask described in section B.1. The photo resist is developed using Shipley Microposit developer and the substrate is etched using a solution of 25 parts phosphoric acid (H_3PO_4), 5 parts acetic acid ($C_2H_4O_2$) and 1 part nitric acid (HNO_3). A rinse in acetone to remove the remaining photo resist completes the fabrication process.

B.4 Device Mounting and Testing.

The device is attached to an Airpax microcircuit package by means of black wax. The lack of bonding facilities requires the use of GC Electronics Silver Print as a bonding agent for the connecting wires. It provides a good electrical contact and can easily be removed for substrate and package reuse.

Device testing is done on the HP 8505 network analyzer, shown in Figure B.2, connected to an HP 9816 computer running time domain software. This allows the measured frequency domain data to be downloaded to the

Figure B.2: HP 8505 network analyzer setup

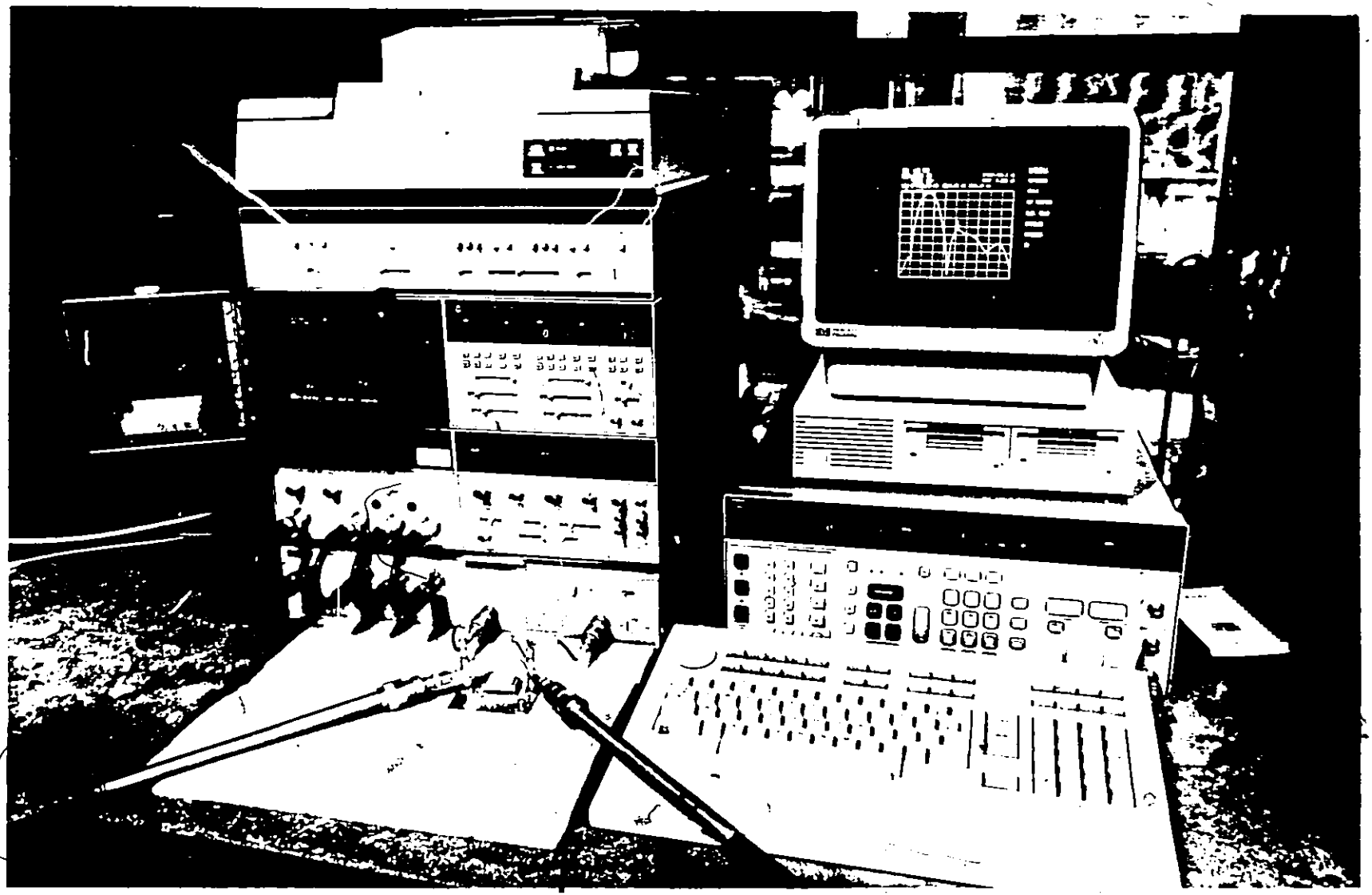

computer and analyzed. It also allows selected components in the impulse response to be gated out and their effect on the frequency response to be determined.

APPENDIX C

COUPLING-OF-MODES COMPUTER PROGRAM

The following pages contain a complete source listing of the Coupling-of-Modes program written by the author to analyze SAW devices. It was compiled using a Microsoft FORTRAN 5 compiler (v. 3.3) on a Texas Instruments Business-Pro micro-computer running a Microsoft DOS operating system (v. 3.05). Graphics are controlled by means of the ZABLIB library available at the University.

The listing includes five modules. COM is the main program that calls the other subroutines. EDIT allows the current SAW device configuration to be defined and displayed. CMPUTE computes the frequency and impulse responses of the SAW device. PLOT displays these responses. Finally, STORAGE allows the user to store and retrieve device configurations as well as their responses.

```
$STORAGE:2
$NOFLOATCALLS
      PROGRAM COM
C*****************************************************************************
C*
C*  SYSTEM TO COMPUTE THE FREQUENCY RESPONSE OF ARBITRARY SURFACE ACOUSTIC
C*  WAVE STRUCTURES USING COUPLING OF MODES THEORY.
C*
C*  BY PETER M. SMITH, MCMASTER UNIVERSITY, HAMILTON, ONTARIO.
C*  VERSION 1 WRITTEN JANUARY 1986
C*  LATEST UPDATE: MAY 1987
C*
C*
C*  VARIABLES USED:
C*
C*       ALLFLG - FLAG INDICATING THAT ALL MATRICES ARE INVALID
C*        KSOFT - LAST SOFTKEY PRESSED
C*    SECLEN(I) - LENGTH OF CURRENT SECTION IN HALF WAVELENGTHS
C*    SECFLG(I) - ARRAY OF FLAGS INDICATING THAT THE MATRICES
C*                DESCRIBING THE I-TH ELEMENT ARE INVALID
C*      TYPE(I) - ARRAY DESCRIBING ELEMENT IN POSITION I OF STRUCTURE
C*                111 - UNAPODIZED INPUT IDT WITH SINGLE FINGERS
C*                112 - APODIZED INPUT IDT WITH SINGLE FINGERS
C*                121 - UNAPODIZED INPUT IDT WITH SPLIT FINGERS
C*                122 - APODIZED INPUT IDT WITH SPLIT FINGERS
C*                211 - UNAPODIZED OUTPUT IDT WITH SINGLE FINGERS
C*                212 - APODIZED OUTPUT IDT WITH SINCLE FINGERS
C*                221 - UNAPODIZED OUTPUT IDT WITH SPLIT FINGERS
C*                222 - APODIZED OUTPUT IDT WITH SPLIT FINGERS
C*                311 - OPEN CIRCUITED REFLECTOR ARRAY
C*                321 - SHORT CIRCUITED REFLECTOR ARRAY
C*                400 - SPACE
C*    VALDAT(I) - ARRAY OF FLAGS INDICATING VALID DATA AVAILABLE
C*                1 - CRYSTAL SUBSTRATE        5 - APERTURE
C*                2 - FREQUENCIES              6 - LOAD IMPEDANCE
C*                3 - STRUCTURE                7 - ALL DATA
C*                4 - NUMBER OF STRIPS
C*
C*****************************************************************************
C*
      INTEGER KSOFT
      INTEGER SUBSTR, SCTION, TYPE(20)
      INTEGER XSCALE, YSCALE, POINTS
      REAL SECLEN(20), FREQ0, FRQMIN, FRQMAX, APRTUR, RS
      REAL FREQ(512), TIME(512)
      COMPLEX OUTSIG(512), OUTTME(512), ZE
      REAL KAPPA, ALPHA, THETA, METRAT
      LOGICAL*2 ALLFLG, VALDAT(8), MATCH
      CHARACTER*14 DATSTR*14, TIMSTR*9, LSTTME*9, PLTTTL*40
      COMMON KSOFT
      COMMON /FLAGS/ ALLFLG, VALDAT
      COMMON /STATUS/ SUBSTR, SCTION, TYPE, FREQ0, FRQMIN, FRQMAX,
     1       SECLEN, APRTUR, ZE, RS, KAPPA, ALPHA, THETA, METRAT
      COMMON /PLTBLK/ XSCALE, YSCALE, POINTS, MATCH, PLTTTL, TMIN, TMAX
      COMMON /RSPBLK/ FREQ, OUTSIG, TIME, OUTTME
C*    SET UP SYSTEM
      CALL SETUP
C*    SHOW DATE AND TIME
    5 CALL CLRGRF
      CALL DISP('@X@7@L04@C20Today is _')
      CALL GETDAT(DATSTR)
      CALL DISP(DATSTR)
```

```
      CALL DISP('@7@L04@C43at _')
      CALL GETIM(TIMSTR)
      CALL DISP(TIMSTR)
      LSTTME = TIMSTR
*     DISPLAY USER OPTIONS
      CALL DISP('@5@L02@C15@UC O M   S A W   A N A L Y S I S   S Y S T E
     1 M@u@4@L08@C09\ F1 \ Recall previous state@L10@C09\ F2 \ Save curr
     2ent state@6@L12@C09\ F5 \ Edit current structure@L14@C09\ F6 \ Edi
     3t plot parameters@7@L16@C09\ F9 \ Compute current response@L18@C09
     4\ F10 \ Plot current response@2@L22@C09\ F12 \ EXIT_')
*     ACTIVATE VALID SOFTKEYS
      CALL KEYON(1)
      CALL KEYON(2)
      CALL KEYON(5)
      CALL KEYON(6)
      CALL KEYON(9)
      CALL KEYON(10)
      CALL KEYON(12)
*     WAIT FOR USER INPUT
   10 CALL GETIM(TIMSTR)
      IF (TIMSTR .NE. LSTTME) THEN
        CALL DISP('@7@L04@C46_')
        CALL DISP(TIMSTR)
      ENDIF
      LSTTME = TIMSTR
      CALL FLUSH
      IF (KSOFT .EQ. 1) THEN
        CALL RECALL
      ELSEIF (KSOFT .EQ. 2) THEN
        CALL SAVE
      ELSEIF (KSOFT .EQ. 5) THEN
        CALL EDIT
      ELSEIF (KSOFT .EQ. 6) THEN
        CALL EDPLOT
      ELSEIF (KSOFT .EQ. 9) THEN
        CALL CMPUTE
      ELSEIF (KSOFT .EQ. 10) THEN
        CALL PLOT
      ELSEIF (KSOFT .EQ. 12) THEN
        GOTO 15
      ENDIF
      IF (KSOFT .NE. 0) THEN
        KSOFT = 0
        GOTO 5
      ELSE
        GOTO 10
      ENDIF
*     DEACTIVATE ALL SOFTKEYS
   15 CALL KEYOFF(1)
      CALL KEYOFF(2)
      CALL KEYOFF(5)
      CALL KEYOFF(6)
      CALL KEYOFF(9)
      CALL KEYOFF(10)
      CALL KEYOFF(12)
*     EXIT TO SYSTEM, CLEAR AND RESET SCREEN TO WHITE
      CALL DISP('@X@7_')
      END
*******************************************************************
      SUBROUTINE SOFTKY
*******************************************************************
*
*  ROUTINE TO FIND NUMBER OF SOFTKEY PRESSED
*
      INTEGER KSOFT
      COMMON KSOFT
```

```
      CALL GETKEY(KSOFT)
      RETURN
      END
*****************************************************************
      SUBROUTINE SETUP
*****************************************************************
*
*  ROUTINE TO SET UP THE SYSTEM
*
      INTEGER I, XSCALE, YSCALE, POINTS
      CHARACTER PLTTTL*40
      LOGICAL*2 ALLFLG, VALDAT(8), MATCH
      INTEGER SUBSTR, SCTION, TYPE(20)
      REAL SECLEN(20), FREQ0, FRQMIN, FRQMAX, APRTUR, RS
      REAL KAPPA, ALPHA, THETA, METRAT
      COMPLEX ZE
      COMMON /FLAGS/ ALLFLG, VALDAT
      COMMON /STATUS/ SUBSTR, SCTION, TYPE, FREQ0, FRQMIN, FRQMAX,
     1       SECLEN, APRTUR, ZE, RS, KAPPA, ALPHA, THETA, METRAT
      COMMON /PLTBLK/ XSCALE, YSCALE, POINTS, MATCH, PLTTTL, TMIN, TMAX
      PI = 4. * ATAN(1.)
*     SET ALL DATA AS INVALID
      ALLFLG = .TRUE.
*     FLAG ALL DATA AS INVALID
      DO 20 I = 1, 7
        VALDAT(I) = .FALSE.
   20 CONTINUE
*     DEFINE SIMULATION CONSTANTS
      RS = 0.
      KAPPA = 200.
      ALPHA = 10.
      THETA = 0.
      METRAT = 0.5
*     DEFINE PLOT PARAMETERS
      XSCALE = 10
      YSCALE = 10
      POINTS = 256
      MATCH = .FALSE.
      PLTTTL = ' '
      TMIN = 0.
      TMAX = 5.E-6
      RETURN
      END
```

```
$STORAGE:2
$NOFLOATCALLS
*****************************************************************
      SUBROUTINE EDIT
*****************************************************************
*
*  ROUTINE TO EDIT CURRENT STRUCTURE TO BE ANALYSED
*
*  BY PETER M. SMITH, MCMASTER UNIVERSITY
*  LATEST UPDATE:   MAY, 1987
*
      INTEGER SUBSTR, SCTION, TYPE(20)
      REAL SECLEN(20), FREQ0, FRQMIN, FRQMAX, APRTUR, RS
      REAL KAPPA, ALPHA, THETA, METRAT
      COMPLEX ZE
      LOGICAL*2 ALLFLG, VALDAT(8), EOSTR
      INTEGER NEWSUB, I, II
      CHARACTER COMAND(82)
      COMMON /FLAGS/ ALLFLG, VALDAT
      COMMON /STATUS/ SUBSTR, SCTION, TYPE, FREQ0, FRQMIN, FRQMAX,
     1       SECLEN, APRTUR, ZE, RS, KAPPA, ALPHA, THETA, METRAT
      EXTERNAL INKEY
      EOSTR = .FALSE.
*     GET A USER COMMAND
    5 CALL STATE
   10 CALL DISP('@7@L24@C05@B\Command\ @b@7_')
      CALL GETSTR(COMAND)
      CALL TRIML(COMAND)
*     DECODE THE COMMAND
      IF (COMAND(1) .EQ. 'C' .OR. COMAND(1) .EQ. 'c') THEN
*       CHANGE THE CRYSTAL SUBSTRATE
        DO 20 I = 1, 81
          COMAND(I) = COMAND(I + 1)
   20   CONTINUE
        CALL TRIML(COMAND)
        READ(COMAND, '(I1)', ERR = 999) NEWSUB
        IF (NEWSUB .LT. 1 .OR. NEWSUB .GT. 3) THEN
          CALL DISP('@2@L25@C05***** INVALID CRYSTAL SUBSTRATE_')
          CALL BELL
          CALL WAIT(20)
        ELSE
          SUBSTR = NEWSUB
          VALDAT(1) = .TRUE.
        ENDIF
      ELSEIF (COMAND(1) .EQ. 'F' .OR. COMAND(1) .EQ. 'f') THEN
*       CHANGE THE FREQUENCY RANGES
        DO 50 I = 1, 81
          COMAND(I) = COMAND(I + 1)
   50   CONTINUE
        CALL TRIML(COMAND)
        CALL CONVERT(COMAND, FRQMIN, EOSTR)
        FRQMIN = FRQMIN * 1.E6
        DO 60 I = 1, 80
          COMAND(I) = COMAND(I + 1)
   60   CONTINUE
        CALL TRIML(COMAND)
        CALL CONVERT(COMAND, FREQ0, EOSTR)
        FREQ0 = FREQ0 * 1.E6
        DO 70 I = 1, 79
          COMAND(I) = COMAND(I + 1)
   70   CONTINUE
        CALL TRIML(COMAND)
```

```
            CALL CONVERT(COMAND, FRQMAX, EOSTR)
            FRQMAX = FRQMAX * 1.E6
            VALDAT(2) = .TRUE.
          ELSEIF (COMAND(1) .EQ. 'S' .OR. COMAND(1) .EQ. 's') THEN
*           CHANGE THE DEVICE STRUCTURE
            II = 1
            DO 71 I = 1, 81
              COMAND(I) = COMAND(I + 1)
 71         CONTINUE
            GOTO 78
 75         DO 76 I = 1, 77
*             REMOVE PREVIOUS CODE FROM COMMAND LINE
              COMAND(I) = COMAND(I + 4)
*76         CONTINUE
*           DECODE EACH CODE IN COMMAND LINE
 78         CALL TRIML(COMAND)
            IF (COMAND(1) .EQ. 'I' .OR. COMAND(1) .EQ. 'i') THEN
*             HAVE INPUT IDT
              IF (COMAND(2) .EQ. 'S' .OR. COMAND(2) .EQ. 's') THEN
*               HAVE SINGLE FINGER INPUT IDT
                IF (COMAND(3) .EQ. 'A' .OR. COMAND(3) .EQ. 'a') THEN
*                 HAVE AN APODISED INPUT IDT WITH SINGLE FINGERS
                  TYPE(II) = 112
                  II = II + 1
                ELSE
*                 HAVE AN UNAPODISED INPUT IDT WITH SINGLE FINGERS
                  TYPE(II) = 111
                  II = II + 1
                ENDIF
              ELSEIF (COMAND(2) .EQ. 'D' .OR. COMAND(2) .EQ. 'd') THEN
*               HAVE DOUBLE FINGER INPUT IDT
                IF (COMAND(3) .EQ. 'A' .OR. COMAND(3) .EQ. 'a') THEN
*                 HAVE AN APODISED INPUT IDT WITH SPLIT FINGERS
                  TYPE(II) = 122
                  II = II + 1
                ELSE
*                 HAVE AN UNAPODISED INPUT IDT WITH SPLIT FINGERS
                  TYPE(II) = 121
                  II = II + 1
                ENDIF
              ELSE
                CALL BELL
              ENDIF
            ELSEIF (COMAND(1) .EQ. 'O' .OR. COMAND(1) .EQ. 'o') THEN
*             HAVE AN OUTPUT IDT
              IF (COMAND(2) .EQ. 'S' .OR. COMAND(2) .EQ. 's') THEN
*               HAVE A SINGLE FINGER OUTPUT IDT
                IF (COMAND(3) .EQ. 'A' .OR. COMAND(3) .EQ. 'a') THEN
*                 HAVE AN APODISED OUTPUT IDT WITH SINGLE FINGERS
                  TYPE(II) = 212
                  II = II + 1
                ELSE
*                 HAVE AN UNAPODISED OUTPUT IDT WITH SINGLE FINGERS
                  TYPE(II) = 211
                  II = II + 1
                ENDIF
              ELSEIF (COMAND(2) .EQ. 'D' .OR. COMAND(2) .EQ. 'd') THEN
*               HAVE A SPLIT FINGER OUTPUT IDT
                IF (COMAND(3) .EQ. 'A' .OR. COMAND(3) .EQ. 'a') THEN
*                 HAVE AN APODISED OUTPUT IDT WITH SPLIT FINGERS
                  TYPE(II) = 222
                  II = II + 1
                ELSE
*                 HAVE AN UNAPODISED OUTPUT IDT WITH SPLIT FINGERS
                  TYPE(II) = 221
                  II = II + 1
```

```
            ENDIF
          ELSE
            CALL BELL
          ENDIF
        ELSEIF (COMAND(1) .EQ. 'R' .OR. COMAND(1) .EQ. 'r') THEN
*         HAVE A REFLECTOR ARRAY
          IF (COMAND(2) .EQ. 'S' .OR. COMAND(2) .EQ. 's') THEN
*           HAVE A SHORTED REFLECTOR ARRAY
            IF (COMAND(3) .EQ. 'T' .OR. COMAND(3) .EQ. 't') THEN
*             HAVE A TAPERED AND SHORTED REFLECTOR ARRAY
              TYPE(II) = 322
              II = II + 1
            ELSE
*             HAVE A NON-TAPERED SHORTED REFLECTOR ARRAY
              TYPE(II) = 321
              II = II + 1
            ENDIF
          ELSEIF (COMAND(2) .EQ. 'O' .OR. COMAND(2) .EQ. 'o') THEN
*           HAVE AN OPEN CIRCUITED REFLECTOR ARRAY
            IF (COMAND(3) .EQ. 'T' .OR. COMAND(3) .EQ. 't') THEN
*             HAVE A TAPERED OPEN REFLECTOR ARRAY
              TYPE(II) = 312
              II = II + 1
            ELSE
*             HAVE A NON-TAPERED OPEN REFLECTOR ARRAY
              TYPE(II) = 311
              II = II + 1
            ENDIF
          ELSE
            CALL BELL
          ENDIF
        ELSEIF (COMAND(1) .EQ. 'S' .OR. COMAND(1) .EQ. 's') THEN
          IF (COMAND(2) .EQ. 'P' .OR. COMAND(2) .EQ. 'p') THEN
*           HAVE A SPACE
            TYPE(II) = 400
            II = II + 1
          ELSE
            CALL BELL
          ENDIF
        ELSEIF (COMAND(1) .EQ. 'M' .OR. COMAND(1) .EQ. 'm') THEN
          IF (COMAND(2) .EQ. 'S' .OR. COMAND(2) .EQ. 's') THEN
*           HAVE A MULTISTRIP COUPLER
            TYPE(II) = 500
            II = II + 1
          ENDIF
        ELSE
*         ASSUME END OF INPUT
          SCTION = II - 1
          GOTO 85
        ENDIF
        GOTO 75
   85   VALDAT(3) = .TRUE.
      ELSEIF (COMAND(1) .EQ. 'N' .OR. COMAND(1) .EQ. 'n') THEN
*       CHANGE THE DIMENSIONS OF THE SECTIONS
        IF (.NOT. VALDAT(3)) THEN
          CALL DISP('@7@L25@C20 ***** MUST INITIALIZE STRUCTURE FIRST_')
          CALL BELL
          CALL WAIT(30)
          CALL ERSLIN(25)
        ELSE
          DO 88 I = 1, SCTION
            SECLEN(I) = 0.
            DO 87 II = 1, 81
              COMAND(II) = COMAND(II + 1)
   87       CONTINUE
            IF (.NOT. EOSTR) THEN
```

```
            CALL TRIML(COMAND)
            CALL CONVERT(COMAND, SECLEN(I), EOSTR)
          ENDIF
 88     CONTINUE
        VALDAT(4) = .TRUE.
      ENDIF
    ELSEIF (COMAND(1) .EQ. 'A' .OR. COMAND(1) .EQ. 'a') THEN
*     CHANGE THE APERTURE
      DO 80 I = 1, 81
        COMAND(I) = COMAND(I + 1)
 80   CONTINUE
      CALL TRIML(COMAND)
      CALL CONVERT(COMAND, APRTUR, EOSTR)
      APRTUR = APRTUR / 1.E3
      VALDAT(5) = .TRUE.
    ELSEIF (COMAND(1) .EQ. 'Z' .OR. COMAND(1) .EQ. 'z') THEN
*     CHANGE THE LOAD IMPEDANCE
      DO 90 I = 1, 81
        COMAND(I) = COMAND(I + 1)
 90   CONTINUE
      CALL TRIML(COMAND)
      CALL CONVERT(COMAND, ZTEMP, EOSTR)
      ZE = CMPLX(ZTEMP, 0.)
      VALDAT(6) = .TRUE.
    ELSEIF (COMAND(1) .EQ. 'M' .OR. COMAND(1) .EQ. 'm') THEN
*     DISPLAY MENU FOR CONSTANTS IN SIMULATION
 95   CALL STATE2
      CALL DISP('@7@L25@C05@B\Command\ @b_')
      CALL GETSTR(COMAND)
      CALL TRIML(COMAND)
      IF (COMAND(1) .EQ. 'R' .OR. COMAND(1) .EQ. 'r') THEN
*       CHANGE THE ELECTRODE RESISTANCE
        DO 100 I = 1, 81
          COMAND(I) = COMAND(I + 1)
100     CONTINUE
        CALL TRIML(COMAND)
        CALL CONVERT(COMAND, RS, EOSTR)
      ELSEIF(COMAND(1) .EQ. 'K' .OR. COMAND(1) .EQ. 'k') THEN
*       CHANGE THE GRATING COUPLING CONSTANT
        DO 110 I = 1, 81
          COMAND(I) = COMAND(I + 1)
110     CONTINUE
        CALL TRIML(COMAND)
        CALL CONVERT(COMAND, KAPPA, EOSTR)
      ELSEIF (COMAND(1) .EQ. 'A' .OR. COMAND(1) .EQ. 'a') THEN
*       CHANGE THE GRATING LOSS COEFFICIENT
        DO 120 I = 1, 81
          COMAND(I) = COMAND(I + 1)
120     CONTINUE
        CALL TRIML(COMAND)
        CALL CONVERT(COMAND, ALPHA, EOSTR)
      ELSEIF (COMAND(1) .EQ. 'M' .OR. COMAND(1) .EQ. 'm') THEN
*       CHANGE THE METALISATION RATIO
        DO 130 I = 1, 81
          COMAND(I) = COMAND(I + 1)
130     CONTINUE
        CALL TRIML(COMAND)
        CALL CONVERT(COMAND, METRAT, EOSTR)
      ELSEIF (COMAND(1) .EQ. 'X' .OR. COMAND(1) .EQ. 'x') THEN
        CALL ERSWL(60, 24, 13)
        GOTO 5
      ENDIF
      CALL ERSWL(60, 24, 13)
      GOTO 95
    ELSEIF (COMAND(1) .EQ. 'Q' .OR. COMAND(1) .EQ. 'q') THEN
*     RETURN TO COMMAND MODE AND SET VALDAT(8) TO TRUE FOR VALID DATA
```

```
      IF (VALDAT(1) .AND. VALDAT(2) .AND. VALDAT(3) .AND. VALDAT(4)
     1      .AND. VALDAT(5) .AND. VALDAT(6)) THEN
        VALDAT(7) = .TRUE.
      ENDIF
      CALL FLUSH
      CALL CLRTXT
      CALL CLRGRF
      RETURN
    ELSE
      GOTO 999
    ENDIF
    CALL ERSWL(60, 24, 13)
    GOTO 5
999 CALL DISP('@7@L25@C20 ***** UNRECOGNIZED COMMAND - _')
    CALL DISP('@7@L25@C50_')
    CALL DISP(COMAND)
    CALL BELL
    CALL ERSWL(60, 24, 13)
    GOTO 10
    END
*****************************************************************
    SUBROUTINE EDPLOT
*****************************************************************
*
*  ROUTINE TO EDIT PLOT PARAMETERS
*
    INTEGER KSOFT
    INTEGER XSCALE, YSCALE, POINTS
    CHARACTER PLTTTL*40
    LOGICAL*2 MATCH
    COMMON KSOFT
    COMMON /PLTBLK/ XSCALE, YSCALE, POINTS, MATCH, PLTTTL, TMIN, TMAX
  5 CALL CLRTXT
    CALL DISP('@6@L03@C25@UP L O T   P A R A M E T E R S@u_')
*   DISPLAY CHOSEN X-SCALE OF PLOT
    IF (XSCALE .EQ. 10) THEN
      CALL DISP('@6@L08@C09\ F1 \ X-axis scale      \10 MHz/div\   5 M
     1Hz/div   2 MHz/div_')
    ELSEIF (XSCALE .EQ. 5) THEN
      CALL DISP('@6@L08@C09\ F1 \ X-axis scale      10 MHz/div   \5 MH
     1z/div\   2 MHz/div_')
    ELSEIF (XSCALE .EQ. 1) THEN
      CALL DISP('@6@L08@C09\ F1 \ X-axis scale      10 MHz/div   5 MHz
     1/div   \2 MHz/div\_')
    ENDIF
*   DISPLAY CHOSEN Y-SCALE OF PLOT
    IF (YSCALE .EQ. 20) THEN
      CALL DISP('@6@L10@C09\ F2 \ Y-axis scale      \20 dB/div\    10
     1dB/div    5 dB/div    2 dB/div_')
    ELSEIF (YSCALE .EQ. 10) THEN
      CALL DISP('@6@L10@C09\ F2 \ Y-axis scale      20 dB/div    \10 d
     1B/div\    5 dB/div    2 dB/div_')
    ELSEIF (YSCALE .EQ. 5) THEN
      CALL DISP('@6@L10@C09\ F2 \ Y-axis scale      20 dB/div    10 dB
     1/div    \5 dB/div\    2 dB/div_')
    ELSEIF (YSCALE .EQ. 2) THEN
      CALL DISP('@6@L10@C09\ F2 \ Y-axis scale      20 dB/div    10 dB
     1/div    5 dB/div    \2 dB/div\_')
    ENDIF
*   DISPLAY CHOSEN NUMBER OF POINTS IN PLOT
    IF (POINTS .EQ. 512) THEN
      CALL DISP('@3@L12@C09\ F3 \ Points            \512\     256
     1128_')
    ELSEIF (POINTS .EQ. 256) THEN
      CALL DISP('@3@L12@C09\ F3 \ Points            512     \256\
     1128_')
```

```
      ELSEIF (POINTS .EQ. 128) THEN
        CALL DISP('@3@L12@C09\ F3 \ Points          512     256     \1
     128\_')
      ENDIF
*     ALLOW WINDOWING FOR TIME DOMAIN CALCULATIONS
*      IF (HANING) THEN
*        CALL DISP('@5@L14@C09\ F4 \ Windowing       \ON\     OFF_')
*      ELSE
*        CALL DISP('@5@L14@C09\ F4 \ Windowing       ON      \OFF\_')
*      ENDIF
*     SIMULATION MATCHING CONDITIONS
      IF (MATCH) THEN
        CALL DISP('@5@L14@C09\ F4 \ Match           \YES\    NO_')
      ELSE
        CALL DISP('@5@L14@C09\ F4 \ Match           YES     \NO\_')
      ENDIF
*     DISPLAY TITLE OF PLOT
      CALL DISP('@7@L16@C09\ F5 \ Title@C32_')
      CALL DISP(PLTTTL)
*     DISPLAY EXIT OPTION
      CALL DISP('@2@L19@C09\ F10 \ EXIT_')
*     ACTIVATE SOFTKEYS
      CALL KEYON(1)
      CALL KEYON(2)
      CALL KEYON(3)
      CALL KEYON(4)
      CALL KEYON(5)
      CALL KEYON(10)
*     WAIT FOR USER INPUT
      KSOFT = 0
   10 CALL FLUSH
      IF (KSOFT .EQ. 1) GOTO 15
      IF (KSOFT .EQ. 2) GOTO 20
      IF (KSOFT .EQ. 3) GOTO 30
      IF (KSOFT .EQ. 4) GOTO 40
      IF (KSOFT .EQ. 5) GOTO 50
      IF (KSOFT .EQ. 10) GOTO 60
      GOTO 10
*     USER SELECTS NEW X-SCALE
   15 IF (XSCALE .EQ. 10) THEN
        XSCALE = 5
      ELSEIF (XSCALE .EQ. 5) THEN
        XSCALE = 1
      ELSEIF (XSCALE .EQ. 1) THEN
        XSCALE = 10
      ENDIF
      GOTO 5
*     USER SELECTS NEW Y-SCALE
   20 IF (YSCALE .EQ. 20) THEN
        YSCALE = 10
      ELSEIF (YSCALE .EQ. 10) THEN
        YSCALE = 5
      ELSEIF (YSCALE .EQ. 5) THEN
        YSCALE = 2
      ELSEIF (YSCALE .EQ. 2) THEN
        YSCALE = 20
      ENDIF
      GOTO 5
*     USER SELECTS NEW NUMBER OF POINTS
   30 IF (POINTS .EQ. 512) THEN
        POINTS = 256
      ELSEIF (POINTS .EQ. 256) THEN
        POINTS = 128
      ELSEIF (POINTS .EQ. 128) THEN
        POINTS = 512
      ENDIF
```

```
      GOTO 5
*     USER SELECTS NEW MATCHING OPTION
   40 IF (MATCH) THEN
        MATCH = .FALSE.
      ELSE
        MATCH = .TRUE.
      ENDIF
      GOTO 5
*     USER SELECTS NEW TITLE
   50 CALL DISP('@7@L25@C05@B\New title\@b _')
      CALL GETSTR(PLTTTL)
      GOTO 5
*     EXIT
   60 CALL KEYOFF(1)
      CALL KEYOFF(2)
      CALL KEYOFF(3)
      CALL KEYOFF(4)
      CALL KEYOFF(5)
      CALL KEYOFF(10)
      CALL CLRTXT
      RETURN
      END
*******************************************************************************
      SUBROUTINE CONVERT(CHRSTR, RENUM, EOSTR)
*******************************************************************************
*
*  ROUTINE TO CONVERT A CHARACTER STRING TO CORRESPONDING REAL NUMBER
*
      CHARACTER CHRSTR(82)
      REAL RENUM
      INTEGER DECPLC
      LOGICAL*2 DECMAL, EOSTR
      EOSTR = .FALSE.
      RENUM = 0.
      SIGN = 1.
      DECMAL = .FALSE.
      IF (CHRSTR(1) .EQ. '-') THEN
        SIGN = -1.
      ENDIF
      DO 10 I = 1, 82
        IF (ICHAR(CHRSTR(I)) .GE. 48 .AND. ICHAR(CHRSTR(I)) .LE. 57
     1      .AND. .NOT. DECMAL) THEN
*         HAVE A DIGIT BEFORE DECIMAL PLACE
          RENUM = RENUM * 10. + FLOAT(ICHAR(CHRSTR(I)) - 48)
        ELSEIF (ICHAR(CHRSTR(I)) .GE. 48 .AND. ICHAR(CHRSTR(I)) .LE. 57
     1      .AND. DECMAL) THEN
*         HAVE A DIGIT AFTER DECIMAL PLACE
          RENUM = RENUM + FLOAT(ICHAR(CHRSTR(I)) - 48) / 10.**DECPLC
          DECPLC = DECPLC + 1
        ELSEIF (CHRSTR(I) .EQ. '.') THEN
*         HAVE A DECIMAL POINT
          DECMAL = .TRUE.
          DECPLC = 1
        ELSEIF (CHRSTR(I) .EQ. '_') THEN
          RENUM = SIGN * RENUM
          EOSTR = .TRUE.
          RETURN
        ELSE
          RENUM = SIGN * RENUM
          RETURN
        ENDIF
        DO 10 J = 1, 81
          CHRSTR(J) = CHRSTR(J + 1)
   10 CONTINUE
      END
```

```
C*************************************************************************
C     SUBROUTINE STATE
C*************************************************************************
C
C  ROUTINE TO DISPLAY THE CURRENT STATE TO BE EDITED
C
      INTEGER SUBSTR, SCTION, TYPE(20)
      REAL SECLEN(20), FREQ0, FRQMIN, FRQMAX, APRTUR, RS
      REAL KAPPA, ALPHA, THETA, METRAT
      COMPLEX ZE
      LOGICAL*2 ALLFLG, VALDAT(8)
      INTEGER I, XPOS, YPOS
      CHARACTER SIDT*25, DIDT*36, SHRRFL*32, OPNRFL*35, SPC*14
      CHARACTER MSC*40, APOD*30
      CHARACTER*85 LINE1, LINE2, LINE3, LINE4, LINE5
      CHARACTER LINE6*85, LINE7*85, TEMP*100, TEMP2*100, TEMP3*10
      COMMON /STATUS/ SUBSTR, SCTION, TYPE, FREQ0, FRQMIN, FRQMAX,
     +       SECLEN, APRTUR, ZE, RS, KAPPA, ALPHA, THETA, METRAT
      COMMON /FLAGS/ ALLFLG, VALDAT
      DATA SIDT/'CR25U40L25D40U7R25U26L25_'/, SPC/'CR25U40L25D40_'/
      DATA DIDT/'CR25U40L25D40U7R25U26L25R5D26R15U26_'/
      DATA SHRRFL/'CR25U40L25D40V25,40PL25CV25,-40_'/
      DATA OPNRFL/'PR25CU40PL25CD40V25,40PL25CV25,-40_'/
      DATA APOD/'PV7,20CV5,-5V5,5V-5,5V-5,-5_'/
      DATA MSC/'CU40PR5CD40PR5CU40PR5CD40PR5CU40PR5CD40_'/
C     CLEAR SCREEN OF TEXT AND GRAPHICS
      CALL CLRGRF
      CALL CLRTXT
C     DRAW STRUCTURE AT TOP OF SCREEN
      IF (VALDAT(3)) THEN
        DO 10 I = 1, SCTION
          XPOS = I * 30
          YPOS = 250
          IF (TYPE(I) .EQ. 111) THEN
C           HAVE AN UNAPODISED INPUT IDT WITH SINGLE FINGERS
            CALL PTCOLR('R')
            CALL DRAWRL(XPOS, YPOS, SIDT)
          ELSEIF (TYPE(I) .EQ. 112) THEN
C           HAVE AN APODISED INPUT IDT WITH SINGLE FINGERS
            CALL PTCOLR('R')
            CALL DRAWRL(XPOS, YPOS, SIDT)
            CALL DRAWRL(XPOS, YPOS, APOD)
          ELSEIF (TYPE(I) .EQ. 211) THEN
C           HAVE AN UNAPODISED OUTPUT IDT WITH SINGLE FINGERS
            CALL PTCOLR('G')
            CALL DRAWRL(XPOS, YPOS, SIDT)
          ELSEIF (TYPE(I) .EQ. 212) THEN
C           HAVE AN APODISED OUTPUT IDT WITH SINGLE FINGERS
            CALL PTCOLR('G')
            CALL DRAWRL(XPOS, YPOS, SIDT)
            CALL DRAWRL(XPOS, YPOS, APOD)
          ELSEIF (TYPE(I) .EQ. 121) THEN
C           HAVE AN UNAPODISED INPUT IDT WITH SPLIT FINGERS
            CALL PTCOLR('R')
            CALL DRAWRL(XPOS, YPOS, DIDT)
          ELSEIF (TYPE(I) .EQ. 122) THEN
C           HAVE AN APODISED INPUT IDT WITH SPLIT FINGERS
            CALL PTCOLR('R')
            CALL DRAWRL(XPOS, YPOS, DIDT)
            CALL DRAWRL(XPOS, YPOS, APOD)
          ELSEIF (TYPE(I) .EQ. 221) THEN
C           HAVE AN UNAPODISED OUTPUT IDT WITH SPLIT FINGERS
            CALL PTCOLR('G')
            CALL DRAWRL(XPOS, YPOS, DIDT)
          ELSEIF (TYPE(I) .EQ. 222) THEN
C           HAVE AN APODISED OUTPUT IDT WITH SPLIT FINGERS
            CALL PTCOLR('G')
```

```
            CALL DRAWRL(XPOS, YPOS, DIDT)
            CALL DRAWRL(XPOS, YPOS, APOD)
          ELSEIF (TYPE(I) .EQ. 321) THEN
            HAVE A NON-TAPERED SHORTED REFLECTOR ARRAY
            CALL PTCOLR('Y')
            CALL DRAWRL(XPOS, YPOS, SHRRFL)
          ELSEIF (TYPE(I) .EQ. 322) THEN
            HAVE A TAPERED SHORTED REFLECTOR ARRAY
            CALL PTCOLR('Y')
            CALL DRAWRL(XPOS, YPOS, SHRRFL)
            CALL DRAWRL(XPOS, YPOS, APOD)
          ELSEIF (TYPE(I) .EQ. 311) THEN
            HAVE AN NON-TAPERED OPEN REFLECTOR ARRAY
            CALL PTCOLR('Y')
            CALL DRAWRL(XPOS, YPOS, OPNRFL)
          ELSEIF (TYPE(I) .EQ. 312) THEN
            HAVE A TAPERED OPEN REFLECTOR ARRAY
            CALL PTCOLR('Y')
            CALL DRAWRL(XPOS, YPOS, OPNRFL)
            CALL DRAWRL(XPOS, YPOS, APOD)
          ELSEIF (TYPE(I) .EQ. 400) THEN
            HAVE AN SPACE
            CALL PTCOLR('W')
            CALL DRAWRL(XPOS, YPOS, SPC)
          ELSEIF (TYPE(I) .EQ. 500) THEN
            HAVE A MULTISTRIP COUPLER
            CALL PTCOLR('W')
            CALL DRAWRL(XPOS, YPOS, MSC)
          END IF
   10   CONTINUE
      ENDIF
      SHOW CURRENT SUBSTRATE
      IF (VALDAT(1)) THEN
        IF (SUBSTR .EQ. 1) THEN
          TEMP = '1 = \YX LiNbO3\  2 = YZ LiNbO3  3 = ST-X Quartz_'
        ELSEIF (SUBSTR .EQ. 2) THEN
          TEMP = '1 = YX LiNbO3  2 = \YZ LiNbO3\  3 = ST-X Quartz_'
        ELSEIF (SUBSTR .EQ. 3) THEN
          TEMP = '1 = YX LiNbO3  2 = YZ LiNbO3  3 = \ST-X Quartz\_'
        ENDIF
      ELSE
        HAVE NO VALID CURRENT SUBSTRATE
        TEMP = '1 = YX LiNbO3  2 = YZ LiNbO3  3 = ST-X Quartz_'
      ENDIF
      CALL CONCAT('@6@L08@C05\ C \ Crystal              _', TEMP, LINE1)
      CALL DISP(LINE1)
      SHOW CURRENT FREQUENCY CHOICES
      IF (VALDAT(2)) THEN
        CALL ENCODE(FRQMIN/1.E6, TEMP, '(F7.2)_')
        CALL DISP('@4@L10@C30Min = @C36_')
        CALL DISP(TEMP)
        CALL ENCODE(FREQ0/1.E6, TEMP, '(F7.2)_')
        CALL DISP('@L10@C46Center = @C55_')
        CALL DISP(TEMP)
        CALL ENCODE(FRQMAX/1.E6, TEMP, '(F7.2)_')
        CALL DISP('@L10@C65Max = @C71_')
        CALL DISP(TEMP)
      ELSE
        CALL DISP('@L10@C30**** NOT INITIALIZED_')
      ENDIF
      CALL DISP('@L10@C05\ F \ Frequency (MHz)      _')
      SHOW STRUCTURE OPTIONS
      TEMP = '@21SU  IDU    @40SU  ODU    @6ROU  RSU    @7SPC_'
      CALL CONCAT('@4@L12@C05\ S \ Structure            _', TEMP, LINE3)
      CALL DISP(LINE3)
      CALL DISP('@L13@C30@21SA  IDA    @40SA  ODA    @6ROT  RST    @7MSC
```

```
     1_')
*    SHOW CURRENT LENGTH OF EACH SECTION
     IF (VALDAT(4)) THEN
       TEMP = '_'
       DO 20 I = 1, SCTION
         TEMP3 = '          '
         CALL ENCODE(SECLEN(I), TEMP3, '(F7.2)_')
         CALL STRPAD(TEMP3, 7)
         CALL CONCAT(TEMP, TEMP3, TEMP2)
         TEMP = TEMP2
20     CONTINUE
     ELSE
       TEMP = ' ***** NOT INITIALIZED_'
     ENDIF
     IF (LEN(TEMP) .LE. 50) THEN
*    CAN FIT WHOLE STRING ON ONE LINE
     CALL CONCAT('@4@L15@C05\ N \ Number of strips      _', TEMP, LINE4)
     CALL DISP(LINE4)
     ELSE
*    NEED TWO LINES TO FIT WHOLE STRING
     TEMP2 = TEMP(50:LEN(TEMP))
     CALL COMPRS(TEMP, 50, LEN(TEMP)-50)
     CALL CONCAT('@4@L15@C05\ N \ Number of strips      _', TEMP, LINE4)
     CALL DISP(LINE4)
     CALL DISP('@L16@C30_')
     CALL DISP(TEMP2)
     ENDIF
*    SHOW CURRENT APERTURE
     IF (VALDAT(5)) THEN
       CALL ENCODE(APRTUR*1000., TEMP2, '(F7.2)_')
       CALL CONCAT(TEMP2, ' mm_', TEMP)
     ELSE
       TEMP = ' ***** NOT INITIALIZED_'
     ENDIF
     CALL CONCAT('@4@L18@C05\ A \ Aperture (mm) '       _', TEMP, LINE5)
     CALL DISP(LINE5)
*    SHOW CURRENT LOAD IMPEDANCE
     IF (VALDAT(6)) THEN
       CALL ENCODE(REAL(ZE), TEMP2, '(F7.2)_')
       CALL CONCAT(TEMP2, ' Ohm_', TEMP)
     ELSE
       TEMP = ' ***** NOT INITIALIZED_'
     ENDIF
     CALL CONCAT('@5@L20@C05\ Z \ Load Impedance        _', TEMP, LINE6)
     CALL DISP(LINE6)
*    SHOW OPTIONS FOR OTHER MENU AND TO QUIT
     CALL DISP('@3@L22@C05\ M \ More simulation constants
    1     @2\ Q \ Quit_')
     RETURN
     END
*******************************************************************
     SUBROUTINE STATE2
*******************************************************************
*
*  ROUTINE TO DIPLAY THE CURRENT CONSTANTS FOR SIMULATION
*
     INTEGER SUBSTR, SCTION, TYPE(20)
     REAL SECLEN(20), FREQ0, FRQMIN, FRQMAX, APRTUR, RS
     REAL KAPPA, ALPHA, THETA, METRAT
     COMPLEX ZE
     CHARACTER*20 TEMP, TEMP2
     COMMON /STATUS/ SUBSTR, SCTION, TYPE, FREQ0, FRQMIN, FRQMAX,
    1        SECLEN, APRTUR, ZE, RS, KAPPA, ALPHA, THETA, METRAT
*    CLEAR SCREEN
     CALL DISP('@X_')
*    SHOW CURRENT ELECTRODE RESISTANCE
```

```
      CALL ENCODE(RS, TEMP2, '(F7.2)_')
      CALL CONCAT(TEMP2, ' Ohm_', TEMP)
      CALL DISP('@5@L08@C05\ R \ Electrode resistance_')
      CALL DISP('@L08@C40_')
      CALL DISP(TEMP)
*     SHOW CURRENT GRATING COUPLING COEFFICIENT
      CALL ENCODE(KAPPA, TEMP2, '(F9.2)_')
      CALL CONCAT(TEMP2, ' / meter_', TEMP)
      CALL DISP('@6@L11@C05\ K \ Grating coupling constant_')
      CALL DISP('@L11@C40_')
      CALL DISP (TEMP)
*     SHOW CURRENT GRATING LOSS CONSTANT
      CALL ENCODE(ALPHA, TEMP2, '(F7.2)_')
      CALL CONCAT(TEMP2, ' / meter_', TEMP)
      CALL DISP('@L13@C05\ A \ Grating loss constant_')
      CALL DISP('@L13@C40_')
      CALL DISP(TEMP)
*     SHOW CURRENT METALISATION RATIO CONSTANT
      CALL ENCODE(METRAT, TEMP2, '(F5.3)_')
      CALL DISP('@L15@C05\ M \ Metallization ratio  _')
      CALL DISP('@L15@C40_')
      CALL DISP(TEMP2)
*     SHOW OPTION TO RETURN
      CALL DISP('@3@L18@C05\ X \ RETURN_')
      RETURN
      END
```

```
$STORAGE:2
$NOFLOATCALLS
*****************************************************************
      SUBROUTINE CMPUTE
*****************************************************************
*
*  ROUTINE TO COMPUTE THE FREQUENCY RESPONSE OF CURRENT STRUCTURE
*
*  WRITTEN BY PETER M. SMITH, MCMASTER UNIVERSITY, HAMILTON, ON
*  LATEST UPDATE: JULY 1987
*
*  VARIABLES USED:
*     APOD(I) - APODISATION FUNCTION FOR CURRENT SECTION
*      APRTUR - APERTURE OF IDT'S
*        BETA - PROPAGATION CONSTANT FOR SAW
*       BETA0 - PROPAGATION CONSTANT AT CENTRE FREQUENCY
*         CFF - CAPACITANCE PER UNIT LENGTH PER FINGER PAIR
*          CS - CAPACITANCE PER FINGER PAIR
*          CT - CAPACITANCE OF IDT
*       DELTA - MEASURE OF FREQUENCY DEVIATION FROM BRAGG FREQUENCY
*        FREQ - CURRENT FREQUENCY OF SIMULATION
*       FREQ0 - RESONANT FREQUENCY OF SIMULATION
*      FRQMAX - MAXIMUM FREQUENCY OF SIMULATION
*      FRQMIN - MINIMUM FREQUENCY OF SIMULATION
*          K2 - ELECTROMECHANICAL COUPLING CONSTANT FOR SUBSTRATE
*      LAMBDA - ONE HALF OF THE WAVELENGTH AT CENTER FREQUENCY
*   LENGTH(I) - LENGTH OF I-TH SECTION
*       NT(I) - NUMBER OF HALF WAVELENGTHS IN I-TH SECTION
*       OMEGA - CURRENT ANGULAR FREQUENCY
*      OUTSIG - OUTPUT SIGNAL FROM DEVICE
*      SCTION - NUMBER OF ELEMENT SECTIONS IN STRUCTURE
*      SUBSTR - SUBSTRATE IN USE:
*                 1 = YZ LITHIM NIOBATE
*                 2 = 128 YX LITHIUM NIOBATE
*                 3 = ST-X QUARTZ
*        T(I) - ACOUSTIC SCATTERING MATRIX FOR I-TH SECTION
*     TYPE(I) - TYPE OF STRUCTURE IN I-TH SECTION:
*                 111 = UNAPODISED INPUT IDT WITH SINGLE FINGERS
*                 112 = APODISED INPUT IDT WITH SINGLE FINGERS
*                 121 = UNAPODISED INPUT IDT WITH SPLIT FINGERS
*                 122 = APODISED INPUT IDT WITH SPLIT FINGERS
*                 211 = UNAPODISED OUTPUT IDT WITH SINGLE FINGERS
*                 212 = APODISED OUTPUT IDT WITH SINGLE FINGERS
*                 221 = UNAPODISED OUTPUT IDT WITH SPLIT FINGERS
*                 222 = APODISED OUTPUT IDT WITH SPLIT FINGERS
*                 311 = NON-TAPERED OPEN CIRCUITED REFLECTOR ARRAY
*                 312 = TAPERED OPEN CIRCUITED REFLECTOR ARRAY
*                 321 = NON-TAPERED SHORT CIRCUITED REFLECTOR ARRAY
*                 322 = TAPERED SHORT CIRCUITED REFLECTOR ARRAY
*                 400 = SPACE
*          V0 - VELOCITY OF SAW ON SUBSTRATE
*     W(I, J) - ACOUSTIC WAVES AT END OF SECTION J
*          Y0 - CHARACTERISTIC ADMITTANCE OF SAW ON SUBSTRATE
*       YLOAD - LOAD ADMITTANCE
*
*****************************************************************
*
      IMPLICIT REAL*8 (P)
      INTEGER SUBSTR, SCTION, TYPE(20), SECTYP, FINTYP, APDTYP
      INTEGER XSCALE, YSCALE, POINTS
      INTEGER II, KSOFT
      CHARACTER PLTTTL*40, CHR*8
```

```
      REAL FREQ0, FRQMIN, FRQMAX, SECLEN(20), APRTUR, RS,RESFRQ(20)
      LOGICAL*2 ALLFLG, VALDAT(8), MATCH
      COMPLEX OUTSIG(512), OUTTME(512), ZE
      COMPLEX*16 NUM, DENOM, PHS2, PHS, YLOAD, YOUT
      COMPLEX*16 T(3, 3, 20), SUBT(3, 3), PHSCNS, THETA12
      COMPLEX*16 ETHETA, CCOSH, CSINH, ATTEN, SIGMA
      COMPLEX*16 TEMP(3, 3), TEMP2(2), TEMP3(2, 2), W(2, 20), B(20)
      COMPLEX*16 TF11, TF12, TF13, TF21, TF22, TF23, TF31; TF32, TF33
      REAL A(20)
      REAL*8 X, PVAL(20), T1, T2, T3, COEFF, SINVAL
      COMPLEX*16 M11, M12, M13, M21, M22, M23, M31, M32, M33
      REAL V0, BETA, APOD(400)
      REAL LENGTH(20), K2, LAMBDA, DELTA, OMEGA
      REAL FRQ(512), TIME(512), RSPNSE(512)
      INTEGER NT(17)
      INTEGER XX(512), YY(512), IX(5), IY(5), WW(4)
      REAL PLTRSP(9, 512), GA
      REAL KAPPA, ALPHA, THETA, METRAT
      COMMON /STATUS/ SUBSTR, SCTION, TYPE, FREQ0, FRQMIN, FRQMAX,
     1       SECLEN, APRTUR, ZE, RS, KAPPA, ALPHA, THETA, METRAT
      COMMON /PLTBLK/ XSCALE, YSCALE, POINTS, MATCH, PLTTTL, TMIN, TMAX
      COMMON /FLAGS/ ALLFLG, VALDAT
      COMMON /RSPBLK/ FRQ, OUTSIG, TIME, OUTTME
      COMMON /LGNDRE/ PVAL, X
      COMMON KSOFT
      DATA IX/0, 499, 499, 0, 0/, IY/0, 0, 219, 219, 0/
      DATA WW/119, 619, 39, 259/

      IF (.NOT. VALDAT(7)) THEN
        CALL DISP('@7@L25@C09*** UNINITIALIZED PARAMETER_')
        CALL BELL
        CALL WAIT(30)
        CALL ERSLIN(25)
        RETURN
      ENDIF
      DISPLAY CURRENT STATE OF COMPUTATION TO RELIEVE BOREDOM
      CALL DISP('@X@4@L24@C05MIN FREQ =@7@C30CURR FREQ =@2@C56MAX FREQ =
     1_')
      CALL ENCODE(FRQMIN / 1.E6, CHR, '(F6.1)_')
      CALL DISP('@4@L24@C16_')
      CALL DISP(CHR)
      CALL ENCODE(FRQMAX / 1.E6, CHR, '(F6.1)_')
      CALL DISP('@2@L24@C67_')
      CALL DISP(CHR)
      BEGIN COMPUTATIONS
      PI = 4. * DATAN(DBLE(1.))
      PI2 = 2. * PI
      IF (SUBSTR .EQ. 1) THEN
        HAVE YZ LITHIUM NIOBATE
        CFF = 4.6438E-10
        V0 = 3488.
        K2 = 0.045
        EPSILON = 8.85E-12 * (1. + 50.)
        Y0 = 0.21
      ELSEIF (SUBSTR .EQ. 2) THEN
        HAVE 128 ROTATED YX LITHIUM NIOBATE
        CFF = 5.E-10
        V0 = 3990.
        K2 = 0.056
        EPSILON = 8.85E-12 * (1. + 50.)
        Y0 = 0.21
      ELSEIF (SUBSTR .EQ. 3) THEN
        HAVE ST-X QUARTZ
        CFF = 5.03385E-11
        V0 = 3158.
        K2 = 0.0016
```

```
        EPSILON = 8.85E-12 * (1. + 4.4)
        Y0 = 0.87
      ENDIF
      Z0 = 1 / Y0
      CS = APRTUR * CFF
*     LAMBDA IS A HALF WAVELENGTH
      LAMBDA = 0.5 * V0 / FREQ0
      OMEGA0 = PI2 * FREQ0
      BETA0 = OMEGA0 / V0
      DO 5 I = 1, SCTION
        LENGTH(I) = SECLEN(I) * LAMBDA
        NT(I) = INT(SECLEN(I))
    5 CONTINUE
*
*     FOR EACH FREQUENCY EVALUATE THE TRANSFER FUNCTION AND PLOT
*
      CALL DISP('@7@L12@C30W A I T . . . _')
      FSTEP = (FRQMAX - FRQMIN) / FLOAT(POINTS)
      CALL KEYON(11)
      X = DCOS(PI * METRAT)
      CALL SETP
      DO 10 II = 1, POINTS
        FREQ = FRQMIN + FLOAT(II) * FSTEP
*       UPDATE FREQUENCY ON SCREEN
        CALL ENCODE(FLOAT(INT(FREQ / 1.E6)), CHR, '(F6.1)_')
        CALL DISP('@7@L24@C42_')
        CALL DISP(CHR)
        OMEGA = PI2 * FREQ
        BETA = OMEGA / V0
        DELTA = (BETA**2 - BETA0**2) / (2. * BETA0)
*
*       COMPUTE TRANSMISSION MATRICES FOR EACH SECTION AT CURRENT FREQUENCY
*
        DO 20 I = 1, SCTION
          SECTYP = TYPE(I) / 100
          IF (SECTYP .LE. 2) THEN
*           HAVE A TRANSDUCER
            FINTYP = TYPE(I) / 10 - SECTYP * 10
            IF (FINTYP .EQ. 1) THEN
*             HAVE SINGLE FINGERS
              RESFRQ(I) = FREQ0
              PHSCNS = CDEXP(DCMPLX(DBLE(0.), -PI/2 * FREQ / RESFRQ(I)))
*             ENTER APODISATION VALUES FOR TRANSDUCER
              APDTYP = MOD(TYPE(I), 10)
              IF (APDTYP .EQ. 1) THEN
*               HAVE AN UNAPODISED TRANSDUCER
                DO 30 J = 1, NT(I), 2
                  APOD(J) = 1.
                  APOD(J + 1) = -1.
   30           CONTINUE
              ELSEIF (APDTYP .EQ. 2) THEN
*               HAVE AN APODISED TRANSDUCER **** SINC FOR THE TIME BEING
                DO 35 J = 1, NT(I), 2
                  VAL = 3. * SNGL(PI) * (-1.+2.*(J - 1)/FLOAT(NT(I)))
                  IF (VAL .GE. 1.E-12) THEN
                    APOD(J) = SIN(VAL) / VAL
                    APOD(J) = 0.54 - 0.46 * COS(PI2*(J-1)/(NT(I)-1))
                    APOD(J + 1) = -APOD(J)
                  ELSE
                    APOD(J) = 1.
                    APOD(J + 1) = -1.
                  ENDIF
   35             CONTINUE
              ENDIF
            ELSEIF (FINTYP .EQ. 2) THEN
*             HAVE SPLIT FINGERS
```

```
      RESFRQ(I) = 2. * FREQ0
      PHSCNS = CDEXP(DCMPLX(DBLE(0.), -PI/2 * FREQ / RESFRQ(I)))
*     NEED TWICE AS MANY FINGERS, SO CORRECT NT(I)
      NT(I) = 2 * NT(I)
*     ENTER APODISATION VALUES FOR IDT
      APDTYP = MOD(TYPE(I), 10)
      IF (APDTYP .EQ. 1) THEN
        HAVE AN UNAPODISED TRANSDUCER
        DO 36 J = 1, NT(I), 4
          APOD(J) = 1.0
          APOD(J + 1) = 1.0
          APOD(J + 2) = -1.0
          APOD(J + 3) = -1.0
36      CONTINUE
      ELSEIF (APDTYP .EQ. 2) THEN
*       HAVE AN APODISED TRANSDUCER **** SINC FOR THE TIME BEING
        DO 37 J = 1, NT(I), 4
          VAL = 3. * SNGL(PI) * (-1.+2.*(J - 1)/FLOAT(NT(I)))
          IF (VAL .GE. 1.E-12) THEN
            APOD(J) = SIN(VAL) / VAL
            APOD(J + 1) = APOD(J)
            APOD(J + 2) = -APOD(J)
            APOD(J + 3) = -APOD(J)
          ELSE
            APOD(J) = 1.
            APOD(J + 1) = 1.
            APOD(J + 2) = -1.
            APOD(J + 3) = -1.
          ENDIF
37      CONTINUE
      ENDIF
    ENDIF
*   FIND OVERALL RESPONSE FOR TRANSDUCER
    N = INT(.5 * FREQ / RESFRQ(I))
    S = .5 * FREQ / RESFRQ(I) - FLOAT(N)
    T1 = DBLE(0.)
    T2 = DBLE(0.)
    T3 = DBLE(0.)
    A(1) = -0.5
    NP1 = N + 1
    DO 52 M = 2, NP1
      A(M) = 0.
      MM1 = M - 1
      DO 52 J = 1, MM1
        A(M) = A(M) - A(J) * P(M - J)
52  CONTINUE
    DO 53 M = 0, N
      T1 = T1 + A(M + 1) * (PP(2 * (N + S) - M, 1) +
     1      (-1.)**(N-M) * PP(N - M + S, -1) * PP(N + 2 *
     2      S - 1, 1) / PP(S - 1, -1))
      T2 = T2 + A(M + 1) * (P(M - 1) + (-1.)**(N-M) *
     1      PP(N - M + S, -1) * P(N) / PP(S - 1, -1))
53  CONTINUE
    SINVAL = DSIN(PI * S)
    T3 = K2 * SINVAL * P(N) / PP(S - 1, -1)
    COEFF = K2 * PI * (S + N)
    PHS2 = PHSCNS**2
    PHS = PHSCNS
    M11 = DCMPLX(DBLE(0.), COEFF * T1)
    M12 = DCMPLX(DBLE(1.), COEFF * T2)
    M13 = DCMPLX(DBLE(0.), T3)
    M21 = M12
    M22 = M11
    M23 = M13
    M31 = Y0 * APRTUR / LAMBDA * M13
    M32 = M31
```

```
*
*           MODIFY PARAMETERS FOR ERROR IN DATTA'S PAPER AS GIVEN IN
*           PANASIK'S PAPER
*
            THETA12 = CDEXP(DCMPLX(DBLE(0.), DATAN(DIMAG(M12) /
     1                                             DREAL(M12))))
            M11 = CDABS(M11) * THETA12 * DCMPLX(DBLE(0.), DBLE(1.))
     1            * PHS2
            M22 = M11
            M21 = DSQRT(1. - CDABS(M11)**2) * THETA12 * PHS2
            M12 = M21
            M13 = M13 * PHS
            M23 = M13
            M31 = M31 * PHS
            M32 = M31
            M33 = M13 * DCONJG(M13) * Y0 * APRTUR / LAMBDA
     1            + DCMPLX(DBLE(0.), DBLE(OMEGA * CS))
*
*           MODIFY PARAMETERS FOR EXTERNAL LOADS
*           THIS INCLUDES INDUCED VOLTAGES ON IDT (-> M11,M12,M21,M22)
*           AS WELL AS VOLTAGE DIVISIONS AT SOURCE (-> OTHER M'S)
*
            YLOAD = DCMPLX(DBLE(1. / REAL(ZE)), DBLE(0.))
            IF (MATCH) THEN
              YOUT = (YLOAD + M33)
              M11 = M11 + M13 * M31 / YOUT
              M12 = M12 + M13 * M32 / YOUT
              M13 = M13 * YLOAD / YOUT
              M21 = M21 + M23 * M31 / YOUT
              M22 = M22 + M23 * M32 / YOUT
              M23 = M23 * YLOAD / YOUT
              M31 = M31
              M32 = M32
              M33 = M33 * YLOAD / YOUT
            ENDIF
*
*           TRANSMISSION PARAMETERS FOR EACH FINGER
*
            TF11 = 1. / M21
            TF12 = -M22 * TF11
            TF13 = -M23 * TF11
            TF21 = -TF12
            TF22 = M12 + M11 * TF12
            TF23 = M13 + M11 * TF13
            TF31 = M31 * TF11
            TF32 = M32 + M31 * TF12
            TF33 = M33 + M31 * TF13
*
*           TRANSMISSION PARAMETERS FOR WHOLE IDT
*
            DO 38 J = 1, 3
              DO 38 K = 1, 3
                IF (J .EQ. K) THEN
                  T(J, K, I) = DCMPLX(DBLE(1.), DBLE(0.))
                ELSE
                  T(J, K, I) = DCMPLX(DBLE(0.), DBLE(0.))
                ENDIF
 38         CONTINUE
            DO 40 J = NT(I), 1, -1
*             MULTIPLY OUT TRANSMISSION MATRICES FOR EACH FINGER
              SUBT(1, 1) = TF11
              SUBT(1, 2) = TF12
              SUBT(1, 3) = TF13 * APOD(J)
              SUBT(2, 1) = TF21
              SUBT(2, 2) = TF22
              SUBT(2, 3) = TF23 * APOD(J)
```

```
            SUBT(3, 1) = TF31 * APOD(J)
            SUBT(3, 2) = TF32 * APOD(J)
            SUBT(3, 3) = TF33 * APOD(J)
            TEMP(1, 1) = SUBT(1, 1) * T(1, 1, I) +
     1                   SUBT(1, 2) * T(2, 1, I)
            TEMP(1, 2) = SUBT(1, 1) * T(1, 2, I) +
     1                   SUBT(1, 2) * T(2, 2, I)
            TEMP(1, 3) = SUBT(1, 1) * T(1, 3, I) +
     1                   SUBT(1, 2) * T(2, 3, I) + SUBT(1, 3)
            TEMP(2, 1) = SUBT(2, 1) * T(1, 1, I) +
     1                   SUBT(2, 2) * T(2, 1, I)
            TEMP(2, 2) = SUBT(2, 1) * T(1, 2, I) +
     1                   SUBT(2, 2) * T(2, 2, I)
            TEMP(2, 3) = SUBT(2, 1) * T(1, 3, I) +
                         SUBT(2, 2) * T(2, 3, I) + SUBT(2, 3)
            TEMP(3, 1) = SUBT(3, 1) * T(1, 1, I) +
     1                   SUBT(3, 2) * T(2, 1, I) + T(3, 1, I)
            TEMP(3, 2) = SUBT(3, 1) * T(1, 2, I) +
     1                   SUBT(3, 2) * T(2, 2, I) + T(3, 2, I)
            TEMP(3, 3) = SUBT(3, 1) * T(1, 3, I) +
     1                   SUBT(3, 2) * T(2, 3, I) + SUBT(3, 3) +
     2                   T(3, 3, I)
            T(1, 1, I) = TEMP(1, 1)
            T(1, 2, I) = TEMP(1, 2)
            T(1, 3, I) = TEMP(1, 3)
            T(2, 1, I) = TEMP(2, 1)
            T(2, 2, I) = TEMP(2, 2)
            T(2, 3, I) = TEMP(2, 3)
            T(3, 1, I) = TEMP(3, 1)
            T(3, 2, I) = TEMP(3, 2)
            T(3, 3, I) = TEMP(3, 3)
   40     CONTINUE
          IF (MOD(II, 2) .EQ. 1) THEN
            IF (I .EQ. 1) THEN
              M33 = T(3, 3, 1) - T(1, 3, I) * T(3, 1, I) / T(1, 1, 1)
              GA = 2 * K2 * CS * FREQ * (NT(I) - 1)**2
              IF (ABS(NT(I) * LAMBDA * DELTA) .GE. 1.E-10) THEN
                GA = GA * (SIN(NT(I) * LAMBDA * DELTA / 2) /
     1                     (NT(I) * LAMBDA * DELTA / 2))**2
              ENDIF
            ENDIF
          ENDIF
        ELSEIF (SECTYP .EQ. 3) THEN
          HAVE A REFLECTOR
            ATTEN = DCMPLX(DBLE(ALPHA), DBLE(DELTA))
            SIGMA = CDSQRT(KAPPA**2 + ATTEN**2)
            CCOSH = 0.5 * (CDEXP(SIGMA * LENGTH(I)) + CDEXP(-SIGMA *
     1              LENGTH(I)))
            CSINH = 0.5 * (CDEXP(SIGMA * LENGTH(I)) - CDEXP(-SIGMA *
     1              LENGTH(I)))
            PHSCNS = CDEXP(DCMPLX(DBLE(0.), DBLE(BETA * LENGTH(I))))
            ETHETA = CDEXP(DCMPLX(DBLE(0.), DBLE(THETA)))
            T(1, 1, I) = (CCOSH + ATTEN * CSINH / SIGMA) * PHSCNS
            T(1, 2, I) = DCMPLX(DBLE(0.), DBLE(KAPPA)) / SIGMA *
     1                   CSINH * PHSCNS * DCONJG(ETHETA)
            T(2, 1, I) = DCMPLX(DBLE(0.), DBLE(-KAPPA)) / SIGMA *
     1                   CSINH * DCONJG(PHSCNS) * ETHETA
            T(2, 2, I) = (CCOSH - ATTEN * CSINH / SIGMA) *
     1                   DCONJG(PHSCNS)
   45     CONTINUE
        ELSEIF (SECTYP .EQ. 4) THEN
          HAVE A SPACE (SEE EQUATION (13))
          T(1, 1, I) = CDEXP(DCMPLX(DBLE(0.), DBLE(BETA * LENGTH(I))))
          T(1, 2, I) = DCMPLX(DBLE(0.), DBLE(0.))
          T(2, 1, I) = DCMPLX(DBLE(0.), DBLE(0.))
          T(2, 2, I) = DCONJG(T(1, 1, I))
```

```
            ELSE
              CALL BELL
              CALL DISP('@7@L25@C09*** ERR 1 - UNKNOWN SECTION TYPE_')
              STOP
            ENDIF
 20       CONTINUE
*
*         FIND THE SCALING FACTOR OF RIGHTMOST WAVE FOR INPUT SIGNAL OF
*         MAGNITUDE 1
*
          NUM = DCMPLX(DBLE(0.), DBLE(0.))
          TEMP(1, 1) = DCMPLX(DBLE(1.), DBLE(0.))
          TEMP(1, 2) = DCMPLX(DBLE(0.), DBLE(0.))
          TEMP(2, 1) = DCMPLX(DBLE(0.), DBLE(0.))
          TEMP(2, 2) = DCMPLX(DBLE(1.), DBLE(0.))
          DO 50 I = 1, SCTION
            SECTYP = TYPE(I) / 100
            IF (SECTYP .EQ. 1) THEN
              TEMP2(1) = TEMP(1, 1) * T(1, 3, I) + TEMP(1, 2) * T(2, 3, I)
              TEMP2(2) = TEMP(2, 1) * T(1, 3, I) + TEMP(2, 2) * T(2, 3, I)
              NUM = NUM + TEMP2(1)
            ENDIF
            TEMP3(1, 1) = TEMP(1, 1)*T(1, 1, I) + TEMP(1, 2)*T(2, 1, I)
            TEMP3(1, 2) = TEMP(1, 1)*T(1, 2, I) + TEMP(1, 2)*T(2, 2, I)
            TEMP3(2, 1) = TEMP(2, 1)*T(1, 1, I) + TEMP(2, 2)*T(2, 1, I)
            TEMP3(2, 2) = TEMP(2, 1)*T(1, 2, I) + TEMP(2, 2)*T(2, 2, I)
            DO 50 J = 1, 2
              DO 50 K = 1, 2
                TEMP(J, K) = TEMP3(J, K)
 50       CONTINUE
          DENOM = TEMP3(1, 1)
          W(1, SCTION) = -NUM / DENOM
          W(2, SCTION) = DCMPLX(DBLE(0.), DBLE(0.))
*
*         WORK THROUGH STRUCTURE AND FIND OUTPUT SIGNAL
*
          OUTSIG(II) = CMPLX(0., 0.)
          DO 60 I = SCTION, 2, -1
            IF (ABS(FREQ-FREQ0) .LE. 1.) THEN
              W1MAG = SNGL(DSQRT(DREAL(W(1,I))**2
     1                     + DIMAG(W(1,I))**2))
              W2MAG = SNGL(DSQRT(DREAL(W(2,I))**2
     1                     + DIMAG(W(2,I))**2))
            ENDIF
            SECTYP = TYPE(I) / 100
            W(1, I - 1) = T(1, 1, I) * W(1, I) + T(1, 2, I) * W(2, I)
            W(2, I - 1) = T(2, 1, I) * W(1, I) + T(2, 2, I) * W(2, I)
            IF (SECTYP .EQ. 1) THEN
*             HAVE AN INPUT TRANSDUCER, SO ADD EFFECT OF INPUT SIGNAL
              W(1, I - 1) = W(1, I - 1) + T(1, 3, I)
              W(2, I - 1) = W(2, I - 1) + T(2, 3, I)
            ELSEIF (SECTYP .EQ. 2) THEN
*             HAVE AN OUTPUT TRANSDUCER, SO ADD OUTPUT SIGNAL TO TOTAL
              B(I) = T(3, 1, I) * W(1, I) + T(3, 2, I) * W(2, I)
              B(I) = B(I) / (YLOAD + T(3, 3, I))
              IF (DABS(DREAL(B(I))) .LT. 1.D-30) THEN
                B(I) = DCMPLX(DBLE(0.), DIMAG(B(I)))
              ENDIF
              IF (DABS(DIMAG(B(I))) .LT. 1.D-30) THEN
                B(I) = DCMPLX(DREAL(B(I)), DBLE(0.))
              ENDIF
              IF (ABS(FREQ-FREQ0) .LE. 1.) THEN
                BMAG = SNGL(DSQRT(DREAL(B(I))**2
     1                       + DIMAG(B(I))**2))
              ENDIF
              OUTSIG(II) = OUTSIG(II) + CMPLX(SNGL(DREAL(B(I))),
```

```
     1                    SNGL(DIMAG(B(I))))
            ENDIF
  60      CONTINUE
          IF (ABS(FREQ-FREQ0) .LE. 1.) THEN
            W1MAG = SNGL(DSQRT(DREAL(W(1,1))**2
     1                    + DIMAG(W(1,1))**2))
            W2MAG = SNGL(DSQRT(DREAL(W(2,1))**2
     1                    + DIMAG(W(2,1))**2))
          ENDIF
          SECTYP = TYPE(1) / 100
          IF (SECTYP .EQ. 2) THEN
            B(1) = T(3, 1, 1) * W(1, 1) + T(3, 2, 1) * W(2, 1)
            B(1) = B(1) / (YLOAD + T(3, 3, 1))
            IF (DABS(DREAL(B(1))) .LT. 1.D-30) THEN
              B(1) = DCMPLX(DBLE(0.), DIMAG(B(1)))
            ENDIF
            IF (DABS(DIMAG(B(1))) .LT. 1.D-30) THEN
              B(1) = DCMPLX(DREAL(B(1)), DBLE(0.))
            ENDIF
            OUTSIG(II) = OUTSIG(II) + CMPLX(SNGL(DREAL(B(1))),
     1                   SNGL(DIMAG(B(1))))
          ENDIF
          FRQ(II) = FREQ
C         ALLOW AN ABORT BY PRESSING F11
          CALL FLUSH
          IF (KSOFT .EQ. 11) THEN
            CALL DISP('@X_')
            ALLFLG = .TRUE.
            CALL KEYOFF(11)
            RETURN
          ENDIF
C         RESET CORRECT LENGTH OF SPLIT FINGER TRANSDUCERS
          DO 70 I = 1, SCTION
            SECTYP = TYPE(I) / 100
            IF (SECTYP .LE. 2) THEN
              FINTYP = TYPE(I) / 10 - SECTYP * 10
              IF (FINTYP .EQ. 2) THEN
                NT(I) = NT(I) / 2
              ENDIF
            ENDIF
  70      CONTINUE
  10    CONTINUE
C
C       COMPUTE IMPULSE RESPONSE
C
C       DISPLAY CURRENT STATE OF COMPUTATION TO RELIEVE BOREDOM
        CALL DISP('@X@4@L24@C05MIN TIME =@7@C30CURR TIME =@2@C56MAX TIME =
       1_')
        CALL ENCODE(TMIN * 1.E6, CHR, '(F6.2)_')
        CALL DISP('@4@L24@C16_')
        CALL DISP(CHR)
        CALL ENCODE(TMAX * 1.E6, CHR, '(F6.2)_')
        CALL DISP('@2@L24@C67_')
        CALL DISP(CHR)
        STEP = PI2 / (POINTS - 1)
        DO 110 I = 1, POINTS
          TIME(I) = TMIN + (TMAX - TMIN) * I / FLOAT(POINTS)
C         UPDATE FREQUENCY ON SCREEN
          CALL ENCODE(TIME(I) * 1.E6, CHR, '(F6.2)_')
          CALL DISP('@7@L24@C42_')
          CALL DISP(CHR)
          OUTTME(I) = CMPLX(0., 0.)
          DO 110 J = 1, POINTS
            OMEGA = PI2 * FRQ(J)
            HAMMING = 0.54 - 0.46 * COS(STEP * (J - 1))
            OUTTME(I) = OUTTME(I) + OUTSIG(J) * HAMMING *
```

```
     1                              CEXP(CMPLX(0., OMEGA * TIME(I)))
  110 CONTINUE
      CALL CLRTXT
      CALL CLRGRF
      CALL DISP('@X_')
      ALLFLG = .FALSE.
      RETURN
      END
*****************************************************************
      DOUBLE PRECISION FUNCTION PP(R, J)
*****************************************************************
*
*     FUNCTION TO COMPUTE THE NONINTEGER FORM OF THE LEGENDRE POLYNOMIAL
*     OF THE FIRST KIND
*
      IMPLICIT REAL*8 (P)
      COMMON /LGNDRE/ PVAL, X
      REAL*8 PI, X, COEFF, PVAL(20)
      DATA INF/19/
      PI = 4. * DATAN(DBLE(1.))
      IF (ABS(FLOAT(NINT(R)) - R) .LE. 1.E-12) THEN
        IF (J .LT. 0) THEN
          IF ((MOD(NINT(R), 2) .EQ. 1 .AND. NINT(R) .GE. 0) .OR.
     1        (MOD(NINT(R), 2) .EQ. 0 .AND. NINT(R) .LT. 0)) THEN
            PP = -P(NINT(R))
          ELSE
            PP = P(NINT(R))
          ENDIF
        ELSE
          PP = P(NINT(R))
        ENDIF
      ELSE
        PP = 0.
        DO 10 N = 0, INF
          IF (J .EQ. 1) THEN
            COEFF = (-1.)**N * (1./(R - N) - 1./(R + N + 1))
          ELSE
            COEFF = 1./(R - N) - 1./(R + N + 1)
          ENDIF
          PP = PP + COEFF * P(N)
   10   CONTINUE
        PP = PP * DSIN(R * PI) / PI
      ENDIF
      RETURN
      END
*****************************************************************
      DOUBLE PRECISION FUNCTION P(N)
*****************************************************************
      COMMON /LGNDRE/ PVAL, X
      REAL*8 PVAL(20), X
      IF (N .LT. 0) THEN
        P = PVAL(-N)
      ELSE
        P = PVAL(N + 1)
      ENDIF
      RETURN
      END
*****************************************************************
      SUBROUTINE SETP
*****************************************************************
*
*     FUNCTION TO COMPUTE THE LEGENDRE POLYNOMIAL OF THE FIRST KIND
*
      COMMON /LGNDRE/ PVAL, X
      REAL*8 PVAL(20), X
      PVAL(1) = DBLE(1.)
```

```
      PVAL(2) = X
      DO 10 I = 2, 19
        PVAL(I + 1) = 2 * X * PVAL(I) - PVAL(I - 1) -
     1                (X * PVAL(I) - PVAL(I - 1)) / I
   10 CONTINUE
      RETURN
      END
```

```
$STORAGE:2
$NOFLOATCALLS
*****************************************************************
      SUBROUTINE PLOT
*****************************************************************
*
*  ROUTINE TO PLOT THE CURRENT COMPUTED FREQUENCY RESPONSE
*
*  BY PETER M. SMITH, MCMASTER UNIVERSITY
*  LATEST UPDATE:  MAY 1987
*
      REAL*4 FREQ(512), TIME(512), RSPNSE(512), XRANGE, YRANGE, YMAX
      REAL*8 MAGN
      COMPLEX OUTSIG(512), OUTTME(512), ZE
      INTEGER*2 W(4), W0(4), IX(5), IY(5), IXY(2), X(512), Y(512)
      INTEGER SUBSTR, SCTION, TYPE(20)
      REAL FREQ0, FRQMIN, FRQMAX, SECLEN(20), APRTUR, RS
      REAL KAPPA, ALPHA, THETA, METRAT
      LOGICAL*2 ALLFLG, VALDAT(8), MATCH
      INTEGER XSCALE, YSCALE, POINTS, NN
      CHARACTER PLTTTL*40, STR*6
      COMMON /STATUS/ SUBSTR, SCTION, TYPE, FREQ0, FRQMIN, FRQMAX,
     1     SECLEN, APRTUR, ZE, RS, KAPPA, ALPHA, THETA, METRAT
      COMMON /FLAGS/ ALLFLG, VALDAT
      COMMON /PLTBLK/ XSCALE, YSCALE, POINTS, MATCH, PLTTTL, TMIN, TMAX
      COMMON /RSPBLK/ FREQ, OUTSIG, TIME, OUTTME
      EXTERNAL INKEY
      DATA IX/0, 499, 499, 0, 0/, IY/0, 0, 219, 219, 0/
      DATA W/119, 619, 39, 259/, W0/0, 719, 0, 299/
*     CHECK THAT HAVE DATA TO PLOT
      IF (ALLFLG) THEN
        CALL DISP('@7@L25@C09 *** NO DATA TO PLOT_')
        CALL BELL
        CALL WAIT(30)
        CALL ERSLIN(25)
        RETURN
      ENDIF
*     COMPUTE MAGNITUDE RESPONSE
      DO 5 I = 1, POINTS
        MAGN = DBLE(REAL(OUTSIG(I)))**2 + DBLE(AIMAG(OUTSIG(I)))**2
        IF (MAGN .GE. 1.D-40) THEN
          RSPNSE(I) = 10. * -SNGL(DLOG10(MAGN))
        ELSE
          RSPNSE(I) = 400.
        ENDIF
    5 CONTINUE
*     SET UP GRAPH AREA
      CALL CLRTXT
      CALL PTCOLR('Y')
      CALL WINDOW(W)
      CALL LINE(5, IX, IY)
      XRANGE = (FRQMAX - FRQMIN) / 1.E6
      YRANGE = 5. * FLOAT(YSCALE)
      CALL AXIS('X', 0, 499, 0, NINT(500. * FLOAT(XSCALE) / XRANGE))
      CALL AXIS('X', 0, 499, 219, NINT(500. * FLOAT(XSCALE) / XRANGE))
      CALL AXIS('Y', 0, 219, 0, NINT(220. * FLOAT(YSCALE) / YRANGE))
      CALL AXIS('Y', 0, 219, 499, NINT(220. * FLOAT(YSCALE) / YRANGE))
*     NORMALIZE RESPONSE FOR PLOTTING
      YMAX = -1.E12
      DO 10 I = 1, POINTS
        IF (RSPNSE(I) .GT. YMAX) YMAX = RSPNSE(I)
   10 CONTINUE
```

```
      IF (YMAX .GT. 0.) THEN
        YMAX = YSCALE * FLOAT(INT(YMAX / YSCALE) + 1)
      ELSE
        YMAX = YSCALE * FLOAT(INT(YMAX / YSCALE))
      ENDIF
      DO 20 I = 1, POINTS
        X(I) = NINT(FLOAT(I) * (500. / FLOAT(POINTS)))
        Y(I) = NINT(219. * (RSPNSE(I) - YMAX + YRANGE) / YRANGE)
   20 CONTINUE
*     PLOT RESPONSE
      CALL PTCOLR('C')
      CALL LINE(POINTS, X, Y)
*     SCALE THE Y-AXIS
      CALL PTCOLR('Y')
      CALL WINDOW(WO)
      IXY(1) = 85
      DO 30 I = 1, 6
        IXY(2) = 37 + (I - 1) * 44
        CALL ENCODE((YMAX - YRANGE) + YSCALE * FLOAT(I - 1), STR,
     1              '(F5.0)_')
        CALL PLTLET(0, IXY, STR)
   30 CONTINUE
*     SCALE THE X-AXIS
      IXY(2) = 30
      NN = INT(XRANGE / FLOAT(XSCALE)) + 1
      DO 40 I = 1, NN
        IXY(1) = 112 + NINT((I - 1) * 500. * FLOAT(XSCALE) / XRANGE)
        CALL ENCODE(FRQMIN/1.E6 + FLOAT(XSCALE * (I - 1)), STR,
     1              '(F5.0)_')
        CALL PLTLET(0, IXY, STR)
   40 CONTINUE
*     LABEL THE X-AXIS
      IXY(1) = 310
      IXY(2) = 5
      CALL LETRH(1, IXY, 'FREQUENCY (MHZ)_')
*     LABEL THE Y-AXIS
      IXY(1) = 40
      IXY(2) = 220
      CALL LETRV(1, IXY, 'MAGNITUDE (DB)_')
*     LABEL THE PLOT
      IXY(1) = 375 - 5 * LEN(PLTTTL)
      IXY(2) = 280
      CALL LETRH(1, IXY, PLTTTL)
*     WAIT FOR / KEY FOR TIME DOMAIN OR FOR RETURN KEY TO EXIT TO
*     COMMAND MODE
      CALL DISP('@7@L24@C68@B\RTN\@b Return_')
      CALL DISP('@7@L25@C68@B\ / \@b Impulse_')
  100 INCHAR = INKEY('1/_')
      IF (INCHAR .EQ. 0) GOTO 100
      IF (INCHAR .EQ. 1) GOTO 110
      CALL CLRTXT
      CALL CLRGRF
      CALL PLTTME
  110 CALL CLRTXT
      CALL CLRGRF
      RETURN
      END
*******************************************************************
      SUBROUTINE PLTTME
*******************************************************************
*
*  ROUTINE TO PLOT THE IMPULSE RESPONSE OF CURRENT FREQUENCY RESPONSE
*
      REAL*4 FREQ(512), TIME(512), RSPNSE(512), XRANGE, YRANGE, YMAX
      COMPLEX OUTSIG(512), OUTTME(512), ZE
      REAL*4 WR(512), WI(512), XX(512), YY(512)
```

```
      INTEGER*2 W(4), W0(4), IX(5), IY(5), IXY(2), X(512), Y(512)
      INTEGER SUBSTR, SCTION, TYPE(20)
      REAL FREQ0, FRQMIN, FRQMAX, SECLEN(20), APRTUR, RS
      REAL KAPPA, ALPHA, THETA, METRAT
      LOGICAL*2 ALLFLG, VALDAT(8), MATCH
      INTEGER XSCALE, YSCALE, POINTS, NN
      CHARACTER PLTTTL*40, STR*6
      COMMON /STATUS/ SUBSTR, SCTION, TYPE, FREQ0, FRQMIN, FRQMAX,
     1       SECLEN, APRTUR, ZE, RS, KAPPA, ALPHA, THETA, METRAT
      COMMON /FLAGS/ ALLFLG, VALDAT
      COMMON /PLTBLK/ XSCALE, YSCALE, POINTS, MATCH, PLTTTL, TMIN, TMAX
      COMMON /RSPBLK/ FREQ, OUTSIG, TIME, OUTTME
      EXTERNAL INKEY
      DATA IX/0, 499, 499, 0, 0/, IY/0, 0, 219, 219, 0/
      DATA W/119, 619, 39, 259/, W0/0, 719, 0, 299/
      COMPUTE MAGNITUDE RESPONSE
      DO 8 I = 1, POINTS
        RSPNSE(I) = SQRT(REAL(OUTTME(I))**2 + AIMAG(OUTTME(I))**2)
    8 CONTINUE
      SET UP GRAPH AREA
      CALL CLRTXT
      CALL PTCOLR('Y')
      CALL WINDOW(W)
      CALL LINE(5, IX, IY)
      CALL AXIS('X', 0, 499, 0, 100)
      CALL AXIS('X', 0, 499, 219, 100)
      CALL AXIS('Y', 0, 219, 0, 44)
      CALL AXIS('Y', 0, 219, 499, 44)
      NORMALIZE RESPONSE FOR PLOTTING
      YMAX = -1.E12
      XMIN = 1.E12
      XMAX = -1.E12
      DO 10 I = 1, POINTS
        IF (RSPNSE(I) .GT. YMAX) YMAX = RSPNSE(I)
        IF (TIME(I) .LT. XMIN) XMIN = TIME(I)
        IF (TIME(I) .GT. XMAX) XMAX = TIME(I)
   10 CONTINUE
      TRANGE = XMAX - XMIN
      IF (ABS(YMAX) .LE. 1.E-20) THEN
        WRITE (*, *) ' YMAX = 0 --> ERROR'
        STOP
      ENDIF
      DO 15 I = 1, POINTS
        RSPNSE(I) = RSPNSE(I) / YMAX
   15 CONTINUE
      DO 20 I = 1, POINTS
        X(I) = NINT(FLOAT(I) * (500. / FLOAT(POINTS)))
        Y(I) = NINT(219. * RSPNSE(I))
   20 CONTINUE
      PLOT RESPONSE
      CALL PTCOLR('C')
      CALL LINE(POINTS, X, Y)
      SCALE THE Y-AXIS
      CALL PTCOLR('Y')
      CALL WINDOW(W0)
      IXY(1) = 85
      DO 30 I = 1, 6
        IXY(2) = 37 + (1 - T) * 44
        CALL ENCODE(0.2 * FLOAT(I - 1), STR, '(F5.2)_')
        CALL PLTLET(0, IXY, STR)
   30 CONTINUE
      SCALE THE X-AXIS
      IXY(2) = 30
      DO 40 I = 1, 6
        IXY(1) = 112 + NINT((I - 1) * 500. * 0.2)
        CALL ENCODE(0.2 * TRANGE * 1.E6 * FLOAT(I - 1), STR, '(F5.1)_')
```

```
      CALL PLTLET(0, IXY, STR)
   40 CONTINUE
*     LABEL THE X-AXIS
      IXY(1) = 340
      IXY(2) = 5
      CALL LETRH(1, IXY, 'TIME (us)_')
*     LABEL THE Y-AXIS
      IXY(1) = 40
      IXY(2) = 200
      CALL LETRV(1, IXY, 'AMPLITUDE_')
*     LABEL THE PLOT
      IXY(1) = 375 - 5 * LEN(PLTTTL)
      IXY(2) = 280
      CALL LETRH(1, IXY, PLTTTL)
*     WAIT FOR / KEY FOR FREQUENCY DOMAIN OR FOR RETURN KEY TO EXIT TO
*     COMMAND MODE
      CALL DISP('@7@L24@C68@B\RTN\@b Return_')
      CALL DISP('@7@L25@C68@B\ / \@b Frequency_')
  100 INCHAR = INKEY('1/_')
      IF (INCHAR .EQ. 0) GOTO 100
      IF (INCHAR .EQ. 1) GOTO 110
      CALL CLRTXT
      CALL CLRGRF
      CALL PLOT
  110 CALL CLRTXT
      CALL CLRGRF
      RETURN
      END
```

```
$STORAGE:2
$NOFLOATCALLS
*****************************************************************
      SUBROUTINE SAVE
*****************************************************************
*
*  ROUTINE TO SAVE THE CURRENT STRUCTURE ONTO FILE 'COM.STT'
*
*  BY PETER M. SMITH, MCMASTER UNIVERSITY
*  LATEST UPDATE:  MAY 1987
*
      INTEGER SUBSTR, SCTION, TYPE(20)
      REAL FREQ0, FRQMIN, FRQMAX, SECLEN(20), APRTUR, RS
      REAL KAPPA, ALPHA, THETA, METRAT
      REAL FREQ(512), TIME(512)
      COMPLEX OUTSIG(512), OUTTME(512), ZE
      LOGICAL*2 ALLFLG, VALDAT(8), MATCH
      INTEGER XSCALE, YSCALE, POINTS
      CHARACTER PLTTTL*40
      COMMON /STATUS/ SUBSTR, SCTION, TYPE, FREQ0, FRQMIN, FRQMAX,
     1        SECLEN, APRTUR, ZE, RS, KAPPA, ALPHA, THETA, METRAT
      COMMON /FLAGS/ ALLFLG, VALDAT
      COMMON /PLTBLK/ XSCALE, YSCALE, POINTS, MATCH, PLTTTL, TMIN, TMAX
      COMMON /RSPBLK/ FREQ, OUTSIG, TIME, OUTTME
*
      OPEN(UNIT = 1, FILE = 'COM.STT', STATUS = 'NEW')
      WRITE(1, *) SUBSTR
      WRITE(1, *) FRQMIN, FREQ0, FRQMAX
      WRITE(1, *) SCTION
      WRITE(1, *) (TYPE(I), I = 1, SCTION)
      WRITE(1, *) (SECLEN(I), I = 1, SCTION)
      WRITE(1, *) APRTUR
      WRITE(1, *) ZE
      WRITE(1, *) RS
      WRITE(1, *) KAPPA
      WRITE(1, *) ALPHA
      WRITE(1, *) THETA
      WRITE(1, *) METRAT
      WRITE(1, *) (VALDAT(I), I = 1, 7)
      WRITE(1, *) ALLFLG
      WRITE(1, *) XSCALE, YSCALE
      WRITE(1, *) POINTS
      WRITE(1, *) MATCH
      WRITE(1, '(A, A40, A)') '''', PLTTTL, ''''
      WRITE(1, *) TMIN, TMAX
      IF (.NOT. ALLFLG) THEN
        DO 10 I = 1, POINTS
          WRITE(1, *) FREQ(I), OUTSIG(I), TIME(I), OUTTME(I)
10    CONTINUE
      ENDIF
      CLOSE(UNIT = 1, STATUS = 'KEEP')
      CALL BELL
      RETURN
      END
*****************************************************************
      SUBROUTINE RECALL
*****************************************************************
*
*  ROUTINE TO RECALL THE LATEST SAVED SYSTEM STATE FROM FILE 'COM.STT'
*
      INTEGER SUBSTR, SCTION, TYPE(20)
      REAL SECLEN(20), FREQ0, FRQMIN, FRQMAX, APRTUR, RS
```

```
      REAL KAPPA, ALPHA, THETA, METRAT
      INTEGER XSCALE, YSCALE, POINTS
      REAL FREQ(512), TIME(512)
      COMPLEX OUTSIG(512), OUTTME(512), ZE
      LOGICAL*2 ALLFLG, VALDAT(8), MATCH
      CHARACTER PLTTTL*40
      INTEGER CHK
      COMMON /FLAGS/ ALLFLG, VALDAT
      COMMON /STATUS/ SUBSTR, SCTION, TYPE, FREQ0, FRQMIN, FRQMAX,
     1       SECLEN, APRTUR, ZE, RS, KAPPA, ALPHA, THETA, METRAT
      COMMON /PLTBLK/ XSCALE, YSCALE, POINTS, MATCH, PLTTTL, TMIN, TMAX
      COMMON /RSPBLK/ FREQ, OUTSIG, TIME, OUTTME

      OPEN(UNIT = 1, FILE = 'COM.STT', STATUS = 'OLD', IOSTAT = CHK)
      IF (CHK .NE. 0) THEN
        CALL DISP('@7@L25@C09*** NO DATA FILE FOUND_')
        CALL BELL
        CALL WAIT(30)
        CALL ERSLIN(25)
        RETURN
      ENDIF
      READ(1, *) SUBSTR
      READ(1, *) FRQMIN, FREQ0, FRQMAX
      READ(1, *) SCTION
      READ(1, *) (TYPE(I), I = 1, SCTION)
      READ(1, *) (SECLEN(I), I = 1, SCTION)
      READ(1, *) APRTUR
      READ(1, *) ZE
      READ(1, *) RS
      READ(1, *) KAPPA
      READ(1, *) ALPHA
      READ(1, *) THETA
      READ(1, *) METRAT
      READ(1, *) (VALDAT(I), I = 1, 7)
      READ(1, *) ALLFLG
      READ(1, *) XSCALE, YSCALE
      READ(1, *) POINTS
      READ(1, *) MATCH
      READ(1, *) PLTTTL
      READ(1, *) TMIN, TMAX
      IF (.NOT. ALLFLG) THEN
        DO 10 I = 1, POINTS
          READ(1, *) FREQ(I), OUTSIG(I), TIME(I), OUTTME(I)
10    CONTINUE
      ENDIF
      CLOSE(UNIT = 1)
      CALL BELL
      RETURN
      END
```

REFERENCES

1. J. H. Collins and L. Masotti (Eds.), Computer-Aided Design of Surface Acoustic Wave Devices, Elsevier: New York, 1976.

2. H. Matthews (Ed.), Surface Wave Filters: Design, Construction and Use, John Wiley: New York, 1977.

3. A. A. Oliner (Ed.), Acoustic Surface Waves, Springer-Verlag: New York, 1978.

4. E. A. Ash and E. G. S. Paige (Eds.), Rayleigh-Wave Theory and Application, Springer-Verlag: Berlin, 1985.

5. D. P. Morgan, Surface-Wave Devices for Signal Processing, Elsevier: Amsterdam, 1985.

6. S. Datta, Surface Acoustic Wave Devices, Prentice-Hall: Englewood Cliffs, N.J., 1986.

7. G. S. Kino, Acoustic Waves: Devices, Imaging & Analog Signal Processing, Prentice-Hall: Englewood Cliffs, N.J., 1987.

8. C. K. Campbell, Course Notes on Surface Acoustic Wave Devices and their Signal Processing Applications, George Washington University, Washington, D.C., 1987.

9. R. M. White and F. W. Voltmer, "Direct Piezoelectric Coupling to Surface Elastic Waves", Applied Physics Letters, Vol. 7, No. 12, pp. 314-316, Dec. 1965.

10. J. Helszajn, Passive and Active Microwave Circuits, Wiley: New York p. 170, 1978.

11. W. S. Jones, C. S. Hartmann, T. D. Sturdivant, "Second Order Effects in Surface Wave Devices", IEEE Trans. on Sonics and Ultrasonics, Vol. SU-19, No. 3, pp. 368-377, July 1972.

12. T. W. Bristol, "Analysis and Design of Surface Acoustic Wave Transducers", Proc. of IEE International Specialist Seminar on Component Performance and Systems Applications of Surface-Acoustic-Wave Devices, pp. 115-129, 1972.

13. C. Flory and M. Tan, "Compensation of Diffraction Effects in SAW Filters Using the Uniform Asymptotic Expansion", IEEE Trans. on Ultrasonics, Ferroelectrics and Frequency Control, Vol. UFFC-34, No. 1, pp. 105-113 Jan 1987.

14. C. S. Hartmann, D. T. Bell and R. C. Rosenfeld, "Impulse Model Design of Acoustic Surface Wave Filters", IEEE Transactions on Microwave Theory and Techniques, Vol. MTT-21, No. 4, pp. 162-175, April 1973.

15. W. R. Smith, "Studies of Microwave Acoustic Transducers and Dispersive Delay Lines", Ph.D. Thesis, Stanford University, 1969.

16. P. S. Cross and R. V. Schmidt, "Coupled Surface-Acoustic-Wave Resonators", Bell System Technical Journal, Vol. 56, No. 8, pp. 1447-1483, Oct. 1977.

17. A. V. Oppenheim and R. W. Schafer, Digital Signal Processing, Prentice Hall: Englewood Cliffs, N.J., Chapter 5, 1975.

18. P. M. Smith, Design of SAW Filters using the Remez Exchange Algorithm, M.Eng. Thesis, McMaster University, 1985.

19. E. A. Ash, "Surface Wave Grating Reflectors and Resonators", IEEE Proceedings of the 1970 G-MTT International Microwave Symposium, pp. 385-386, 1970.

20. C. S. Hartmann, W. S. Jones and H. Vollers, "Wideband Unidirectional Interdigital Surface Wave Transducers", IEEE Trans. on Sonics and Ultrasonics, Vol. SU-19, No. 2, pp. 378-381, July 1972.

21. F. G. Marshall, E. G. S. Paige, A. S. Young, "New Unidirectional Transducer and Broadband Reflector of Acoustic Surface Waves", Electronics Letters, Vol. 7, No. 21, pp. 638-640, Sep. 1971.

22. F. G. Marshall and E. G. S. Paige, "Novel Acoustic-Surface-Wave Directional Coupler With Diverse Applications", Electronics Letters, Vol. 7, pp. 460-462, 1971.

23. R. B. Brown, "Low-Loss Device Using Multistrip Coupler Ring Configuration", IEEE Proceeding of the 1986 Ultrasonics Symposium, pp. 71-76, 1986.

24. C. K. Campbell and C. B. Saw, "Analysis and Design of Low-Loss SAW Filters Using Single-Phase Unidirectional Transducers", IEEE Trans. on Ultrasonics, Ferroelectrics and Frequency Control, Vol. UFFC-34, No. 3, pp. 357-367, May 1987.

25. M. F. Lewis, "SAW Filters Employing Interdigitated Interdigital Transducers", IEEE Proceedings of the 1982 Ultrasonics Symposium, pp. 12-17, 1982.

26. J. R. Pierce, "Coupling of Modes of Propagation", Journal of Applied Physics, Vol. 25, pp. 179-183, 1954.

27. H. Kogelnik, "Coupled Wave Theory for Thick Hologram Gratings, Bell System Technical Journal, Vol. 48, No. 9, pp. 2909-2947, Nov. 1969.

28. A. Yariv, "Coupled-Mode Theory for Guided-Wave Optics", IEEE Journal of Quantum Electronics, Vol. QE-9, No. 9, pp. 919-933, Sep. 1973.

29. P. V. Wright, "A Coupling-of-Modes Analysis of SAW Grating Structures", Ph.D. Thesis, Massachusetts Institute of Technology, Cambridge, MA, 1981.

30. D. P. Chen and H. A. Haus, "Analysis of Metal-Strip SAW Gratings and Transducers", IEEE Transactions on Sonics and Ultrasonics, Vol. SU-32, No. 3, pp. 395-408, May 1985.

31. C. B. Saw, "Low-Loss SAW Filters for Front-End Signal Processing", M.Eng. Thesis, McMaster University, Hamilton, Ont., 1986.

32. C. S. Hartmann, P. V. Wright, R. J. Kansy and E. M. Garber, "An Analysis of SAW Interdigital Transducers with Internal Reflections and the Application to the Design of Single-Phase Unidirectional Transducers", IEEE Proceedings of the 1982 Ultrasonics Symposium, pp. 40-45, 1982.

33. C. M. Panasik and B. J. Hunsinger, "Scattering Matrix Analysis of Surface Acoustic Wave Reflections and Transducers", IEEE Trans. on Sonics and Ultrasonics, Vol. SU-28, No. 2, pp. 79-91, March 1981.

34. S. Datta and B. J. Hunsinger, "An Analytical Theory for the Scattering of Surface Acoustic Waves by a Single Electrode in a Periodic Array on a Piezoelectric Substrate", Journal of Applied Physics, Vol. 51, No. 9, pp. 4817-4823, Sep. 1980.

35. H. Bateman, Higher Transcendental Functions, New York: McGraw Hill, p. 167, 1953.

36. C. A. Balanis, Antenna Theory: Analysis and Design, New York: Harper & Row, Chapter 6, 1982

37. W. P. Robins, Phase Noise in Signal Sources, London: Peregrinus, Chapter 5, 1982.

38. Solution 4 from Innovative Measurement Solutions, Atlanta, Georgia.

39. P. J. Edmonson, C. K. Campbell and P. M. Smith, "Narrow-Band SAW Filters Using Stepped-Resonators With Tapered Gratings", IEEE Proceedings of the 1984 Ultrasonics Symposium, pp. 235-238, 1984.

40. C. K. Campbell, Y. Ye and J. J. Sferrazza Papa, "Wide-Band Linear Phase SAW Filter Design Using Slanted Transducer Fingers", IEEE Transactions on Sonics and Ultrasonics, Vol. SU-29, No. 6, pp. 224-228, July 1982.

41. D. B. Leeson, "Simple Model of a Feedback Oscillator Noise Spectrum", Proceedings of the IEEE, Vol. 54, No. 2, pp. 329-330, Feb 1966.

42. User's manual for the HP 5390A frequency stability analyzer phase noise program, HP part number 05390-90011, November 1977.

43. C. B. Saw, P. M. Smith, P. J. Edmonson and C. K. Campbell, "Mode Selection in a Multimode SAW Oscillator Using FM Chirp Mixing Signal Injection", accepted for publication in the IEEE Transactions on Ultrasonics, Ferroelectrics and Frequency Control.